# Posttranslational regulation and effector specificity of the type VI secretion system

Julie Michelle Silverman

A dissertation

submitted in partial fulfillment of the

requirements for the degree of

Doctorate of Philosophy

University of Washington

2013

Joseph Mougous, chair

Matthew Parsek

Beth Traxler

Program Authorized to offer Degree:

Microbiology

University of Washington

# ABSTRACT

Posttranslational regulation and effector specificity of the type VI secretion system

Julie Michelle Silverman

Chair of Supervisory Committee:

Professor Joseph D. Mougous

Microbiology

Bacteria mediate interactions with their surroundings by exporting a variety of proteins into the extracellular environment. Gram-negative bacteria have evolved at least six dedicated secretory pathways to accomplish this task, each exporting a discrete set of proteins through complex and genetically divergent systems. One such system is the type VI secretion system (T6SS), which is a contact-dependent protein export pathway that delivers toxic effectors into target bacterial and eukaryotic cells. The export of effectors is controlled by sophisticated regulatory networks that can be triggered by specific environmental cues. The characterization of these regulatory pathways has yielded new insight into the physiologically relevant conditions in which these systems are active. In this thesis work, the Hcp secretion island I (HSI-I)-encoded T6SS (H1-T6SS) of the opportunistic pathogen, *Pseudomonas aeruginosa*, was used as a model system to investigate the factors that govern T6S activity. Specifically, this work describes two distinct

posttranslational regulatory pathways – mediated by H1-T6SS associated proteins – that coordinate T6S apparatus assembly and effector export. One of these regulatory pathways, the threonine phosphorylation pathway (TPP), is stimulated when *P. aeruginosa* is subjected to surface-associated growth conditions. In contrast, the second pathway, which is mediated by a negative regulator, TagF, does not respond to surface or planktonic growth conditions and, instead, is likely stimulated by an unknown cue. As productive H1-T6S-dependent toxin delivery requires close cell contact, the presence of these regulatory pathways may provide a means to efficiently initiate H1-T6S activity under appropriate environmental conditions. Another important aspect of the T6SS and secretion systems in general, is the mechanisms used to specifically select substrates for export. This thesis work has uncovered a mechanism for substrate recognition by the T6SS. I found that specific interactions between T6S-effectors and a secreted T6S component, Hcp (haemolysin co-regulated protein), are essential for effector export. Thus, Hcp plays a central role in T6S substrate discrimination. Together, these findings have advanced our understanding of the T6SS and have shed light on the diverse mechanisms by which proteins can be exported by bacteria.

TABLE OF CONTENTS

# ACKNOWLEDGEMENTS

I am grateful to many individuals who have provided endless support, invaluable advice, persistent encouragement and kindness over the course of my graduate studies.

Most importantly, I would like to thank my graduate school advisor, Joseph Mougous, for being an inspiring scientist and mentor. I am indebted to Joseph for his fundamental role in my accomplishments and overall development as a scientist. His positive attitude, words of encouragement and constructive criticism have helped me to improve my writing and speaking skills, and to think deeply about my research projects. Additionally, Joseph's genuine passion for science has made the lab an exciting, fun and enriching place to work and learn.

I thank my graduate advisory committee, Matthew Parsek, Beth Traxler, Pete Greenberg, Tamir Gonen and Carlos Catalano, for their continuous support over the course of my graduate studies. I greatly appreciate the time they have dedicated to my committee meetings and beyond. Their insightful questions, eye for experimental detail and thoughtful feedback have helped me progress scientifically.

I would like to thank the Department of Microbiology at University of Washington for giving me this incredible opportunity. The events hosted by the department, including, seminars, journal clubs and retreats, have connected me to other amazing scientists and have helped me improve my communication skills. Additionally, I thank the graduate students in the Microbiology

graduate program. Together, we have supported each other through the ups and downs of graduate school.

I have had the great fortune to work alongside, and in collaboration with, many remarkable colleagues during my time in the Mougous laboratory. Sandra Schwarz, FoSheng Hsu, Yin-Yin Wang, Tuzun Güvener, Rex Trinidad, Brooks Olson, Laura Austin, Justin Leon, Delia Pinto-Santini, Rachel Hood, Mo Li, Mike Carl, Michele LeRoux, Alistair Russell, Nick Andring, Danielle Agnello, Seemay Chou, Max Ferrin, Phil Tatman, Taylor Gardiner, Guillaume DéJean, Brook Peterson and John Whitney have provided both moral and scientific support. The espresso machine has been the center for many insightful discussions that have guided my research. In addition to fostering an enriching scientific environment, Joseph Mougous and Mougous lab members have made “lab outings” and camping trips truly memorable events.

My high school, undergraduate and graduate school professors laid the foundation for my scientific career. My enthusiastic and brilliant high school chemistry teacher, Mr. Reed, initially provoked my passion for science. I wish to thank my undergraduate research advisor, David Davies, who gave me the opportunity to train under his supervision and who encouraged me to pursue microbiology research.

I also wish to thank my family and friends for their constant support and love. My parents, Susan and Daniel Silverman, have ceaselessly encouraged me to follow my love of science. Thank you to my brothers, Eric and Ian Silverman, my sister-in-law, Lauren Weintraub, my best friend,

Marianne DiNapoli, and my boyfriend, Ashish Gupta who have been there to celebrate my successes, support me through the hurdles of graduate school and have enriched my life.

# CHAPTER I:

## Introduction to the type VI secretion system of Gram-negative bacteria

**Specialized secretory systems of Gram-negative bacteria.**

Bacteria must interact with their surroundings and adapt to environmental changes in order to survive. Indeed, bacteria can experience shifts in nutrient availability, come in contact with surfaces and encounter competing or symbiotic organisms. To interact dynamically with their extracellular surroundings, bacteria secrete proteins, including nutrient scavenging molecules, enzymes, toxins and adhesins (85). The transport of these proteins out of the cell is a regulated process mediated by specialized secretory systems.

Secretion in Gram-negative bacteria involves the transport of proteins across the inner and outer membranes. To date, six secretory pathways have been identified in Gram-negative bacteria, termed the type I-VI secretion systems (72). Each system exports a unique group of substrates that are involved in a wide-range of cellular processes. Although these six secretion systems operate in distinct ways, they share common features, including at least one secretion ATPase that energizes the system, a receptor for substrate recognition and a channel that guides substrate transit. The six specialized secretory pathways of Gram-negative bacteria are briefly described below.

The type I secretion system (T1SS), also known as the ATP-binding cassette (ABC) transporter, catalyzes the secretion of proteins from the bacterial cytoplasm into the extracellular space in a single step, without a periplasmic intermediate (111). Known substrates transported by T1SSs include a pore-forming hemolytic toxin, HlyA, of *Escherichia coli*, a metalloprotease, PrtG, of *Erwinia chrysanthemi* and adhesins, BapA and SiiE, of *Salmonella enterica* (93, 138, 237, 251). These substrates are secreted in a unfolded, or partially unfolded, state through a simple

apparatus comprised of three components: an ABC transporter, a membrane fusion protein (MFP) and an outer membrane protein (OMP) (111). The inner membrane localized ABC transporter specifically binds substrates and provides the energy required for secretion. The periplasmic MFP creates a channel bridging the inner and outer membranes, allowing substrates to transit the cellular envelope without undergoing a periplasmic intermediate state. The MFP is thought to stimulate a conformation change of the OMP, inducing channel opening and substrate release across the outer membrane.

The type II secretion system (T2SS) is the main terminal branch of the general secretory pathway (GSP) of Gram-negative bacteria (191). A subset of proteins delivered to the periplasm via the Sec (Secretory) pathway or Tat (Twin arginine-translocation) pathway are translocated, in a fully folded form, across the outer membrane by the T2SS. Many substrates exported by the T2SS are known virulence determinants, including cholera toxin of *Vibrio cholerae*, exotoxin A of *P. aeruginosa* and pectinase of *Erwinia caratovora* (53, 152, 208). T2SSs are also found in non-pathogenic organisms, such as *Shewanella oneidensis*, which exports outer membrane cytochromes required for metal oxide reduction (220). T2S substrates are exported by an apparatus built from 12-15 proteins that comprise four subassemblies spanning the cellular envelope (131). The outer membrane complex interacts with substrates and forms a channel for translocation. The inner membrane complex associates with the secretion ATPase and the periplasmic localized filament, the pseudopilus. The secretion ATPase drives elongation of the pseudopilus, which is thought to generate the force required to drive substrates across the outer membrane.

Type III secretion systems (T3SSs) are frequently found in bacteria that live in close association with eukaryotic cells, symbiotically or pathogenically (54). These secretion systems transport effector proteins through a needle-like complex directly from the bacterial cytoplasm into host cells. The many T3SS substrates characterized to date display a range of activities that specifically target host cell processes, for example, by modifying actin, repressing the immune response or inhibiting apoptosis (91). The structure of the T3SS injectisome, which is evolutionarily related to the bacterial flagellum machinery, is composed of approximately 25 different subunits (92). An extracellular needle filament is built from the membrane spanning basal body complex. Effector recognition and secretion are dependent on a T3S-ATPase that associates with the basal body subunit. Finally, translocator proteins assemble at the tip of the needle, directly contact the host cell membrane and permit effector delivery into the cytosol.

Type IV secretion systems (T4SS) are complex molecular machines that have the capacity to deliver virulence factors directly into a target cell and exchange genetic material with eukaryotes and prokaryotes. Two subgroups of T4SSs exist, both related to conjugation systems: T4ASS and T4BSS (51). T4ASSs are related to the *Agrobacterium tumefaciens* T-DNA transfer system, which is a well-studied virulence-associated pathway that delivers effectors and DNA into plant cells. T4BSSs are related to IncI Tra DNA transfer system (51). *Legionella pneumophila* encodes a T4BSS that promotes bacterial survival and replication in host cells. Although the T4ASS and T4BSS are genetically divergent, they exhibit several commonalities in their structural modules, including several inner membrane-associated ATPases involved in substrate recognition, a transport channel that spans the cellular envelope, and a periplasmic and outer membrane spanning structure that mediates interactions with target cells. Depending on the T4SS, substrates

can be exported directly into target cells in a contact-dependent manner or into the extracellular milieu in a contact-independent manner.

Compared to the type I-IV secretion systems, the Type V secretion system (T5SS), also known as the autotransporter system, is a relatively simple protein export pathway. The T5SS transports periplasmic proteins, delivered by the Sec pathway, across the outer membrane (105). Examples of T5S-substrates include an adhesin, AIDA-I, of *E. coli*, a protease, IgA, of *Neisseria gonorrhea* and a multifunctional eukaryotic toxin, VacA, of *Helicobacter pylori* (57, 169, 231). These substrates contain a C-terminal domain that forms a beta-barrel in the outer membrane. The N-terminal passenger domain is transported across the outer membrane through the beta-barrel, where it either remains attached or is cleaved to produce a soluble protein.

**Overview of the type VI secretion system.**

The type VI secretion system (T6SS) is the most recently described specialized secretory pathway found in proteobacteria (27). These secretory pathways mediate interactions with bacterial or eukaryotic cells through the delivery of effector molecules. The components of T6SSs are encoded within large gene clusters on the chromosome, composed of, on average, 20 kilobases (216). The genes within these clusters were first suggested to encode a new secretory pathway involved in inhibiting root nodule formation by *Rhizobium leguminosarum* (20). Shortly after this report, secretion of the haemolysin co-regulated protein (Hcp), now known as a general marker of T6S activity, was found to be dependent on several genes within a similar locus in *Edwardsiella tarda* (195). Since these early observations, hundreds of T6S (type VI secretion) clusters have been identified in diverse species. Phylogenetic analysis of all known

T6SS gene clusters, showed that T6SSs diverge into five distinct clades (27). Interestingly, many species possess more than one genetically distinct T6S cluster. For example, five T6SSs are found in *Burkholderia thailandensis*, which, based on their phylogeny, are considered non-redundant systems (18). Two of the five T6S clusters that have been studied in *B. thailandensis* display divergent activities – one delivering a toxic effector to eukaryotic host cells, and the other delivering toxins to bacterial cells (88, 216). Ongoing investigations will reveal the molecular factors that drive the distinct functions of these complex machines.

**Components of the type VI secretion apparatus.**

The T6S apparatus is composed of at least 13 different components, named TssA-TssM (Type six secretion A-M), which are generally conserved in all T6SSs and are, thus, considered the core elements of the T6SS (18, 41). In addition to the core components, accessory elements, termed Tag (Type six accessory gene), are encoded within these clusters. The *tag* genes are not well conserved among T6SSs and do not appear to play a direct role in T6S apparatus function. Instead, several studies have indicated that these accessory proteins function as regulators that modulate T6SS activity (223).

Unlike the T3SS and T4SS, where an ultrastructure of the apparatus has been visualized by electron microscopy, it is not known how the T6S components assemble into a higher-order structure (245, 252). Nonetheless, a model of the T6SS apparatus is beginning to take shape based on sequence analysis as well as protein interaction and structural studies. These findings have revealed that the T6S machinery is composed of at least two subassemblies, a membrane-

spanning complex and a bacteriophage tail-like complex, which are described in more detail below **(Figure 1.1)**.

*Membrane-spanning assembly*

The membrane-spanning assembly is comprised of the integral membrane proteins, TssM and TssL, and a membrane-associated protein TssJ **(Figure 1.1)** (8). TssM and TssL share homology with two inner membrane proteins of the *L. pneumophilia* T4BSS, IcmF and DotU, respectively. In the T4BSS, IcmF and DotU are co-dependent for stability and are required for the stabilization of other apparatus components (217, 241). While TssM and TssL do not appear to contribute to stability of the T6S apparatus, these proteins are essential for apparatus assembly and substrate secretion (258). TssM is an integral inner membrane protein that contains a cytoplasmic N-terminal domain, and a periplasmic C-terminal domain (81). The C-terminal domains of many TssM homologs contain a Walker A nucleotide binding motif. Interestingly, the requirement for this motif in T6S function varies between T6SSs. For example, while in *E. tarda*, the Walker A motif is not required for Hcp secretion, it is essential for secretion in *A. tumefaciens* and enteroaggregative *Escherichia coli* (EAEC) (156, 258). Also of note is that the Walker A motif is absent or degenerate in several TssM homologs, further indicating that nucleotide binding is likely required only for a subset of T6SSs.

The C-terminal periplasmic domain of TssM directly interacts with the outer membrane protein, TssJ (81, 258). This interaction is required for T6S in EAEC and has also been confirmed in *A. tumefaciens* and *E. tarda.* Interestingly, the C-terminal domain of TssM of *Citrobacter rodentium* encodes a truncated form of TssM, resulting in a shorter C-terminal domain (97).

While this system is still functional, it is not known whether the interaction between TssM and TssJ is required in all organisms or is a specific case for EAEC.

TssL is localized to the inner membrane through a C-terminal transmembrane segment. Similar to IcmF and DotU, TssL directly interacts with TssM (156). Interestingly, in many organisms TssL contains a peptidoglycan-binding (PGB) domain, while in some cases a related PGB domain containing protein is encoded by a separate open reading frame within the T6S locus (9). For example, TagL, a T6S protein of the Sci-1 T6SS in EAEC, is anchored to the inner membrane and contains a periplasmic PGB domain that is required for T6S activity (8). *In vivo* and *in vitro* analysis of the PGB domain verified its PGB activity. In addition to TagL–peptidoglycan interactions, a direct interaction between TagL and TssL has been reported. This finding is consistent with the observation that TssL often carries a PGB domain. The network of interactions formed between TssL, TssM and TssJ demonstrates that components of the T6S apparatus span the bacterial cell envelope, anchoring at the inner membrane, outer membrane and peptidoglycan cell wall **(Figure 1.1)**.

*Bacteriophage-like complex*

The T6S proteins, VgrG (Valine-glycine repeat protein G), Hcp, TssB, TssC and TssE, share homology and structural properties with proteins of tailed bacteriophage, specifically bacteriophage T4 and λ **(Figure 1.1)** (142). These bacteriophages belong to the order Caudovirales (2). Both phages contain a tail tube (T4=gp19, λ=gpV) that serves as a channel for bacteriophage genomic DNA translocation into target cells (143). The bacteriophage T4 tail spike complex, gp5/gp27, assembles at the tip of the tube and is required for puncturing the

target cell membrane (126). As opposed to the tails of bacteriophage λ, which are noncontractile, the tails of bacteriophage T4 contain a sheath (gp18) that undergoes a contraction event during infection (4). During the DNA ejection process, a conformational change occurs that triggers sheath contraction. This contraction event energizes the release of the tail tube and tail spike toward the target bacterial cell and allows DNA ejection from the bacteriophage head.

Hcp proteins, which are abundantly secreted in a T6S-dependent manner, are structurally homologous to bacteriophage tail tube proteins (125, 142, 166, 184). gpV, which is functionally homologous to the bacteriophage T4 tail tube protein gp19, adopts a similar fold and oligomeric structure as Hcp (166, 184). The X-ray crystallographic structures of Hcp proteins from *P. aeruginosa* and *E. tarda* highlight these similarities (124, 166, 179). Hcp forms a homohexameric ring with an external diameter of 85 Å and an internal diameter of 40 Å. Within the X-ray crystal lattice, these hexamers stack in a head-to-tail or head-to-head manner, resembling the tail tube of bacteriophage. In bacteriophage, DNA is transferred through the pore formed by gp19 (141). Analogously, small or partially unfolded substrates are thought to transit through the 40 Å pore of an Hcp tube. However, there is no experimental evidence to support this hypothesis. Moreover, Hcp tubes have only been observed under crystallographic or *in vitro* conditions, thus the physiological relevance of Hcp tube formation remains unknown (12, 166).

A second secreted component of the T6SS is VgrG. The X-ray crystal structure of the N-terminal domain of VgrG from uropathogenic *E. coli* shows that VgrG forms a trimer that is remarkably similar to the $(gp5/gp27)_3$ complex of bacteriophage T4 (126, 142). Although the full structure was not determined, the C-terminus of VgrG has predicted β –strand repeats, which are thought

to form a β-helix, similar that of gp5. In bacteriophage T4, $(gp5/gp27)_3$ assembles at the tip of the tail tube. During infection, the β –helix domain is used to disrupt the target cell membrane (126). Due to their extracellular localization and their structural homology to the cell-puncturing component of bacteriophage, Hcp and VgrG are thought to make up an extracellular structure of the T6S apparatus that participates in target cell membrane breaching and effector delivery.

The T6SS proteins, TssB and TssC, interact and form oligomeric tubule structures that resemble the bacteriophage T4 tail sheath (25, 151). Analysis of the purified TssB/TssC complex by electron microscopy indicated that filaments of varying length displayed a total diameter of 300 Å and central pore of approximately 100 Å in diameter (42). These dimensions are comparable to the 240 Å outer and 90 Å inner diameter of the bacteriophage sheath in its extended conformation (141). TssB/TssC tubules have also been visualized *in vivo by* electron cryotomography in *V. cholerae* cells, where they appear anchored to the inner membrane and extend into the cytoplasmic space (14, 127). In this study TssB/TssC tubules appeared in two conformations, an extended and contracted form. This observation has supported a model that TssB/TssC may act in a similar manner as the sheath of contractile bacteriophage.

Early characterization of the T6SS has revealed that the AAA+ (ATPase associated with various cellular activities) family protein, ClpV, is essential for T6S function (25, 166). Due to its ATPase activity and its similarity to proteins involved in protein remodeling, it was hypothesized that ClpV was directly involved in energizing the translocation of effectors, through a threading mechanism. Several studies have indicated that ClpV may not be directly involved in substrate processing. Instead, these reports have found that ClpV binds directly to TssC and facilitates the

disassembly of TssB/TssC tubules (25, 166). Together, these findings suggest that ClpV initiates the recycling of TssB and TssC components following assembly and contraction of TssB/TssC tubules during T6S.

In addition to the T6S proteins with structural similarity to bacteriophage proteins, it has been noted that TssE shares sequence and structural homology with gp25, a component of the bacteriophage baseplate (142). Little is known about the remaining core T6S proteins, TssA, TssF, TssG and TssK. These proteins are required for a functional T6SS; however, they have not been ascribed a predicted role in this process due to the lack of known functional homologs and biochemical analysis

In comparison to the process of DNA ejection by bacteriophage, the mechanism of substrate secretion by the T6SSs is still poorly understood. Due to the shared features of T6SSs and bacteriophage tails, a bacteriophage-based model for the mechanism of T6S has emerged **(Figure 1.1)**. In this model, TssB and TssC form a sheath around an Hcp tube that is capped by VgrG. When the system is activated, the TssB/TssC sheath contracts, driving Hcp and VgrG out of the cell. This force may allow Hcp and VgrG to puncture the target cell and deliver effector molecules. One could also speculate that the membrane-spanning complex may play a role in tethering the bacteriophage-like assembly to the inner and outer membranes.

**Type VI secretion systems export functionally diverse effectors.**

While many studies have noted that the T6SS is implicated in various phenotypes, including virulence, host-cell interactions, conjugation or biofilm formation, the molecular basis for only a

limited number of these observed effects has been defined (7, 59, 76, 248). By studying the substrates of several T6SSs, it has become clear that these pathways have the capacity to mediate interactions with bacterial cells or eukaryotic cells through the delivery of effector proteins.

The first studies that identified a direct mechanism for the T6SS in virulence were performed in *V. cholerae* (154, 155, 192, 193). These studies reported that the T6SS of *V. cholerae*, the virulence-associated secretion (*vas*) system, translocates an effector with actin cross-linking activity directly into eukaryotic cells. Delivery of this effector is required for defense against amoebae predation, cytoxicity in macrophages and intestinal inflammation in infant mice. Notably, the gene encoding the actin-crosslinking effector is translationally fused to the C-terminus of a VgrG homolog, a core component of the T6SS. In this case, VgrG secretion, which possibly mediates host cell perforation, occurs simultaneously with effector translocation. Due to the fact that effector activity in *V. cholerae* is covalently linked to the T6S apparatus suggests that, in some cases, VgrG proteins can be bifunctional– acting as a structural component of the apparatus and as an effector with specific activity.

A VgrG homolog that contains a C-terminus with enzymatic activity is also found in *Aeromonas hydrophila* (230). The T6SS of *A. hydrophila* translocates a VgrG homolog fused to an ADP ribosyltransferase domain into mammalian cells where it induces toxicity through actin modification. Interestingly, further bioinformatic and experimental studies have indicated that only a small percentage of VgrG family proteins carry extended C-terminal domains, also referred to as “specialized” VgrGs (22, 62, 192). These VgrG proteins have a variety of predicted functions and include S-type pyocins, lipases, metalloproteases, peptidoglycan hydrolases and

chitosanases. Several instances have also been noted wherein Hcp homologs appear to carry extra domains with predicted antibacterial functions. For example, a predicted S-type pyocin protein of uropathogenic *Escherichia coli*, Usp, is fused to the C-terminus of an Hcp homolog (180). In many of these cases, the activity of specialized VgrG and Hcp proteins and their link to T6S remains to be experimentally tested.

The observation that the majority of VgrG and Hcp proteins lack C-terminal extensions was an early indication that other kinds of T6S effectors existed. The first independently encoded effectors were identified for the H1-T6SS of *P. aeruginosa*, termed Tse1-3 (type VI secretion exported 1-3) (113). Whereas *vgrG* and *hcp* genes are frequently encoded within T6S gene clusters, *tse1-3* are found scattered throughout the bacterial chromosome. The identificataion of Tse1-3 led to the breakthrough discovery that the H1-T6SS delivers these effectors into other bacterial cells in a contact-dependent manner. In this original study, delivery of one of these toxic substrates, Tse2, was shown to provide a growth fitness advantage against susceptible bacterial cells that were growing in close proximity (113). An immunity protein, Tsi2 (type VI secretion immunity 2), encoded adjacent to *tse2* on the bacterial chromosome directly inhibits Tse2 toxicity. It is now known that the other two effectors, Tse1 and Tse3, have peptidoglycan degrading activities, are specifically delivered into bacterial cells, and are also encoded in bicistrons adjacent to cognate immunity genes (204).

Following the initial findings in *P. aeruginosa*, bacterial targeting T6SSs have been identified in other species, including *V. cholerae, E. coli, B. thailandensis, Serratia marcescens, Acinetobacter baumannii* and *C. rodentium* (32, 39, 75, 97, 157, 216). The discovery of other

bacterial targeting T6SS has also been powered by the identification of a superfamily of type VI amidase effectors (Tae), which includes Tse1. This class of effectors was identified based on several shared characteristics: they are encoded in a bicistron adjacent to a gene predicted to encode a periplasmic localized immunity protein (Tai, Type VI secretion amidase immunity), they lack a signal sequence, they have a pI > 8, are less than 200 AA and contain a catalytic Cys. From the work by Russell et al., 2012, 51 *tae* genes were identified, which are broadly distributed among β-, δ-, and γ-proteobacteria. These findings demonstrate the abundance of Tae proteins and suggest that many T6SS have evolved antibacterial targeting capabilities.

In addition to the anti-eukaryotic activity of the *vas* T6SS of *V. cholerae*, this system possesses bacterial targeting capabilities. The bacterial targeting activities of *vas* are dependent on the secretion of a specialized VgrG containing a muramidase domain with peptidoglycan degrading activity. This finding suggests that this T6SS can be promiscuous with regard to targeting diverse cell types. Other examples of dual roles for T6SSs have not yet been reported, thus the generality of this observation remains uncertain.

More recently, a family of T6S effectors displaying phospholipase activity has been identified (69, 205). Similar to the anti-bacterial functions of Tse1-3 proteins, these newly identified effectors, termed Tle1-5 (type VI secretion lipase effector 1-5), are also encoded adjacent to cognate immunity genes (*tli1-5*, type VI secretion lipase immunity). Biochemical and *in vivo* characterization of several Tle proteins showed that they display antibacterial activity, specifically by targeting the bacterial membrane (205). Due to the conserved nature of phospholipids in eukaryotes and prokaryotes, it was hypothesized that T6SSs that export Tle

family effectors may have dual targeting capabilities. Indeed, Tle2 in *V. cholerae* provided a T6S-dependent fitness advantage against bacteria and amoeba (69). This capacity for interdomain targeting has raised interesting questions about the evolution of T6SSs.

**Regulation of type VI secretion activity** (Section from: Silverman J.M., Brunet, Y.R., Cascales E. and Mougous J.D. Structure and regulation of the type VI secretion system. 2012. *Annual Review of Microbiology*. 66:453-72.)

Even though our understanding of T6S function has grown considerably in recent years, its role in nature remains unclear. For instance, many bacteria of significant health concern possess one or more T6SSs; however, the pathogenic relevance of most of these systems is unknown. The majority of organisms with T6SSs are not pathogens and, instead, are found in marine environments, the rhizosphere, and soil, or they are associated with higher organisms as symbionts or commensals (18, 27). Defining the signals and conditions that control the expression and activation of T6S under the highly varied environments such bacteria occupy will be critical for revealing its role in these contexts. Below we provide examples of regulatory pathways and signals that modulate T6S expression. We discuss how environmental cues that influence these pathways might provide insights into the physiological function of the system. This review of T6S regulation is not comprehensive; therefore, we refer readers interested in further details to more exhaustive recent reviews (17, 146).

*Environmental Signals*

Recent findings have demonstrated various classes of regulators sensitive to environmental cues that specifically modulate the activity of the T6SS. Further defining the signals that stimulate T6SSs is essential for understanding the physiological context in which these systems act.

Iron.

The ferric-uptake regulator (Fur) protein is a key modulator of iron-dependent gene expression in bacteria (38). This regulator generally represses transcription through Fe(II)-dependent dimerization and subsequent DNA binding to a consensus sequence called the Fur box located within promoter regions. Transcriptional activation and iron-independent regulation by Fur also occur (36, 100). In addition to its important role in regulating iron acquisition and homeostasis, Fur regulates genes and processes that are not directly involved in iron metabolism. Some examples of these include toxins, adhesins, motility, and resistance to reactive oxygen species (34, 36, 38, 103, 197).

Expression of T6S in two opportunistic enteric pathogens, *E. tarda* and EAEC, is repressed directly at the transcriptional level by Fur **(Figure 1.2)** (31, 45). *E. tarda* is primarily a pathogen of fish; however, consumption of contaminated seafood can lead to gastroenteritis in humans (210). Infection models suggest that T6S plays an important role in the virulence of *E. tarda* and its close relative, *Edwardsiella ictaluri*, against fish (164, 202, 258). Deletion of genes encoding core components of the *E. tarda* Evp (*E. tarda* virulence proteins) T6SS, or insertional disruption of a gene encoding a putative effector of this system, *evpP*, attenuated the organism approximately 100-fold in blue gourami.

Fur-dependent regulation of the Evp T6SS was recently demonstrated by Mok and colleagues (45). Their work showed that Fur confers iron-dependent repression of production and export of an Hcp homolog (EvpC) and that the Fur protein binds directly to a Fur box sequence upstream of *evpP*, the first gene in the evp cluster. Fur-based repression of the *evp* genes is consistent with the contribution of the system to pathogenesis, as Fur repression would likely be alleviated inside iron-depleted host tissues.

EAEC is an emerging enteric pathogen characterized by its propensity to self-adhere and form biofilms on the intestinal mucosa (174). Infections with EAEC result in diarrhea and can be acute or chronic in nature; it is currently the second most common cause of diarrhea in persons traveling to developing countries (101, 234). The Sci-1 T6SS of EAEC is required for biofilm formation and is regulated by iron availability through a pathway involving DNA adenine methyltransferase (Dam)-catalyzed methylation and Fur repression (31). Two Fur boxes and three Dam methylation sites are present upstream of the Sci-1 gene cluster. Interestingly, one of the Fur-binding sites overlaps with a Dam methylation site, and Fur binding prohibits methylase access to the site. In the absence of iron, Fur dissociates and allows RNA polymerase to bind and initiate transcription. Similarly, the loss of Fur also permits methylation at the site, which inhibits the reassociation of Fur. Thus, low cytoplasmic Fe(II) yields stable on-state expression of the Sci-1 T6SS. It is not currently understood how *sci-1* expression is returned to the off-state, as the binding of Fur to hemimethylated sequences that would be generated following DNA replication was not investigated (31).

The physiological consequences of *sci-1* regulation by Fur are not yet known and depend on the abundance and form of iron present in a given environment. The anaerobic environment of the intestinal lumen favors the ferrous [Fe(II)] form of the ion. In support of this, studies of Salmonella have shown that genes under control of Fur remain repressed prior to tissue invasion (116, 122). Furthermore, *Salmonella* pathogenicity island I, which encodes a T3SS required for Salmonella invasion, is activated by iron-bound Fur (74). Extending these findings to EAEC Sci-1 suggests that the T6SS may remain repressed by Fur in vivo. This is congruent with studies demonstrating that T6S does not contribute to the virulence of EAEC in animal infection models (7, 71). However, an important consideration when interpreting these data is that the animal models employed are unlikely to accurately recapitulate chronic EAEC infection. It is conceivable that ferrous iron becomes depleted within stable intestinal biofilm communities of EAEC, thereby leading to Sci-1 T6SS activation. Sci-1 activation mediated by Fur depression is likely to occur in an environmental context, where its role in promoting adhesion could be exploited as an adaptation to oxidative stress or iron starvation (7, 63).

σ54-dependent activators.

Sigma factor 54 (σ54)-dependent activator proteins, also termed bacterial enhancer-binding proteins (bEBPs), are a diverse group of proteins that mediate the translation of environmental signals to changes in gene expression in bacteria (196). bEBPs regulate gene expression by catalyzing the closed-to-open transition of σ54-RNAP holoenzyme transcription complexes. This activity is ATP-dependent and, as described below, can be regulated by signal binding and phosphorylation. bEBPs are generally composed of three domains: an N-terminal regulatory domain, an internal AAA+-family ATPase domain, and a C-terminal DNA-binding domain that

typically mediates sequence-specific interactions with activator sequences 100 to 200 nucleotides upstream of the promoter (214). The N-terminal activation domain and the C-terminal DNA-binding domain are highly variable among bEBP homologs (221). This low conservation is partly responsible for the diversity of signals bEBP homologs detect and the distinct DNA sequences they bind.

A broad range of cellular processes, including nitrogen assimilation, motility, and virulence, are regulated by bEBPs (221). This class of proteins also serves a general role in the regulation of T6S (**Figure 1.2**). Bioinformatic analyses identified bEBPs encoded within phylogenetically diverse T6S gene clusters (16, 27). These analyses have further revealed probable σ54-binding sequences within the respective T6S promoter regions (16). A subset of T6S-associated bEBPs, including representatives from *V. cholerae*, *A. hydrophila*, *Pectobacterium atrosepticum*, and *Marinomonas spp*., were investigated using in vitro binding experiments and reconstituted transcriptional reporter assays. These studies confirmed the predicted role of the proteins in σ54-dependent transcriptional activation of T6S promoters.

The bEBP encoded within the virulence-associated secretion (*vas*) gene cluster, VasH, is a key regulator of *V. cholerae* T6S (129, 193). Reflecting its important regulatory role, T6S-dependent defense against *Dictyostelium discoideum* and killing of *E. coli* in this organism require VasH (157, 192). An analysis of *vasH* homologs in 26 *V. cholerae* strains identified an enrichment of nonsynonymous single nucleotide polymorphisms in the N-terminal regulatory domain (129). Amino acid changes within this domain could provide a mechanism for variable T6S expression response profiles within *V. cholerae* strains exposed to environmental signals. Interestingly, N-

terminal domains of bEBPs can act as intramolecular activators or repressors (254). In *V. cholerae* V52, this domain appears to be a positive regulator, as vas T6S expression was decreased by an N-terminally truncated VasH allele (129). Notably, polymorphisms in *vasH* do not appear to underlie the significant differences in vas expression and activation observed between non-O1/non-O139 strains (e.g., V52) and pandemic disease strains (e.g., N16961, C6706, and A1552). Instead, this variability is explained likely by differences in the strength of repression through quorum-based signaling and by the novel regulator TsrA (type VI secretion system regulator A) (119, 259).

The activity of bEBPs can be regulated by specific phosphorylation events catalyzed by sensor histidine kinases and low-molecular-weight phosphodonors (161, 221). An example is the well-characterized bEBP NtrC (nitrogen regulatory protein C), which is activated through phosphorylation by NtrB (249). In addition, NtrC efficiently autophosphorylates in vitro in the presence of acetyl phosphate, and evidence suggests that acetyl phosphate is also relevant to its signaling properties in vivo (82). A sensor kinase that acts on T6S bEBPs has not been identified; however, these proteins autophosphorylate in vitro in the presence of acetyl phosphate (16). This finding suggests that upstream events such as environmental sampling by sensor kinases or changes in metabolism leading to the accumulation of low-molecular-weight phosphodonors could have a significant impact on σ54-dependent T6S expression.

Surface association. Surface association can promote dramatic changes to bacterial cell physiology. An analysis of global gene expression changes in *Salmonella* Typhimurium demonstrated that one-third of its genes ahow altered expression during surface-growth

conditions (246). Such changes may be caused by signaling systems that directly detect surfaces or that respond to concomitant alterations in the local environment. Cells adhered to surfaces can develop into sessile communities, sometimes referred to as biofilms, in which long-term cell-cell contact is enhanced relative to planktonic cells (55). According to the current understanding of T6S-mediated effects, these conditions are favorable to its contact-dependent mechanism of effector delivery.

The H1-T6SS of *P. aeruginosa* is posttranslationally activated by a threonine phosphorylation pathway (TPP) in response to surface growth of the organism (222) (**Figure 1.2**). Components of this pathway include PpkA, an inner-membrane-spanning serine/threonine kinase, and Fha1, a forkhead-associated domain-containing protein that is activated by PpkA via phosphorylation (115, 167). Activated Fha1 promotes H1-T6S-apparatus assembly and effector secretion. Unlike planktonically grown *P. aeruginosa*, strains placed on an agar surface for 4 h assemble an activated apparatus and contain elevated levels of phosphorylated Fha1 (222). Genetic analysis of the requirements for competitive fitness mediated by the H1-T6SS further established the role of the TPP in surface-dependent H1-T6SS activation and ruled out the involvement of a second phosphorylation-independent pathway. Surface activation of T6S by the TPP may be a general phenomenon, as components of the pathway are found in approximately 30% of identified T6S gene clusters (27).

Though the mechanism(s) is not yet clear, sessile growth may also serve as a cue for regulatory changes that elevate T6S expression. Recent findings demonstrated that cellular levels of TssC1, an H1-T6S component, are elevated in a biofilm compared with planktonically grown cells

(256). Consistent with this observation, the protein Hcp is abundant in *P. aeruginosa* biofilms (209).

*Bacteria-Derived Signals*

Often functioning as a cell contact-dependent bacterial interaction pathway, it is not surprising that the sensing of other bacteria plays an important role in modulating T6S activity. Here we describe several examples of bacteria-derived signals that influence T6S expression.

The Gac/Rsm pathway. The Gac/Rsm signaling pathway couples extracellular bacteria-derived signals with marked changes in target mRNA translation (137). The pathway is initiated by the GacS/GacA two-component system, which upon stimulation leads to elevated expression of one or more small regulatory RNA (sRNA) molecules, variably termed *rsmY* and *rsmZ*. These sRNA molecules interact with and sequester an mRNA-binding protein known as RsmA or CsrA. This protein generally acts as an inhibitor of translation by associating with sequences near or overlapping the ribosome-binding site. Thus, sRNA expression typically facilitates increased translation of specific mRNA targets. In some cases, mRNA binding by RsmA/CsrA can activate translation; however, the mechanism is less clear in these instances.

In the pseudomonads, the Gac/Rsm pathway is a key regulator of many important processes, including biocontrol and virulence factor production, cellular aggregation, and quorum sensing (95). Studies have revealed that *P. aeruginosa*, *P. fluorescens*, and *P. syringae* also use this pathway to regulate the expression of T6S (102, 166, 199) (**Figure 1.2**). This was first noted in *P. aeruginosa*, wherein microarray analyses of strains lacking *retS* or *ladS*, which encode a

repressor and activator of GacA/S signaling, respectively, strongly implicated RsmA in the stability of HSI-I transcripts (96, 242). Later functional analyses demonstrated that assembly, activation, and effector secretion and targeting by the H1-T6SS are stimulated in the Δ*retS* background (113, 166, 167). The most definitive evidence for the involvement of the Gac/Rsm pathway in HSI-I regulation is found in recent work by Brencic & Lory (28), which demonstrates direct RsmA binding to the 5' leader sequence of two HSI-I transcripts.

The incorporation of the H1-T6SS into the global regulon of the *P. aeruginosa* Gac/Rsm pathway has yielded valuable insights into the settings relevant to its function. In *P. aeruginosa*, the Gac/Rsm pathway directly or indirectly regulates the expression of approximately 500 genes (29, 96). Within this expansive set, researchers have noted reciprocal regulation of factors associated with planktonic and sessile growth—leading to the hypothesis that the Gac/Rsm pathway coordinates this physiological transition of the organism (255). In the Gac/Rsm regulon, H1-T6SS expression occurs coincident with factors having experimentally demonstrable roles in sessile community formation, such as two aggregation and adhesion-promoting exopolysaccharides, Pel and Psl. This early regulatory link implied that T6SS activity is relevant to closely interfacing bacteria; however, in what capacity remained unknown. This question has been answered—at least in part—by more recent studies demonstrating the role of the H1-T6SS in contact-dependent interbacterial interactions and the involvement of the system in biofilm-specific antibiotic resistance (113, 204, 256). Notably, the Gac/Rsm pathway of *P. protegens*, which is closely related to that of *P. aeruginosa*, responds to signals generated by other pseudomonads and certain *Vibrio spp*. (70).

Quorum Sensing. Quorum sensing (QS) is a bacterial regulatory mechanism that modulates gene expression based on concentrations of self-produced signals (90, 176). A quorum is sensed by the accumulation of diffusible signaling molecules, which are themselves typically under quorum control. Regulation of quorum-controlled genes is achieved either by direct or indirect effects that signal molecules impart on the DNA-binding properties of dedicated regulatory proteins. A prevailing model is that quorum sensing regulates social behavior of bacteria, both within and between species (181). One piece of evidence in support of this model is that secreted products are disproportionally abundant in the quorum regulon of many species (107). Given this, it is not surprising that many instances of quorum-sensing-regulated T6SSs have arisen in the literature (94, 118, 128, 145, 150, 257, 259).

In *V. cholerae*, two chemically distinct QS systems, autoinducer-2 (AI-2) and cholera autoinducer-1 (CAI-1), collaborate to influence density-dependent gene expression (176) (**Figure 1.2**). Signal molecules from these pathways are detected by two sensor kinases, LuxQ and CqsS, respectively. The pathways converge on the phosphotransfer protein LuxU, which acts on LuxO, a DNA-binding response regulator protein. Phosphorylated LuxO activates the expression of four sRNA molecules (qrr1–4) that in turn repress the production of HapR, a TetR-family global transcriptional regulator.

The majority of studies on *V. cholerae* T6S have been conducted in the serotype O37 strain V52. The V52 strain is a valuable model for studying T6S within the species, as Hcp and VgrG proteins are abundantly exported from the strain, its vas genes are highly expressed, and it exhibits strong Vas-dependent phenotypes against prokaryotic and eukaryotic cells (157, 192,

193). However, under similar in vitro conditions, most strains of *V. cholerae*, including O1 and O139 pandemic strains, display markedly lower vas expression and as a result do not exhibit Vas-dependent phenotypes (118, 119, 259).

Recent studies have suggested that differences in direct QS-dependent expression of vas genes are partially responsible for T6S variability in *V. cholerae*. Ishikawa et al. (118) observed a striking correlation between HapR and Hcp expression among a panel of O1 isolates. Furthermore, a deletion of luxO was shown to strongly induce vas expression in two serotype O1 strains, A1552 and C6707 (118, 259). Consistent with current models of QS circuitry in *V. cholerae*, activation of vas expression in Δ*luxO* required *hapR* and Δ*hfq* recapitulated the effects of the *luxO* deletion.

Despite robust vas expression in O1 strains lacking *luxO*, the secretion system can remain functionally quiescent in this background (259). Thus, levels of HapR do not fully reconcile T6S-related phenotypic differences observed between *V. cholerae* strains. Briefly, complete activation of T6S in pandemic *V. cholerae* strains appears to involve additional factors such as high osmolarity, low temperature, and relief of repression imposed on the system by the TsrA protein (119, 259).

The adaptive role of quorum control over T6S remains to be elucidated. In addition to its role in intraspecies sensing, QS might play a role in perceiving cells of other species (80). This seems particularly probable for the AI-2 pathway, as the dedicated signal synthase involved in AI-2 synthesis, LuxS, is widely conserved. Therefore, AI-2 signal levels could serve as a cue for *V.*

*cholerae* to activate antibacterial defenses, such as its T6SS, in response to potential competitors. If the signal was self-derived, coregulated immunity proteins might ameliorate the detrimental consequences of self-targeting (204).

Not all T6SSs regulated by QS are induced at high cell densities. For example, in *P. aeruginosa* the H1-T6SS is repressed at high cell densities by a direct or indirect mechanism involving LasR, an acyl homoserine lactone-type quorum regulator (145). Interestingly, the two other T6SSs of *P. aeruginosa* are regulated reciprocally with the H1-T6SS by quorum sensing. The two T6SSs of *Vibrio parahaemolyticus* also display reciprocal regulation by quorum sensing (94). Differential regulation of T6S by QS, particularly those cases wherein this occurs within one bacterium, suggests that the system can act in a wide range of contexts and underscores its functional versatility.

**Effector recognition mechanisms of Gram-negative specialized secretory pathways.**

Due to the vast number of proteins present in the bacterial cytoplasm, efficient substrate recognition is a key process for all secretory systems. Similar aspects of substrate selectivity often exist among secretory systems. A recurring theme in substrate recognition is the presence of a receptor protein associated with the secretory apparatus and a signal sequence or motif that is localized to a distinct region on protein substrates. In addition, secretion system-associated chaperones, which bind substrates prior to their interaction with the apparatus, are commonly required for recognition and specificity.

Effector recognition mechanisms have been studies in great detail for T3SSs. An N-terminal signal sequence of 20-30 AAs in length is sufficient for T3S export and permits secretion of hybrid reporters (139, 226). In *S. enterica*, this sequence interacts directly with the T3S-specific ATPase, InvC, which energizes effector translocation through the apparatus (3). Many effectors also require a T3S chaperone for efficient delivery to the ATPase. These effectors interact with cognate T3S-chaperones via a sequence ranging in length of 60-100 AAs, located downstream of the N-terminal signal sequence (19, 188, 227). Chaperones facilitate partial unfolding of effectors, which promote recognition by the ATPase (3). Prior to export, the chaperone-effector complex is disrupted via ATPase activity and, subsequently, the effector is threaded through the T3S apparatus in an ATP-dependent manner. Although T3S chaperones are variable at the amino acid sequence level, most T3S chaperones are small, acidic and dimeric proteins and are stucturally similar (228).

For many effectors secreted through the T4ASS and T4BSS, a cluster of residues at the C-terminus is required (172, 243). The sequence motif varies between organisms and classes of T4SSs; key residues are either positively charged or hydrophobic and may be clustered together or split into two regions along the length of the substrate (213). An essential component involved in T4SS is the T4 coupling protein (T4CP), an ATPase that is anchored at the inner membrane and interacts with the T4S apparatus. Effector recognition has been well characterized for the T4ASS of *A. tumefaciens* (6). In this case, the T4CP recognizes effectors through the signal sequence and provides the energy for effector translocation through the system. DotL is an ATPase of the *L. pneumophilia* T4BSS that is thought to act analogously to the T4CP of *A. tumefaciens*. Several lines of evidence also suggest that IcmS and IcmW, which form a stable

complex and are required for T4BSS function, may be involved in substrate recongition (232). However, a direct function for the IcmS/IcmW complex has not been determined.

In comparison to our knowledge of T3SS and T4SS substrate recognition mechanism, little is known about effector export by the T6SS. While only recently discovered, no reports regarding a possible signal sequence or motif have been made. This thesis work has made advancements towards understanding this process of effector recognition in T6SSs.

**The H1-T6SS of *Pseudomonas aeruginosa.***

*P. aeruginosa* is a Gram-negative γ-proteobacterium that is capable of persisting in a broad range of environments, including in soil, water and in close association with animals. The metabolic versatility of *P. aeruginosa* is one of its outstanding characteristics, allowing it to thrive in the presence of various carbon sources, under nutrient limiting conditions and both in both anoxic and aerobic habitats (177, 229). *P. aeruginosa* is also equipped with numerous genetically encoded pathways that mediate interactions with other organisms in the environment. These pathways contribute significantly to the remarkable success and adaptability of this bacterium. *P. aeruginosa* is also an opportunistic human pathogen that causes infections in immunocompromised individuals, including patients with diabetes, cystic fibrosis (CF) or burn wounds. These infections can become problematic, as *P. aeruginosa* is intrinsically resistant to many antibiotics.

Approximately 80% of CF patients become chronically infected with *P. aeruginosa* by adulthood (171). Due to the strong association between CF patients and *P. aeruginosa*, the pathogenesis of this organism has become a central focus of research. Long-term studies of *P.*

*aeruginosa* populations isolated from the cystic fibrosis lung have revealed that a significant amount of genetic diversification occurs (225). Several mutations in known *P. aeruginosa* biological processes are frequently identified and appear to be enriched over the lifetime of chronically infected cystic fibrosis patient (58). Mutations causing loss of swimming motility, decreased in T3SS expression, increased in T6SS expression, enchanced antibiotic resistance, misregulated quorum sensing and alterations in surface molecules are frequently isolated. Acquisition of these mutations is thought to contribute to the successful adaptation of *P. aeruginosa* in the human host. A growing number of studies have focused on characterizing the metabolic pathways and bacterial processes that are activated or repressed over the course of chronic infection.

Several pieces of evidence have implicated the H1-T6SS in CF. For example, a signature tagged mutagenesis (STM) screen performed with a pool of *P. aeruginosa* mutants that were inoculated in the lungs of rats, a model for chronic infection, found that mutations in various HSI-I genes caused a loss in fitness (190). Additionally, a secreted component of the H1-T6SS apparatus, Hcp1, can be readily detected in sputum of CF patients, suggesting the system may be active under these conditions (166). Although the role of the H1-T6SS in chronic infection has not been determined, the fact that lung infections of CF patients is often polymicrobial has led to the hypothesis that *P. aeruginosa* may use the H1-T6SS to outcompete other organisms and alter the outcome of chronic infection. Interestingly, many of the organisms isolated from the lungs of CF patients harbor at least one T6SS. The prevalence of these systems in Gram-negative bacteria that frequently colonize the CF lung further suggest a possible role for these systems in

polymicrobial environments and could have a significant impact on the outcome of these infections.

**Objectives of this thesis.**

Over the past 10 years, several studies have underscored the importance of the T6SS in bacterial interactions with other organisms. However, many questions remain pertaining to the physiological significance and the molecular underpinnings of the T6SS. The goal of this thesis was to 1) characterize the factors that regulate T6S activity and to 2) further our understanding of effector recognition and export by the T6S apparatus. The H1-T6SS of *P. aeruginosa* was used as a model system for these studies, as it is genetically tractable and its T6SS has been relatively well characterized. The findings generated from this work have contributed to the rapidly expanding field of T6S.

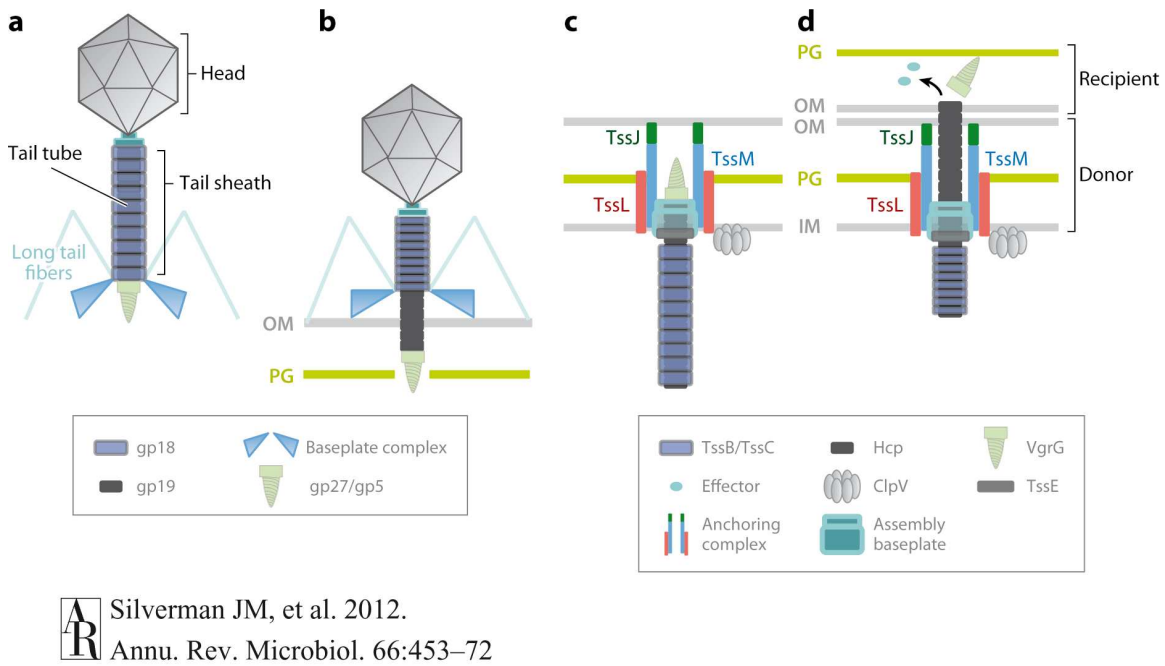


Silverman JM, et al. 2012.
Annu. Rev. Microbiol. 66:453–72

**Figure 1.1**: **Schematic representation comparing proposed models of bacteriophage T4 and the T6S apparatus.** Homologs and analogs of T6S are colored the same as their T4 phage counterparts. (*a*) The bacteriophage T4 tail tube is surrounded by the tail sheath and terminated by the cell-puncturing device (gp27/gp5). (*b*) Upon host cell binding, the bacteriophage T4 baseplate undergoes a conformational change that triggers tail sheath contraction and results in puncturing of the outer membrane (OM) and DNA delivery. Models of (*c*) inactivated and (*d*) activated states of T6S based on protein localization and interactions between T6S subunits. The three membrane-associated proteins TssL, TssM, and TssJ form a complex bound to the peptidoglycan (PG) layer via TssL. The T6S appendix formed by an Hcp tube and a VgrG trimer is thought to be anchored at the cell envelope by the membrane-associated complex. It has been hypothesized that an assembly baseplate can participate in T6S appendix assembly. (*c*) TssB and TssC may form a sheath-like structure enclosing the Hcp tube within the periplasmic space. (*d*) Activation of the T6SS results in effector delivery to a target cell through the Hcp tube. By analogy with bacteriophage T4, the sheath-like structure could propel, through contraction, the Hcp tube toward the cell exterior or directly to the target cell.

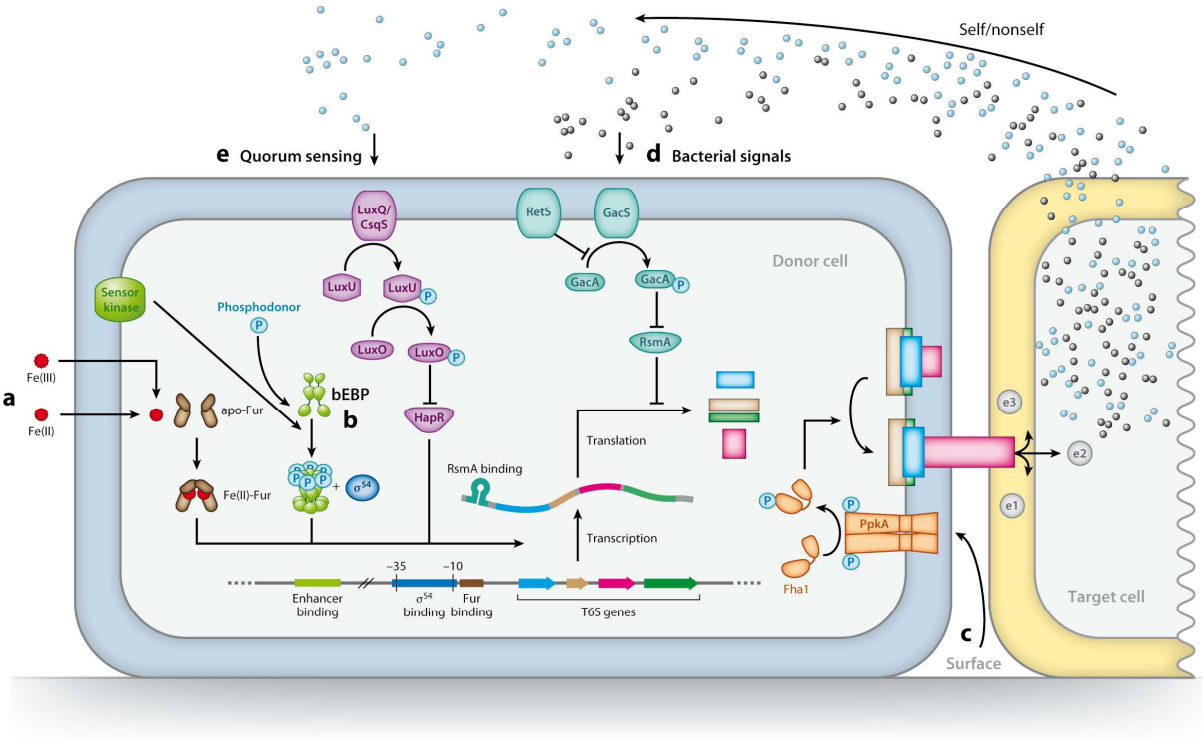


Silverman JM, et al. 2012.
Annu. Rev. Microbiol. 66:453–72

**Figure 1.2: Schematic representation of the diverse regulatory systems that modulate T6S expression and activation in assorted bacteria.** Only those regulatory pathways emphasized in this review are depicted. Pathways are labeled *a–e* corresponding to the order of their presentation in the text. (*a*) Fur represses T6S transcription in the presence of iron. (*b*) bEBPs function in conjunction with $\sigma^{54}$ to activate T6S transcription. (*c*) The TPP posttranslationally activates T6S in response to surface association. Self- and nonself-derived bacterial signals modulate T6S (*d*) posttranscriptionally through the Gac/Rsm pathway or (*e*) transcriptionally via quorum sensing. At right is a target bacterium undergoing intoxication by Tse1–3 effectors (e1–3).

# CHAPTER II:

## Separate inputs modulate phosphorylation-dependent and -independent type VI secretion activation

Published as: Silverman J.M., Austin L.S., Hsu F., Hicks K.G., Hood R.D., and Mougous J.D. 2011. *Molecular Microbiology.* 82(5), 1277-1290.

**ABSTRACT**

Productive intercellular delivery of cargo by secretory systems requires exquisite temporal and spatial choreography. Our laboratory has demonstrated that the H1-T6SS of *P. aeruginosa* transfers effector proteins to other bacterial cells. The activity of these effectors requires cell contact-dependent delivery by the secretion apparatus, and thus their export is highly repressed under planktonic growth conditions. Here we define regulatory pathways that orchestrate efficient secretion by this system. We identified a T6S-associated protein, TagF, as a posttranslational repressor of the H1-T6SS. Strains activated by TagF derepression or stimulation of a previously identified threonine phosphorylation pathway (TPP) share the property of secretory ATPase recruitment to the T6S apparatus, yet display different effector output levels and genetic requirements for their export. We also found that the pathways respond to distinct stimuli; we identified surface growth as a physiological cue that activates the H1-T6SS exclusively through the TPP. Coordination of posttranslational triggering with cell contact-promoting growth conditions provides a mechanism for the T6SS to avoid wasteful release of effectors.

**INTRODUCTION**

In Gram-negative bacteria six secretion systems (types I-VI) have been identified, with specialized functions ranging from general cellular maintenance and physiology to host and bacterial cell interactions (72). The T6SS is found broadly among the Proteobacteria, including many important environmental and human-associated taxa (215). These systems are encoded by gene clusters composed of 13 conserved genes, *tss*, and additional accessory genes, *tag*, that vary in number and content (27). Core components of the T6SS include ClpV, a AAA+ family

ATPase, TssM, a homolog of the type IV secretion protein IcmF, and VgrG and Hcp, two extracellular structural proteins (9, 18, 41). Interestingly, several conserved components of the T6SS share sequence and structural similarity to bacteriophage tail and baseplate proteins (125, 142, 166, 184). Based on this relatedness, the system has been proposed to function as an outward facing puncturing device at the surface of the cell.

The T6SS has been implicated in diverse processes including host-cell interactions (154, 218), biofilm formation (7), and gene regulation (123, 248). Recent studies indicate that the T6SS plays a critical role in interbacterial interactions (215). This was first reported in *P. aeruginosa*, where it was observed that H1-T6SS-dependent export of a toxin, Tse2, can provide a fitness advantage to the organism when cultivated in direct contact with another *P. aeruginosa* strain lacking a Tse2-specific immunity protein, Tsi2 (113). Antibacterial activity has also been attributed to T6SSs of *B. thailandensis* (T6SS-1), *S. marcescens* and *V. cholerae* (Vas), however in these instances the effector proteins involved have not been identified (157, 170, 216).

Like other specialized secretion systems, expression of T6S and export of its effectors are stringently regulated (17). For the H1-T6SS of *P. aeruginosa*, regulation at the transcriptional, posttranscriptional, and posttranslational levels has been studied. The system is transcriptionally repressed by the quorum sensing regulator, LasR (145). The binding of LasR to HSI-I promoters has not been shown, leaving the mechanism of repression unknown. Regulation of the H1-T6SS at the posttranscriptional level is governed by the RNA-binding protein RsmA (28, 96). The Rsm pathway appears to coordinate reciprocal regulation of factors important for planktonic and sessile modes of *P. aeruginosa* growth (29, 33, 96, 255). Consistent with the requirement for

long-term cell contact in T6S-dependent effector delivery between cells, the system was found to be co-regulated by RsmA with factors required for adhesion between cells and to surfaces (28, 96, 166, 242). Furthermore, studies have found *P. aeruginosa* T6S proteins abundantly produced in biofilms relative to planktonic culture (209, 256).

Our laboratory has found that the H1-T6SS is posttranslationally triggered by a TPP (134, 167). Stimulation of the TPP results in export of extracellular structural components of the apparatus, including Hcp1, VgrG1, VgrG4, and substrates, including Tse1-3 (113). At least four proteins, TagR, PpkA, PppA and Fha1, all encoded within HSI-I, participate in the TPP. According to our current model, the H1-T6SS becomes activated by dimerization of PpkA, a membrane-spanning Hanks-type serine/threonine kinase. The environmental cue responsible for inducing PpkA dimerization is unknown; however, TagR, a periplasmic protein, functions upstream of PpkA and promotes activation of the kinase (115). Dimerization of PpkA leads to autophosphorylation, which recruits Fha1 through interactions between the phosphorylated activation loop of the kinase and the Forkhead-associated (FHA) domain of Fha1. Fha1 associated with activated PpkA is phosphorylated by the kinase at Thr362 (*p*-Fha1), in turn promoting H1-T6SS activation by an unknown mechanism (167). Fha1 resides in a complex with ClpV1, suggesting the possibility that recruitment of the ATPase to the apparatus could underlie activation. A PP2C family protein phosphatase, PppA, acts as an antagonist of the TPP by dephosphorylating Fha1, and, possibly, PpkA. Deletion of *pppA* results in constitutive secretion of Hcp1, VgrG1, VgrG4, and Tse1-3.

The genes encoding known TPP components are found in a putative HSI-I operon that also contains four conserved T6S genes (*tssJ1, K1, L1, M1*) and four uncharacterized *tag* genes (*tagQ, S, T, F*) **(Figure 2.1A)**. Sequence analysis of the *tag* genes indicates that *tagS* and *tagT* encode proteins with homology to lipoprotein transport and sorting components, LolE and LolD, respectively (173). The *tagQ* gene encodes a predicted outer membrane lipoprotein, and *tagF*, a predicted cytoplasmic protein with unknown function.

In this study, we sought to define additional regulatory elements of the H1-T6SS. Based on the proximity of *tagQ, S, T,* and *F* to genes encoding known posttranslational regulators of the system, and their variability amongst other T6SSs, we hypothesized that these genes also encode H1-T6SS regulators. In the course of this search, we identified TagF as a posttranslational regulatory protein that represses the activation of the H1-T6SS by a mechanism distinct from the TPP. Inactivation of *tagF* triggers Hcp1 secretion to levels observed in Δ*pppA*, however effector secretion is dampened in Δ*tagF* relative to a strain lacking *pppA*. Also, TagF regulates the activity of the H1-T6SS in a manner that does not require *p*-Fha1, PpkA, or other Tag proteins. Despite these differences, both the TPP and TagF-mediated activation pathways require Fha1 and recruit ClpV1 to the secretion apparatus. We also investigated the physiological significance of posttranslational regulation of the H1-T6SS. Interestingly, we discovered that the H1-T6SS is activated when *P. aeruginosa* is grown on a surface. This occurs via the TPP, as it requires PpkA and involves increased *p*-Fha1 levels.

## RESULTS

**H1-T6SS activity is negatively regulated by TagF.** In the course of our efforts to define the function of HSI-I genes, we noted that the putative HSI-I operon encoding PpkA, PppA, Fha1 and TagR, which constitute all known components of the TPP, also encodes additional non-conserved Tag proteins (TagQ, PA0070; TagS, PA0072; TagT, PA0073; TagF, PA0076) **(Figure 2.1A)**. Based on their genomic context and lack of conservation in other T6SSs (27), we hypothesized that these genes also encode regulators of the H1-T6SS. To ascertain their role in regulating H1-T6SS activity, we introduced individual in-frame deletions of *tagQ, S, T,* and *F* into *P. aeruginosa hcp1–V,* and monitored the effect on Hcp1 secretion. This strain contains a chromosomal fusion of *hcp1* to the vesicular stomatitis virus G protein (VSV-G) epitope tag (*hcp1–V*) (166). We also introduced deletions with known effects on Hcp1 secretion (Δ*tagR,* Δ*ppkA,* Δ*pppA,* or Δ*tssM1*) into this genetic background as controls (115, 166, 167). Consistent with earlier findings, Δ*pppA* displayed high levels of Hcp1 secretion, whereas secretion from Δ*tagR,* Δ*ppkA,* and Δ*tssM1* did not exceed the wild-type **(Figure 2.1B)**. Interestingly, Hcp1 secretion from Δ*tagF* was increased relative to the wild-type strain. Deletions in *tagQ, S,* and *T* did not induce Hcp1 export, and none of the mutations significantly influenced cellular Hcp1 levels.

Hcp1 is considered a structural component of the T6SS; therefore, secretion of the protein is not necessarily indicative of an activated system. As an additional measure of H1-T6SS activation, we probed the effects of the same panel of deletions on the secretion of Tse1, a previously identified effector protein (113). While we observed reproducibly lower levels of secreted Tse1 from Δ*tagF* than from Δ*pppA* (discussed below), the strains showed a similar trend as that observed for Hcp1 secretion, suggesting that a *tagF* deletion results in constitutive activation of

the H1-T6SS **(Figure 2.1C)**. Based on these data, we sought to further define the role of *tagF* in T6S regulation.

**TagF posttranslationally represses the H1-T6SS.** The *tagF* open reading frame is located immediately upstream of *pppA* in the genome of *P. aeruginosa* **(Figure 2.1A)**. To verify that the secretion phenotype of Δ*tagF* is not due to polar effects on *pppA* or other downstream genes, we genetically complemented the strain using an ectopic expression plasmid. Western blot analyses demonstrated that *tagF* expression returns secretion of Hcp1 and Tse1 to parental levels in the Δ*tagF* background **(Figure 2.2A)**. We further confirmed that Hcp1 and Tse1 export in Δ*tagF* occurs in a T6S-dependent manner. The addition of a *clpV1* deletion to Δ*tagF* abrogated secretion of Hcp1 and Tse1 (25, 166). Secretion of both proteins was restored by genetic complementation of the *clpV1* gene **(Figure 2.2B)**.

Possible explanations for the influence of TagF on Hcp1 and Tse1 export by the H1-T6SS apparatus include changes in the expression levels of these proteins, translational or transcriptional induction of the secretion apparatus as a whole, and posttranslational activation of the secretory apparatus. Overall levels of Hcp1 and Tse1 were unaltered in Δ*tagF* **(Figure 2.1B and 2.1C)**, suggesting that increased expression of these proteins does not underlie the secretion phenotype observed. To investigate whether TagF imparts a general influence on T6S expression levels, we employed translational *lacZ* fusion reporters to the *fha1* and *tssA1* genes, which are located immediately downstream of previously identified HSI-I promoters (28). Inactivation of *tagF* did not influence the activities of these reporters; however, as described previously, both were strongly induced in a strain lacking a repressor of the Rsm pathway (RetS) **(Figure 2.2C**

**and 2.2D)** (28). From these data we conclude that TagF represses activation of the H1-T6SS on a posttranslational level.

**TagF mediates activation of the H1-T6SS independently of *p*-Fha1.** Next we considered whether TagF regulates the H1-T6SS via the TPP or independently of this pathway. Several lines of evidence suggest that TagF acts through the TPP. *TagF* orthologs are not located outside of T6S gene clusters, and within these clusters the gene is often found in a subgroup of locally syntenic genes that also includes orthologs of *ppkA* and *pppA* **(Figure 2.3)**. Furthermore, in several instances, including the T6S gene clusters of *A. tumefaciens, Nitrococcus mobilis* and *R. leguminosarum*, *tagF* and *pppA* orthologs appear fused, thereby generating one open reading frame with apparent dual function **(Figure 2.3)**. Such fusion events are enriched among genes encoding interacting proteins or proteins participating in common pathways (77, 224). However, there is also strong genomic-based evidence arguing against TagF participation in the TPP. Most notably, *tagF* orthologs are sometimes present in T6S clusters lacking TPP components, including *fha1* **(Figure 2.3)**.

Previous reports have shown that elevated levels of *p*-Fha1 lead to posttranslational activation of the H1-T6SS. Therefore, we postulated that if TagF directs activation of the H1-T6SS through the TPP, *p*-Fha1 levels might be elevated in a Δ*tagF* strain. To test this, we took advantage of an established SDS-PAGE mobility-based assay for monitoring *p*-Fha1 levels in *P. aeruginosa* (167). Our analyses indicate that unlike Δ*pppA*, the Δ*tagF* strain does not possess *p*-Fha1 levels above those of the parental strain **(Figure 2.4A)**.

Based on our finding that *p*-Fha1 levels are unaffected by *tagF* deletion, we tested the hypothesis that TagF acts independently of the TPP, and thus, *p*-Fha1 should be dispensable in Δ*tagF*. We observed that *fha1* deletion in the Δ*tagF* background inactivates the H1-T6SS as judged by Hcp1 secretion **(Figure 2.4B)**. This implies either that Fha1 must be phosphorylated at a basal level for TagF-mediated activation or that it functions in an important capacity independent of its phosphorylation. The latter is supported by genomic analyses, which found that one quarter of T6S gene clusters containing *fha1* orthologs do not encode identifiable kinase or phosphatase genes (27). To distinguish between the two possibilities, we conducted Δ*fha1* genetic complementation studies in the Δ*tagF* and Δ*pppA* backgrounds using wild-type *fha1* or an allele encoding non-phosphorylatable Fha1 ($fha1_{T362A}$). Wild-type *fha1* restored secretion apparatus function in both backgrounds, however only Δ*tagF* Δ*fha1* was functional when complemented with $fha1_{T362A}$ **(Figure 2.4B)**. Together, these data conclusively demonstrate that Fha1 performs an important function in the T6SS independent of its phosphorylation state, and that TagF activation of the H1-T6SS proceeds independently of *p*-Fha1.

To further probe the relationship between TagF and TPP-mediated T6S activation, we conducted epistasis experiments monitoring Hcp1 and Tse1 secretion. Immediately upstream of Fha1 in the TPP is PpkA, which catalyzes Fha1 phosphorylation and is essential for T6S-apparatus assembly in a constitutively active background (Δ*pppA*) (115). While *ppkA* is essential for Hcp1 and Tse1 secretion in the Δ*pppA* background, we found that the gene is dispensable for these functions in Δ*tagF* **(Figure 2.4C)**. Further upstream of PpkA in the TPP is TagR. This protein appears to regulate the kinase, as inactivation of *tagR* decreases *p*-Fha1 levels, and ectopic expression of PpkA overrides the requirement for *tagR* in H1-T6SS activation (115). Three additional *tag*

genes flank *tagR* (*tagQ, S,* and *T*), and have been postulated to also participate in the TPP. Remarkably, deletion of the four *tag* genes in conjunction with deletions of *ppkA* and *pppA*, did not influence Tse1 or Hcp1 secretion via the H1-T6SS in the Δ*tagF* background. In contrast, the H1-T6SS failed to export these proteins when *tagF* was present in this background **(Figure 2.4D)**. Together, these data show that the *tagF* deletion is epistatic to deletions in genes encoding the TPP core component PpkA and the TPP positive regulatory protein TagR. This suggests that TagF represses activation of the H1-T6SS by acting independently of the TPP. The role of *tagQ, S,* and *T* remains unknown, however our results show that these genes also encode proteins that are dispensable for H1-T6SS effector secretion in a *P. aeruginosa* background lacking *tagF*.

**The TagF and TPP-mediated pathways differentially influence Hcp1 and Tse1 secretion.** The finding that a deletion in *tagF* alleviates the requirement for *ppkA*, suggests that TagF acts either downstream or independently of the TPP. To investigate this, we conducted quantitative analyses comparing Hcp1 and Tse1 secretion from strains with H1-T6S derepressed in either of the pathways (Δ*tagF* or Δ*pppA*) or both (Δ*tagF* Δ*pppA*). Only if the pathways act independently or partially independently would we anticipate observing additive or synergistic effects on secretion. Surprisingly, we found that the double deletion of *pppA* and *tagF* had differential effects on Hcp1 and Tse1 secretion relative to the single deletion strains. Levels of secreted Hcp1 were similar in the three deletion strains, whereas the deletion of the regulators influenced Tse1 export in an additive fashion **(Figure 2.5)**. The observation that one output of the pathways–effector secretion–is induced additively upon their activation suggests that TagF does not act purely by repressing downstream of the TPP. Furthermore, our quantitative analyses proved consistent with our qualitative observation that more Tse1 is exported by Δ*pppA* than Δ*tagF*

**(Figure 2.1C and Figure 2.2A)**. This is noteworthy, as this difference in output is also inconsistent with a simple epistatic relationship between the pathways.

**The TPP and TagF-mediated activation pathways converge on ClpV1 recruitment.** Using fluorescence microscopy (FM), our laboratory previously demonstrated that a chromosomally encoded functional green fluorescent protein fusion to the H1-T6SS ATPase ClpV1 (ClpV1–GFP) is recruited to secretion foci in the cell upon activation of the apparatus via *p*-Fha1 (167). The formation of these foci is thought to reflect maturation of the secretion system, as their presence and intensity correlates with the level of secreted Hcp1 and deletion of essential apparatus components results in their dissolution. Notably, while recruitment of ClpV1 to the H1-T6S apparatus is enhanced by Fha1 phosphorylation, the physical interaction between these proteins is phosphorylation independent (115). Thus, we reasoned that if TagF-mediated activation converges on the TPP downstream of *p*-Fha1, ClpV1 recruitment to the H1-T6S-apparatus should also be observed in the Δ*tagF* strain. To test this hypothesis, we introduced *clpV1–gfp* to the Δ*tagF* background and examined the cells by FM. The absence of *tagF* promoted ClpV1–GFP recruitment to an extent similar to that observed in the Δ*pppA* control, and ectopic expression of *tagF* in the Δ*tagF* background fully complemented the phenotype **(Figure 2.6)**. The formation of these foci required *ppkA* in the Δ*pppA* background, but not the Δ*tagF* background. This mirrors the requirement for *ppkA* with regard to Tse1 and Hcp1 secretion in these two backgrounds, and indicates that the formation of foci correlates with a functional active secretory apparatus **(Figure 2.6)**. Further consistent with the functional significance of ClpV1-GFP foci, we found that a strain lacking both *pppA* and *tagF* displayed higher levels of ClpV1-GFP foci than those with individual deletions in these genes. Therefore,

ClpV1 recruitment to foci is proportional to effector export from these strains. Differences in the number of ClpV1-GFP foci-positive cells among the strains were not due to altered levels of the ClpV1 protein **(Figure 2.6)**. Based on these data, we conclude that TagF and TPP-mediated T6S activation share a convergence in mechanism at the level of ClpV1–GFP recruitment to the secretion apparatus. Interestingly, previous work from our laboratory had led us to conclude that PpkA is an essential structural component of the H1-T6SS (115). Our current work clearly indicates that the structural requirement for PpkA is conditional on TagF. This in part reconciles the observation that PpkA orthologs are absent from the majority of identified T6SSs (167).

**The H1-T6SS is activated by surface growth.** The H1-T6SS efficiently targets Tse2 to other *P. aeruginosa* cells. If recipient cells lack the Tse2-specific immunity protein, Tsi2, their fitness is decreased relative to donors actively exporting Tse2 through a functional H1-T6S apparatus (Hood *et al*., 2010). Here, we used the self-targeting capability of the H1-T6SS as a means to probe the functional consequences of mutations that posttranslationally activate the H1-T6SS (Δ*pppA* and Δ*tagF*).

The influence of regulatory mutations on intercellular effector targeting by the H1-T6SS was assessed by measuring the fitness of donor strains competed against a susceptible recipient (Δ*tse2* Δ*tsi2*). Interbacterial transfer of effectors by the T6SS requires intimate cell contact; therefore, competition assays were performed between strains co-inoculated on a solid growth substrate. When competed in this manner, the parental donor strain displayed a 3.2-fold fitness advantage relative to the recipient. This effect was T6S-dependent, as the deletion of *clpV1* in the donor strain negatively impacted its fitness advantage. Donor strains lacking *pppA* or *tagF*

showed a fitness advantage comparable to the parental. All strains displayed equal fitness when cultivated in liquid media, consistent with the known requirement for intimate cell contact in T6S-dependent fitness changes **(Figure 2.7A)** (113, 216).

The finding that Δ*pppA* and Δ*tagF* did not increase T6S-dependent fitness of *P. aeruginosa* was unexpected, and led us to hypothesize that – unlike in our secretion assays – the apparatus is posttranslationally activated under conditions of the competition experiments. To investigate further the posttranslational activation state of the H1-T6SS under competition assay conditions, we probed the requirement for *ppkA* in the fitness advantage of Δ*pppA* against recipient bacteria. We reasoned that if the TPP was triggered, deletion of the kinase – even in an activated Δ*pppA* background – should inactivate the system. However, if TagF-mediated repression was fully relieved (as in Δ*tagF*), a strain lacking both *ppkA* and *pppA* should remain functional, as was observed in secretion and apparatus assembly assays **(Figure 2.4D and Figure 2.6)**. Interestingly, the Δ*pppA* Δ*ppkA* strain does not possess a T6S-dependent fitness advantage over recipient bacteria. This is not attributable to inactivation of the apparatus due to the loss of PpkA, as Δ*tagF* Δ*ppkA* retained the full fitness advantage of the parental strain **(Figure 2.7A)**. In total, these results suggest that the H1-T6SS is activated posttranslationally by the TPP under the conditions of our *in vitro* growth competition assay.

Next we sought to directly measure the activation state of the H1-T6SS under growth competition assay conditions. We considered three substantive differences between the conditions of our secretion and competition assays that might underlie the apparent change to the activation state of the H1-T6SS: 1) the time period over which the two experiments were

conducted (secretion, 4 hr; competition, 18 hr), 2) the number of discrete *P. aeruginosa* genetic backgrounds present, and 3) propagation in liquid (secretion assay) versus solid (competition assay) media. Multiple lines of evidence indicated that the latter difference was most likely the key determinant of activation of the secretion system under competition conditions. In particular, we noted that all T6SS-dependent interactions observed to date require intimate cell contact. The release of effectors into the milieu is not productive, which is exemplified in the observation that strains bearing mutations leading to strong constitutive activation of the H1-T6SS have no fitness advantage over highly susceptible recipients in liquid cultures (113, 204). Thus, it is logical that bacteria should repress T6S during planktonic growth and relieve this repression when grown in an environment containing a high density of closely interacting bacteria that could be effectively targeted.

If surface growth was responsible for H1-T6SS posttranslational activation under competition conditions, we would expect to observe changes in substrate secretion and *p*-Fha1 levels in the wild-type background relative to those observed in liquid secretion assays performed under otherwise similar conditions (see Methods). Densitometry analysis of *p*-Fha1 levels observed by Western blot indicated that growth on a surface strongly promotes Fha1 phosphorylation; approximately 20.1% of the protein was phosphorylated after growth on a solid surface, whereas the phosphorylated species was only 4.3% of total Fha1 in liquid grown cells **(Figure 2.7B)**. Enhanced Fha1 phosphorylation incurred during surface growth required PpkA, consistent with our model of posttranslational activation by the TPP.

To probe more directly the activation state of the H1-T6SS during growth on a solid substrate, we measured Hcp1 secretion from surface grown cells. For this experiment, it was necessary to place cells harvested from the substratum into liquid medium for a brief period to allow the accumulation of secreted proteins. H1-T6S-dependent secretion of Hcp1 was greatly increased by surface growth of *P. aeruginosa*. Indeed, levels of the secreted protein were comparable between parental and constitutively triggered backgrounds **(Figure 2.7C)**. It is noteworthy that the TPP and TagF-mediated pathways appear to have no role in promoting H1-T6SS activation beyond that observed during surface growth. This finding explains our aforementioned observation that wild-type, Δ*pppA*, and Δ*tagF* strains display equal T6S-dependent fitness **(Figure 2.7A)**. In addition, our finding that Δ*tagF* is activated through the TPP during surface growth (*p*-Fha1 levels equal to wild-type), suggests that the fitness advantage exhibited by this mutant is phenotypically equivalent to Δ*tagF* Δ*pppA*.

## DISCUSSION

The results of our current study lead us to propose a new model of posttranslational activation of the H1-T6SS **(Figure 2.8)**. As in previous models, Fha1 remains a pivotal protein in the activation process. However, it is now clear that ClpV1 recruitment to the apparatus and apparatus activation can occur via Fha1 phosphorylation-dependent (TPP-mediated) and independent processes (TagF-mediated). We propose that distinct inputs received by the cell regulate these two convergent mechanisms of H1-T6SS activation. Our data argue that TPP-dependent activation, which requires PpkA, is stimulated by a cue deriving from the physiological changes encountered during surface growth. On the other hand, phosphorylation-independent activation, which is strongly repressed by TagF and does not require PpkA in any

capacity, appears not to occur under such circumstances. One appealing hypothesis is that TagF posttranslational derepression of the H1-T6SS is modulated by sensing of non-*P. aeruginosa* bacterial species. Our current study was limited to analyses of H1-T6SS activation during intraspecies growth competition experiments **(Figure 2.7A)**. Intriguingly, we note that in addition to the *P. aeruginosa* H1-T6SS, two other bacterial cell-targeting T6SSs, *B. thailandensis* T6SS-1 and the T6SS of *S. marcescens,* appear to utilize TagF proteins. *P. aeruginosa* and *B. thailandensis* encode six additional T6SSs – none of which have been implicated in interbacterial interactions. Among these, only *B. thailandensis* T6SS-6 possesses a *tagF* ortholog (113, 216). The vas system of *V. cholerae* complicates this simple correlation between bacterial cell targeting and the presence of TagF. This system appears to target both bacteria and eukaryotic cells and does not possess a *tagF* gene (157).

At this point, we cannot exclude the assertion that TagF prevention of phosphorylation-independent T6S activation is static (structural) rather than dynamic (regulatory). For example, TagF may act simply as a barrier that prevents non-phosphorylated Fha1 or downstream H1-T6S-components from activating the H1-T6SS. One compelling argument against this model is that TagF appears in many T6SSs that lack Fha1, PpkA and PppA orthologs **(Figure 2.3)** (27). This strongly suggests that phosphorylation-independent posttranslational activation mechanisms for T6S are likely to exist. In addition, this observation leads us to speculate that TagF and TPP-mediated activation converge downstream of Fha1. Another indication that TagF is part of a dynamic regulatory pathway derives from our comparison of Hcp1 and Tse1 secretion from *P. aeruginosa* strains with H1-T6S activity derepressed as the result of mutations in one versus both pathways. We observed Hcp1 secretion is enhanced equally by individual deletions in *tagF* and

*pppA*, and that in combination the deletions do not display an additive effect on secretion of the protein. On the contrary, the absence of the negative regulators triggers Tse1 secretion to different extents, and, in combination, the mutations display an additive effect on the export of this effector and apparatus assembly. This latter result argues that TagF is not simply a downstream repressor of the TPP and suggest that inputs received from TagF and the TPP are used to tune effector export by the H1-T6SS.

The X-ray crystal structure of TagF was recently determined as part of a structural genomics effort **(Figure 2.9)** (83). In the structure, TagF is found to associate as a homodimer with nearly identical monomers composed of α and β elements assembled as a three-layer sandwich (α-β-α). The TagF monomer is not closely related to other solved structures, however it bears some similarity to the N-terminal regulatory domain of the eukaryotic SNARE protein, Sec22b (DALI, r.m.s.d. = 3.3 Å over 87 residues; Z score = 3.9) **(Figure 2.10)** (112, 203). SNARE proteins mediate vesicle trafficking and membrane fusion; therefore, it is unlikely that direct functional parallels between TagF and Sec22b can be drawn. Nonetheless, the structures of Sec22b and TagF contain homology to the actin regulatory protein profilin (133). In particular, they share the surface used by profilin to bind poly-proline sequences. It is conceivable that TagF interacts with proline-rich proteins via this motif. Interestingly, Fha1 has an extensive proline-rich domain of unknown function (amino acids 173-294; 36% proline) located between its N-terminal FHA domain and its C-terminal domain that is phosphorylated by PpkA (167). So far we have not detected an interaction between these proteins. An important future direction will be to elucidate components of the TagF-mediated activation pathway by identifying TagF-interacting proteins.

Our finding that the H1-T6SS is activated by the TPP when *P. aeruginosa* is grown on a surface fits well with our current understanding of the environmental conditions physiologically relevant to T6SS function. It first became apparent that the system might be important to the sessile lifestyle of *P. aeruginosa* through circumstantial evidence, including the discovery that HSI-I is stringently co-regulated with exopolysaccharides involved in cellular aggregation and adhesion to surfaces (96, 166). Later, interactions between bacteria mediated by the T6SS were shown to be exquisitely dependent on intimate cell contact – ameliorated entirely in liquid medium (113). Perhaps the strongest evidence linking sessile physiology and T6S function is our recent finding that in the absence of T6SS-1, *B. thailandensis* is rapidly displaced from a flow-cell chamber by *P. putida* (216). One candidate signaling molecule that may directly or indirectly be responsible for TPP activation during surface growth is cyclic-di-GMP. This molecule is a secondary messenger that modulates the expression of traits important for the transition between sessile and planktonic lifestyles of certain bacteria, including *P. aeruginosa* (106). Direct regulation by c-di-GMP has been observed at both transcriptional and posttranslational levels (24, 78, 108, 182). Given the requirement for sessile growth in T6S function and the precedent for c-di-GMP acting as a posttranslational regulator, it is reasonable to speculate that this molecule might directly or indirectly be responsible for TPP activation during surface growth. Indeed, c-di-GMP-dependent regulation of T6S in *P. aeruginosa* was recently reported by Filloux and colleagues (165). This study showed that c-di-GMP levels in *P. aeruginosa* Δ*retS* correlate to cellular Hcp1 levels, however the point(s) of regulation at which the signaling molecule acts was not determined, raising the possibility that c-di-GMP regulates the H1-T6SS on the posttranslational level as well.

Highly regulated triggering of effector export is likely to be a critical factor in the potency and efficiency of bacterial intercellular protein delivery machines. While the great majority of evidence for this claim derives from studies of the type III secretion system (64, 86), our work on posttranslational activation of the H1-T6SS suggests that it may be equally true in this system. Our data indicate that the products of at least eight HSI-I genes are involved in regulating the activation state of the H1-T6S apparatus. Seven of these are wholly dispensable for the function of the system, suggesting that they are dedicated regulatory proteins. The complexity of T6S regulation rivaling that of type III is not surprising when one considers the consequences of either system releasing effectors out of step with target cell interaction. Effectors from both systems lack the ability to reach their ultimate sites of action without target cell engagement; therefore, a failure to precisely spatially and temporally coordinate effector release is a complete loss of the metabolic investment in their synthesis.

## MATERIALS AND METHODS

**Bacterial strains, plasmids and growth conditions.** The sequenced *P. aeruginosa* strain, PAO1, was used for this study (229). *P. aeruginosa* strains were grown in Luria-Bertani (LB) medium at 37°C supplemented with 30 μg $mL^{-1}$ gentamicin, 300 μg $mL^{-1}$ carbenicillin, 25 μg $mL^{-1}$ carbenicillin, 100 μg $mL^{-1}$ tetracyclin, 25 μg $mL^{-1}$ irgasan, 5% w/v sucrose, 0.2% w/v arabinose or 0.5 mM IPTG as required. Plasmids and strains used in this study are shown in **Table 2.1**. Plasmids used for inducible expression in *P. aeruginosa* included pPSV35 (Fha1 and $Fha1_{T362A}$ complementation) and pPSV35-CV (complementation with TagF fused to C-terminal VSV-G tag) (115, 200), pSW196 (ClpV1 complementation) (15), and pUC18-mini-Tn7 (*lacZ*20::PA0081, *lacZ*20::PA0082 *yfp, cfp* reporters) (28, 136). pPSV18 (201) was used for

constitutive expression of Tse2 and Tsi2. *tse2* and *tsi2* were cloned into pPSV35 using primers 591 and 743 and were subcloned into pPSV18 using restriction sites SacI and XbaI. *E. coli* strains, DH5α and SM10, were used for plasmid maintenance and conjugal transfer and were grown at 37°C. *P. aeruginosa* strains were transformed with plasmids by electroporation or conjugation with *E. coli* SM10.

**Chromosomal fusions and mutations in *P. aeruginosa.*** Chromosomal fusions and in-frame deletions were generated by allelic replacement using the pEXG2 suicide plasmid (166, 200). The sequences used for these constructs were made by splicing by overlap extension PCR and cloned into the 5' XbaI and 3' HindIII sites of pEXG2. The primers used for amplification were designed such that the first several codons were fused to the last several codons with an intervening sequence of 5'- TTCAGCATGCTTGCGGCTCGAGTT -3'. For *tagQ, tagS, tagT, tagF, pppA tagF* deletion constructs, upstream DNA flanking sequences were amplified using primer pairs 871/872, 471/472, 774/775, 291/292 and 291/292, respectively. Downstream flanking DNA sequences were amplified with primer pairs 873/874, 473/474, 776/777, 293/294 and 564/565, respectively. For the deletion of the accessory gene cluster (PA0070–PA0075 and PA0070–PA0076), flanking and overlapping primers were made for the 5' and 3' genes. Chromosomal VSV-G epitope tagged *hcp1, tse1* and *fha1* were also generated by splicing by overlap extension PCR and cloned into pEXG2 (166, 167). The VSV-G sequence 5-TATACAGATATTGAAATGAATAGATTAGGAAAATGA -3' was used to replace the stop codon of each gene. Upstream and downstream primer pairs used to generate *tse1-VSV-G* were 596/597 and 598/599. Strains harboring *clpV1-gfp* chromosomal fusions were generated as described previously (167). The pUC18-mini-Tn7 and pSW196 derivatives were transformed

into *P. aeruginosa* by conjugation. All chromosomal mutations were confirmed through PCR analysis.

**β-Galactosidase assay.** A chromosomal insertion vector carrying a fusion of *lacZ* to the *fha1* or *tssA1* promoters, pUC18-mini-Tn7-*lacZ*20-Gm::PA0081 and pUC18-mini-Tn7-*lacZ*20-Gm::PA0082, respectively, were used to generate all strains for analysis. The sequences used for these fusions contained the promoter of each indicated strain, the 5' leader sequence and the first several coding nucleotides (28). The plasmids were introduced into *P. aeruginosa* by four parental mating conjugation or electroporation (47). The vector backbones were not removed, except for strains MLS 1526 and MLS 2715. Overnight cultures were diluted 1:1000 in LB with 50 mM MOPS pH 7 and grown to mid-log phase. Cells were permeabilized with chloroform (15% chloroform) and assayed using the Tropix Galacon-Plus® reagents (Tropix, Bedford, MA). Luminescence was measured by using a GENios Pro-Basic microplate reader (Tecan Group Ltd. Mannedorf, Switzerland). Values were normalized to the optical density at 600 nm for each strain. All β-galactosidase assays were performed in triplicate. Statistical significance was determined using a one-way analysis of variance (ANOVA) and Tukey's post-hoc test.

**Preparation of proteins and Western blotting.** Protein samples from liquid grow cultures were prepared as previously described (115). Specifically, overnight cultures of *P. aeruginosa* were used to inoculate 2 mL of LB (1:1000) supplemented with appropriate additives. Cultures were grown at 37°C with shaking at 250 r.p.m. Samples were harvested at mid-log phase by centrifugation at 9,000 r.p.m. for 3 minutes and 1.3 mL of the supernatant were centrifuged a second time to remove contaminating bacterial cells. After this second step, 1 mL of the

supernatant fractions was treated with 110 μL 100% w/v Trichloroacetic acid (final concentration of 10%). To collect precipitated proteins, the samples were centrifuged at for 30 minutes at 13,500 r.p.m. Supernatants were removed and the protein pellets were washed with 1 mL of 100% acetone and centrifuged at 4°C for 15 minutes at 13,500 r.p.m. The protein pellets were resuspended in 20 μL of SDS-PAGE sample loading buffer. To isolate cell-associated protein samples, the cell pellets were resuspended in 100 μL of Buffer 1 (0.5 M NaCl, 50 mM Tris pH 7.5 and 10% glycerol) and mixed 1:2 with SDS-PAGE sample loading buffer. The secreted and cell-associated protein samples were analyzed by Western blotting as previously described (166) using rabbit α-VSV-G (1:5000, Sigma) or rabbit α-Fha1 (diluted 1:5000) and detected with α-rabbit horseradish peroxidase-conjugated secondary antibodies (Sigma). Mouse α-GFP (1:1000, Roche) or mouse α-RNA polymerase β-subunit antibody (1:2000, Neoclone) and α-mouse horseradish peroxidase-conjugated antibodies (Sigma) were used to detect ClpV1-GFP or RNAP. Western blots were developed using chemiluminescent substrate (SuperSignal West Pico Substrate, Thermo Scientific) and imaged with a FluorChemQ (ProteinSimple).

For surface grown strains, overnight cultures were diluted 1:100 in LB and 3 mL of this dilution was spotted onto a 0.2mM polycarbonate membrane placed on onto LB agar. After approximately 4 hours of growth at 37°C the cells were resuspended by placing the filter in 2 mL of LB and incubating at 37°C with shaking (250 r.p.m.) for 5 minutes. Cell and supernatant samples were then collected as described above

Densitometry was performed using AlphaView®Q software (ProteinSimple). The percentage of phosphorylated Fha1 was determined by measure band intensity of phosphorylated and total

Fha1 from three independent experiments. The values were normalized to Δ*ppkA*, which was set at 0% *p*-Fha1.

**Preparation of supernatant protein samples for quantitative analysis.** Supernatant samples analyzed for Tse1 and Hcp1 in the Δ*pppA* Δ*tagF* backgrounds were prepared using a filter based method. A total of 4 mL were grown for each strain (2 mL/tube) and were harvested by centrifugation in a 15 mL Falcon tube (Becton Dickinson) at 4,000 r.p.m. in a swing bucket rotor for 5 minutes. The supernatants were filtered over through a 0.2 μM Supor® Membrane (Pall Life Sciences) into two 2 mL microcentrifuge tubes containing 250 μL of 100% w/v Trichloroacetic acid. The precipitation and acetone wash were carried out as described in the previous section. Washed samples were then resuspended in 50 μL of SDS-PAGE sample loading buffer. Densitometry was performed using AlphaView®Q software (ProteinSimple). Statistical significance was determined using ANOVA and Tukey's post-hoc test.

**Fluorescence microscopy.** *P. aeruginosa* strains were cultured in an identical manner as described for protein sample preparations. All samples were harvested at mid-log phase by centrifuging at 7,000 r.p.m and resuspending the pellet to an optical density (600 nm) of 5 with PBS supplemented with 0.5mM TMA-DPH, for membrane staining. Three microliters of the mixture were spotted onto a 1% PBS agarose pad. All images were acquired with the same exposure settings on a Nicon 80i microscope with a 100X PlanAprochromat objective (numerical aperature 1.4) and Chroma Technology Corp. filter sets. Images were recorded using a CoolSnap HQ camera (Photometerics). DAPI and GFP were used for imaging TMA-DPH and ClpV1-GFP, respectively. MetaMorph 6.3r2 software was used (115). Three randomly selected

frames containing $200 \leq N \leq 700$ cell were chosen for the analysis of GFP foci. Statistical significance was determined using ANOVA and Tukey's post-hoc test.

**Interbacterial growth competition assays and quantification.** Overnight cultures were mixed at a 1:1 ratio to a total density of approximately $1.0x10^8$ CFU/mL in 1 mL LB medium. In each experiment the donor and recipient strain contained constitutively expressing yellow fluorescent protein (YFP) or cyan fluorescent protein (CFP), respectively. To construct these strains the mini-Tn7 system, pUCP18-mini-Tn7 containing *yfp* or *cfp*, was inserted on the PAO1 chromosome at the neutral phage attachment site, *attB*, downstream of the *glmS* (136). The plasmids were introduced into *P. aeruginosa* via four-parental mating conjugation or electroporation (47). The vector backbones were not removed. For our assays, over-expression of Tse2 and Tsi2 in the donor strain was required for the H1-T6S-dependent fitness advantage. Donor strains harbored pPSV18::PA2702 PA2703 for constitutive expression of Tse2 and Tsi2. Recipient strains harbored the empty vector, pPSV18 (201). Competitions were grown on 0.2mM polycarbonate membranes on LB agar for 18 hours at 37°C, or in 2 mL of LB with shaking. Cells were resuspended in LB medium and spotted onto 1.0% agarose PBS pads and imaged as described above for FM. YFP and CFP filters were used to image the two cell populations. Assays were performed in triplicate. Three fields containing 100 to 200 cells were imaged for each competition. To determine the competitive index (the number of YFP positive cells to CFP positive cells) MetaMorph® computer-assisted morphometry based on area was used. Thresholds were set identically for each image generated using YFP and CFP filters. The areas of the thresholded regions were calculated using MetaMorph® software and the ratios of

YFP and CFP labeled cells were calculated. Statistical significance was determined using ANOVA and Tukey's post-hoc test. Grubbs' test was used to detect outlier data points.

**Generation of TagF structure images.** PyMOL was used to generate molecular graphic images (http:://www.pymol.org) (211). The TagF (PA0076) X-ray crystal structure (Protein Data Bank, http://www.rcsb.org accession code 2QNU) was solved by the Midwest center for structural genomics (83). Structural superpositions were determined by DALI (112).

**Table 2.1: Strains and plasmids used in Chapter II.**

| Strain # | Relevant genotype (*P. aeruginosa* PAO1) | Reference |
|---|---|---|
| JDM 62 | PA0085-VSV-G | (167) |
| MLS 2256 | ΔPA0070 PA0085-VSV-G | This study |
| MLS 2384 | ΔPA0071 PA0085-VSV-G | (115) |
| MLS 3552 | ΔPA0072 PA0085-VSV-G | This study |
| MLS 3553 | ΔPA0073 PA0085-VSV-G | This study |
| MLS 2139 | ΔPA0074 PA0085 VSVG | (167) |
| JDM 117 | ΔPA0075 PA0085-VSV-G | (167) |
| MLS 1235 | ΔPA0076 PA0085-VSV-G | This study |
| MLS 3549 | ΔPA0077 PA0085-VSV-G | (166) |
| MLS 2213 | ΔPA0074 ΔPA0076 PA0085-VSV-G | This study |
| MLS 1584 | ΔPA0075 ΔPA0076 PA0085-VSV-G | This study |
| MLS 223 | PAO1 PA0081-VSV-G | (167) |
| MLS 1597 | ΔPA00074 PA0081-VSV-G | (167) |
| MLS 1596 | ΔPA0075 PA0081-VSV-G | (167) |
| MLS 1594 | ΔPA0076 PA0081-VSV-G | This study |
| MLS 3558 | ΔPA0074 ΔPA0075 PA0081-VSV-G | (167) |
| MLS 1627 | PA1844-VSV-G | This study |
| MLS 3555 | ΔPA0070 PA1844-VSV-G | This study |
| MLS 3554 | ΔPA0071 PA1844-VSV-G | This study |
| MLS 3556 | ΔPA0072 PA1844-VSV-G | This study |
| MLS 3557 | ΔPA0073 PA1844-VSV-G | This study |
| MLS 3551 | ΔPA0074 PA1844-VSVG | This study |
| MLS 1607 | ΔPA0075 PA1844-VSV-G | This study |
| MLS 1720 | ΔPA0076 PA1844-VSV-G | This study |
| MLS 3550 | ΔPA0077 PA1844-VSV-G | This study |
| MLS 2797 | ΔPA0074 ΔPA0076 PA1844-VSV-G | This study |
| MLS 1810 | ΔPA0075 ΔPA0076 PA1844-VSV-G | This study |
| MLS 724 | PA0090-GFP | (167) |
| MLS 3560 | ΔPA0074 ΔPA0075 PA0090-GFP | This study |
| MLS 3546 | ΔPA0076 PA0090-GFP | This study |
| MLS 3547 | ΔPA0074 ΔPA0076 PA0090-GFP | This study |
| MLS 3548 | ΔPA0075 PA0090-GFP | (167) |
| MLS 3639 | ΔPA0075 ΔPA0076 PA0090-GFP | This study |
| MLS 3566 | ΔPA0076 ΔPA0090 PA0085-VSV-G | This study |
| MLS 3567 | ΔPA0076 ΔPA0090 PA1844-VSVG | This study |
| MLS 2252 | ΔPA0076 ΔPA0081 PA0085-VSV-G | This study |
| MLS 3653 | ΔPA0075 ΔPA0081 PA0085-VSV-G | This study |
| MLS 2402 | ΔPA0076 attTn7::*yfp* | This study |
| MLS 2403 | ΔPA0075 attTn7::*yfp* | This study |
| MLS 2404 | ΔPA0090 attTn7::*yfp* | This study |

| | | |
|---|---|---|
| MLS 2092 | PAO1 attTn7::*yfp* | This study |
| MLS 3545 | ΔPA0074 ΔPA0076 attTn7::*yfp* | This study |
| MLS 2076 | ΔPA2702 ΔPA2073 attTn7::*cfp* | This study |
| MLS 3559 | ΔPA0074 ΔPA0075 attTn7::*yfp* | This study |
| MLS 3568 | ΔPA0070 ΔPA0071 ΔPA0072 ΔPA0073 ΔPA0074 ΔPA0075 PA0085-VSV-G | This study |
| MLS 2257 | ΔPA0070 ΔPA0071 ΔPA0072 ΔPA0073 ΔPA0074 ΔPA0075 PA0076 PA0085-VSV-G | This study |
| MLS 3569 | ΔPA0070 ΔPA0071 ΔPA0072 ΔPA0073 ΔPA0074 ΔPA0075 PA1844-VSV-G | This study |
| MLS 3570 | ΔPA0070 ΔPA0071 ΔPA0072 ΔPA0073 ΔPA0074 ΔPA0075 ΔPA0076 PA1844-VSV-G | This study |
| MLS 2715 | ΔPA0076 PA0085-VSV-G PA0082-lacZ20 | This study |
| MLS 1526 | PA0085-SV-G PA0082-lacZ20 | Thus study |
| MLS 3571 | ΔPA2234 ΔPA3064 ΔPA4856 attTn7::PA0082 lacZ20 | Thus study |

| **Plasmid name** | **Relevant features** | **Reference** |
|---|---|---|
| pEXG2 | Allelic replacement vector containg *sacB* | (200) |
| pPSV35-CV | Expression vector with *lacI*, *lacUV5* promoter, C-terminal VSV-G tag | (115, 200) |
| pPSV18 | Expression vector with *lac* promoter | (201) |
| pSW196 | MiniCTX1 plasmid, araC pBAD | (15) |
| pPSV35-CV::PA0076 | *tagF-VSV-G* in pPSV35-CV | This study |
| pPSV35::PA0081 | *fha1* in pPSV35, for complementation studies | (167) |
| pPSV35::PA0081 T362A | *fha1* T362A in pPSV35, for complementation studies | (167) |
| pSW196::PA0090 | *clpV1* in mini CTX1 plasmid, araC pBAD | (113) |
| pUC18-mini-Tn7-lacZ20-Gm::PA0081 | miniTn7 with *lacZ* translational reporter fusion to the *fha1* promoter | (28) |
| pUC18-mini-Tn7-lacZ20-Gm::PA0082 | miniTn7 with *lacZ* translational reporter fusion to the *tssA* promoter | (28) |
| pEXG2::ΔPA0070 | *tagQ* deletion allele in pEXG2 | This study |
| pEXG2::ΔPA0071 | *tagR* deletion allele in pEXG2 | (115) |
| pEXG2::ΔPA0072 | *tagS* deletion allele in pEXG2 | This study |
| pEXG2::ΔPA0073 | *tagT* deletion allele in pEXG2 | This study |
| pEXG2::ΔPA0074 | *ppkA* deletion allele in pEXG2 | (167) |
| pEXG2::ΔPA0075 | *pppA* deletion allele in pEXG2 | (167) |
| pEXG2::ΔPA0076 | *tagF* deletion allele in pEXG2 | This study |
| pEXG2::ΔPA0077 | *tssM* deletion allele in pEXG2 | (166) |
| pEXG2::ΔPA0081 | *fha1* deletion allele in pEXG2 | (167) |
| pEXG2::ΔPA0090 | *clpV1* deletion allele in pEXG2 | (166) |
| pEXG2::ΔPA00074 ΔPA0075 | *ppkA–pppA* deletion allele in | (167) |

| | | |
|---|---|---|
| | pEXG2 | |
| pEXG2::ΔPA00075 ΔPA0076 | *pppA–tagF* deletion allele in pEXG2 | This study |
| pEXG2::ΔPA0070-ΔPA0076 | *tagQ–tagF* deletion allele in pEXG2 | This study |
| pEXG2::ΔPA0070-ΔPA0075 | *tagQ–pppA* deletion allele in pEXG2 | This study |
| pEXG2::PA0085-VSV-G | For generating chromosomal *hcp1* with C-terminal VSV-G tag | (166) |
| pEXG2::PA1844-VSV-G | For generating chromosomal *tse1* with C-terminal VSV-G tag | This study |
| pEXG2::PA0081-VSV-G | For generating chromosomal *fha1* with C-terminal VSV-G tag | (167) |
| pPSV18::PA2702 PA2703 | Expression vector with *tse2* and *tsi2* | This study |
| pUC18-mini-Tn7::*yfp* | mini Tn7 for YFP tagging *P. aeruginosa* | (136) |
| pUC18-mini-Tn7::*cfp* | mini Tn7 for CFP tagging *P. aeruginosa* | (136) |
| pCGFP::PA0090 | For generating chromosomal *clpV1-gfp* fusion | (167) |

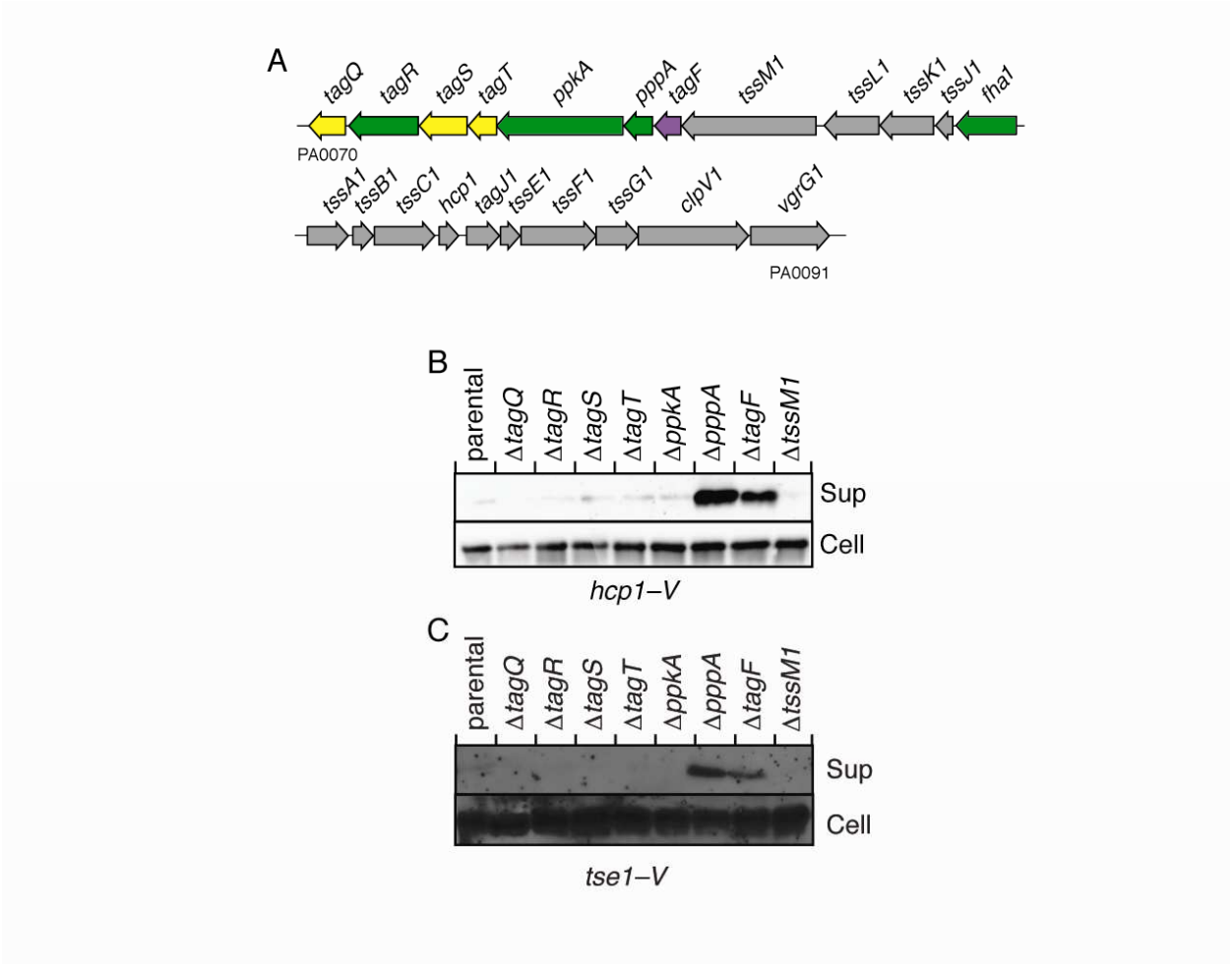


**Figure 2.1: The HSI-I genes, *tagF* and *pppA*, repress Hcp1 and Tse1 secretion.** (A) Genomic organization of *P. aeruginosa* HSI-I. The gene encoding TagF is highlighted in purple. Genes colored in green are known components of the TPP and those colored in yellow are uncharacterized *tag* genes. (B and C) Hcp1 and Tse1 secretion is repressed by *tagF* and *pppA*. Western blot analysis of Hcp1–V and Tse1–V in supernatant (Sup) and cell-associated (Cell) fractions of the genetic backgrounds of *P. aeruginosa* indicated below the blots. Unless otherwise indicated, all blots in this and subsequent figures were probed with antibodies specific to the VSV-G epitope.

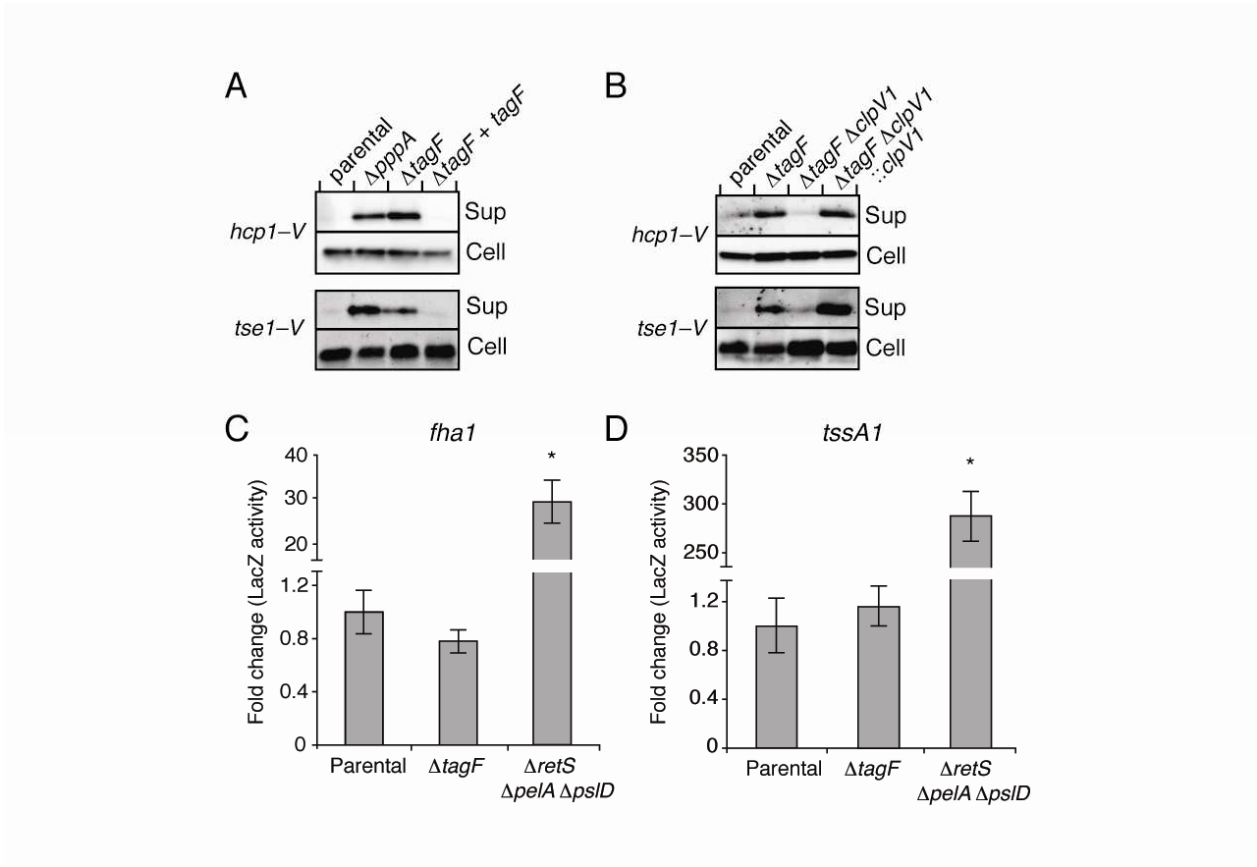


**Figure 2.2: TagF is a negative posttranslational regulator of the H1-T6SS.** (A) Western blot results demonstrating Hcp1 and Tse1 secretion phenotypes of Δ*tagF* can be genetically complemented. (B) Hcp1 and Tse1 secretion in Δ*tagF* requires a functional H1-T6S apparatus. Western blot analysis of Hcp1–V and Tse1–V in supernatant (Sup) and cell-associated (Cell) fractions of the indicated genetic backgrounds of *P. aeruginosa*. (C and D) HSI-I expression is not altered by the deletion of *tagF*. β-galactosidase activity was measured from the indicated *P. aeruginosa* strains carrying a chromosomally-encoded *lacZ* translational fusion to *fha1* (C) or *tssA1* (D) (28). Genes involved in the production of the Pel and Psl polysaccharides were deleted in the Δ*retS* background to prevent cell clumping during growth (52, 207). Error bars represent standard deviation based on three independent replicates. Asterisks indicate statistically significant ($P < 0.001$) differences between Δ*retS* Δ*pelA* Δ*pslD* and wild-type or Δ*tagF* as determined by one-way ANOVA and Tukey's post-hoc tests.

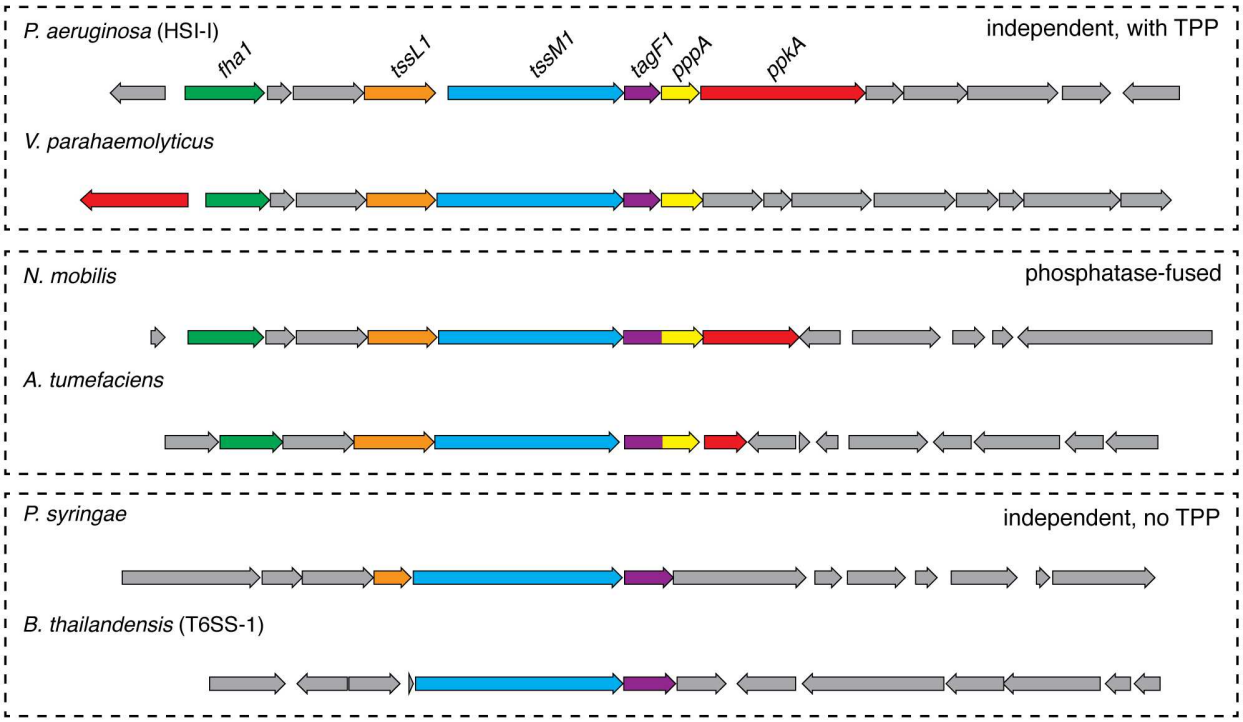


**Figure 2.3: Genetic organization of representative T6S gene clusters containing tagF orthologs.** Colored genes are those that either encode known components of the TPP (*ppkA*, *pppA* and *fha1*) or, for clarity, those that consistently cluster with *tagF* (*tssM* and *tssL*). Apparent orthologs of the HSI-I genes in other clusters are designated with matching colors. *P. aeruginsoa* (HSI-I) and *V. parahaemolyticus* both contain an independent tagF gene (PA0076 and VV_0440) and TPP components (*fha1*, *pppA* and *ppkA*). *N. mobilis* and *A. tumefaciens* also contain TPP components, but, in these cases, the tagF and pppA genes are fused (AGR_L_1064 and NB231_12224). T6SSs of *Pseudomonas syringae* and *B. thailandensis* (T6SS-I) are examples in which tagF is present without TPP components (BTH_I2955 and PSPPH_0124).

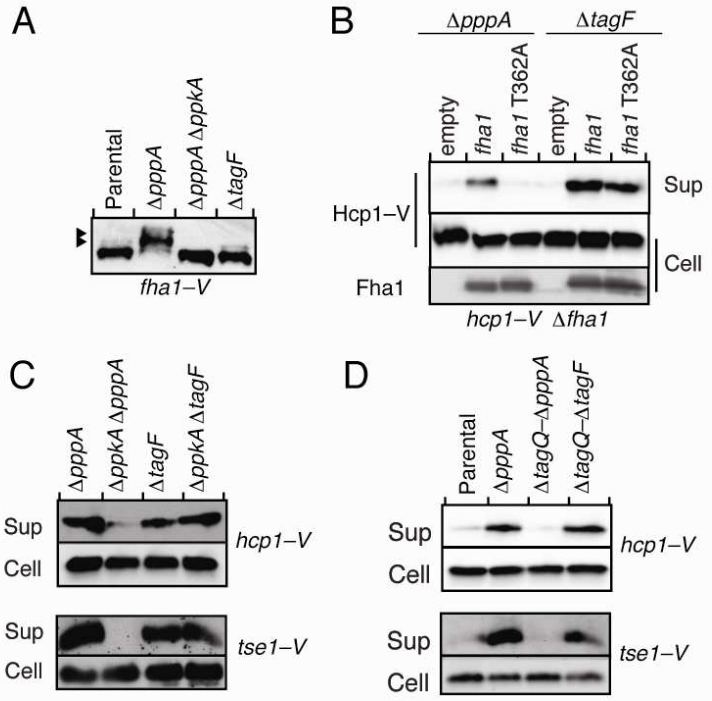


**Figure 2.4: TagF-mediated activation of the H1-T6SS occurs independently of the TPP.** (A) The deletion of *tagF* does not promote elevated levels of *p*-Fha1. Western blot analysis of Fha1–V in the indicated genetic backgrounds of *P. aeruginosa.* Phosphorylated Fha1 species (denoted by arrowheads) are separated from non-phosphorylated Fha1 by their electrophoretic mobility (167). (B) Fha1, but not its phosphorylation, is required for TagF-mediated Hcp1 secretion. Western blot analysis of Hcp1–V secretion and cellular Fha1 levels in the indicated strains of *P. aeruginosa*. Expression plasmids used in each lane are indicated. Fha1 was detected with α-Fha1 antibodies. (C and D) HSI-I genes encoding TPP components and other *tag* genes are not required for Hcp1 and Tse1 secretion in *P. aeruginosa* strains lacking *tagF*. Western blot analysis of Hcp1–V and Tse1–V in the indicated *P. aeruginosa* strains. (Δ*tagQ*-Δ*pppA,* Δ*tagQ* Δ*tagR* Δ*tagS* Δ*tagT* Δ*ppkA* Δ*pppA;* Δ*tagQ*-Δ*tagF,* Δ*tagQ* Δ*tagR* Δ*tagS* Δ*tagT* Δ*ppkA* Δ*pppA* Δ*tagF*).

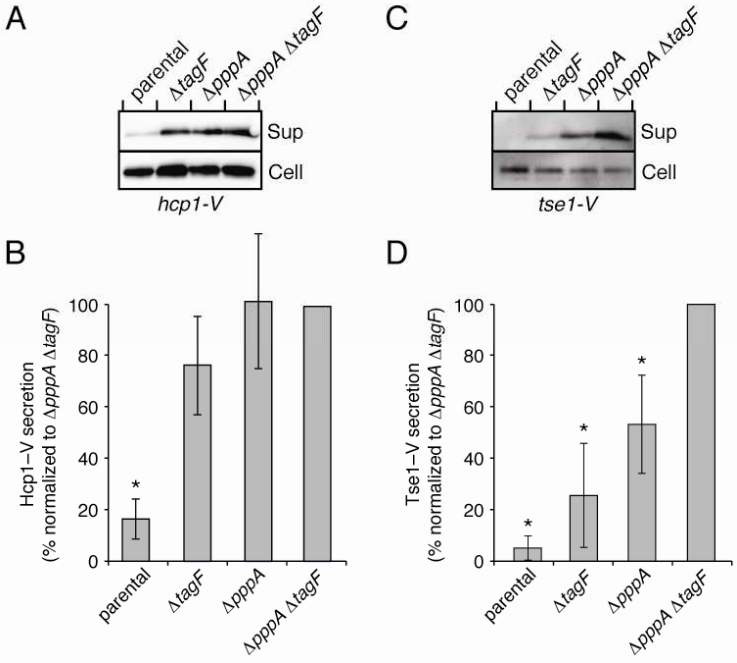


**Figure 2.5: Hcp1 and Tse1 secretion are differentially regulated by the TPP and TagF-mediated pathways.** (A-D) Representative Western blots of Hcp1–V (A) and Tse1–V (C) secretion from the indicated genetic backgrounds of *P. aeruginosa*. (B and D) Quantitative analyses of Hcp1 (B) and Tse1 (D) secretion based on band densitometry from independent Western blot experiments similar to those shown in A and C, respectively. Data are normalized to Δ*pppA* Δ*tagF*. Error bars represent standard deviation based on three independent replicates. Asterisks indicate secretion is significantly less than the Δ*pppA* Δ*tagF* background based on ANOVA and Tukey's post-hoc test ($P < 0.05$).

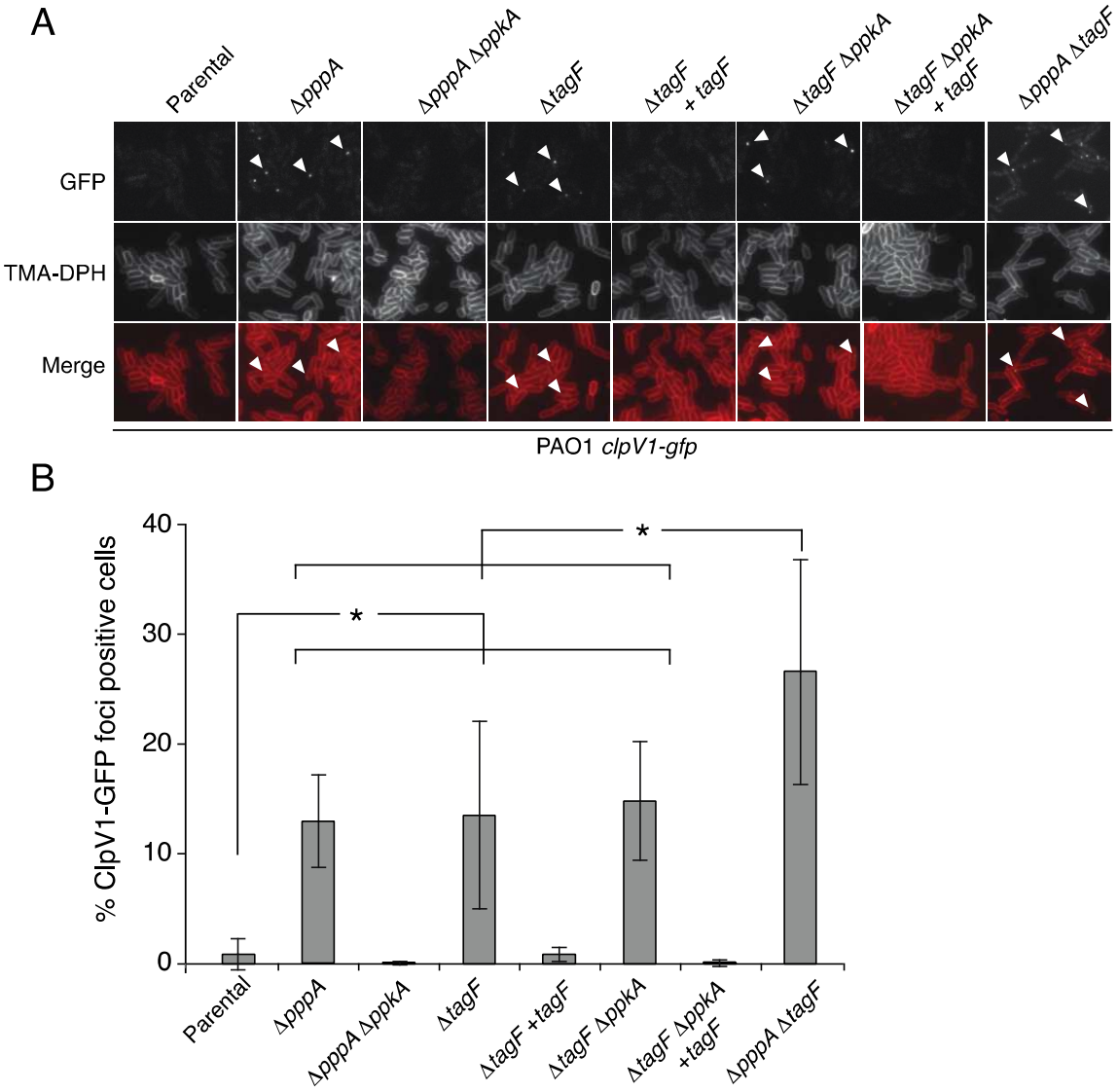


**Figure 2.6: ClpV1 recruitment to the H1-T6S-apparatus is triggered by TagF-mediated activation.** (A) Increased ClpV1–GFP recruitment to the H1-T6S-apparatus is promoted by a *tagF* deletion and occurs independent of the kinase (Δ*tagF* Δ*ppkA*) as observed by the formation of punctate foci using fluorescence microscopy (indicated by white triangles). The lipophilic dye, TMA-DPH, was used to visualize bacterial membranes. (B) Quantitative analysis of ClpV1–GFP foci positive cells in the indicated backgrounds (parental background PAO1 *clpV1–gfp*). Error bars represent standard deviation based on three independent replicates. Asterisks indicate the number of ClpV1–GFP foci per cell are statistically higher than the parental or lower than Δ*pppA* Δ*tagF* based on ANOVA and Tukey's post-hoc test ($P < 0.002$).

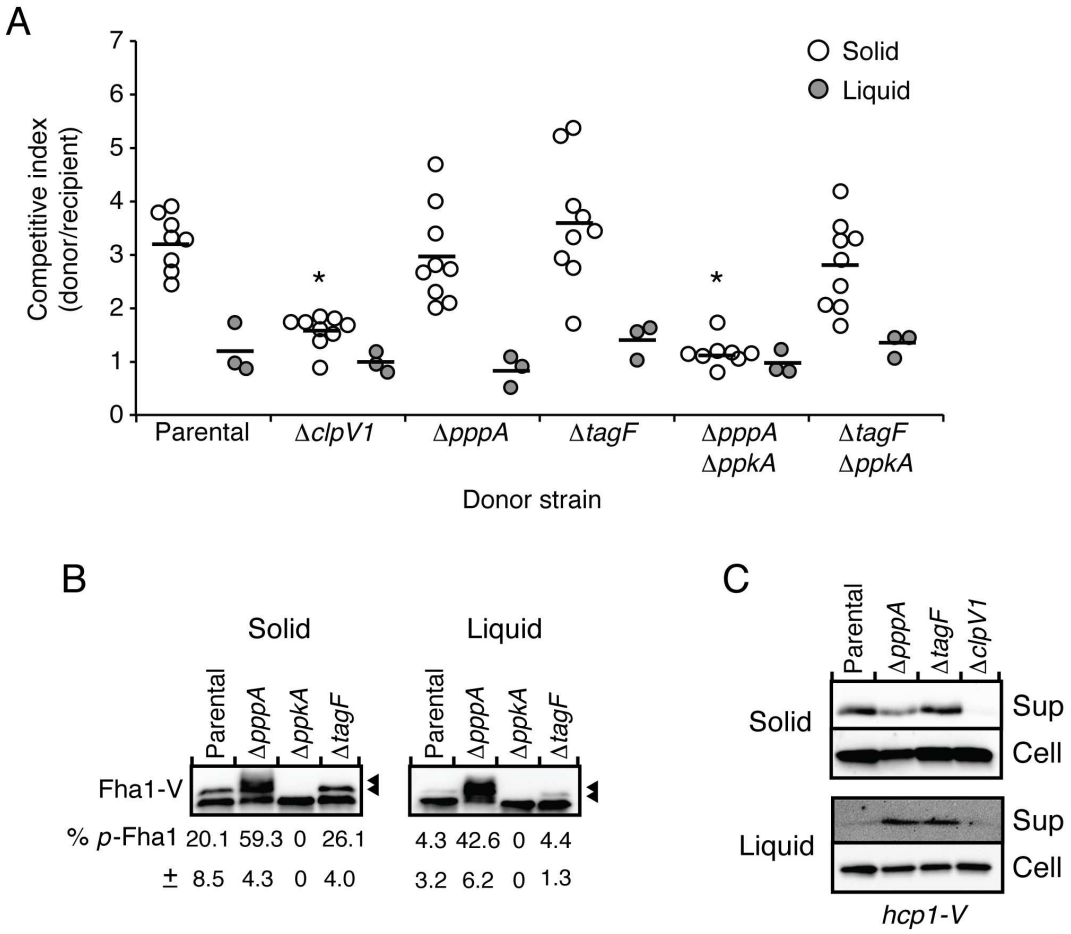


**Figure 2.7: The H1-T6SS is posttranslationally activated by the TPP when *P. aeruginosa* is grown on a surface.** (A) Deletions in *pppA* or *tagF* do not influence T6S-dependent fitness. Results of growth competition assays conducted on a solid surface (open circles) or in liquid media (filled circles) between the indicated donor strains and a susceptible recipient (Δ*tse2* Δ*tsi2*). Asterisks indicate a competitive index that is statistically lower than the parental strain based on ANOVA followed by Tukey's post-hoc test ($P < 0.05$). (B) *p*-Fha1 levels are increased when *P. aeruginosa* is grown on a surface. Arrowheads denote *p*-Fha1 species. For each strain, the percentage of total Fha1–V in the *p*-Fha1–V form based on band densitometry is provided. Data are normalized to Δ*ppkA*. Error provided is standard deviation based on three independent replicates. (C) Secretion of Hcp1 by the H1-T6SS is triggered by surface growth. Western blot analysis of secreted and cell-associated Hcp1–V.

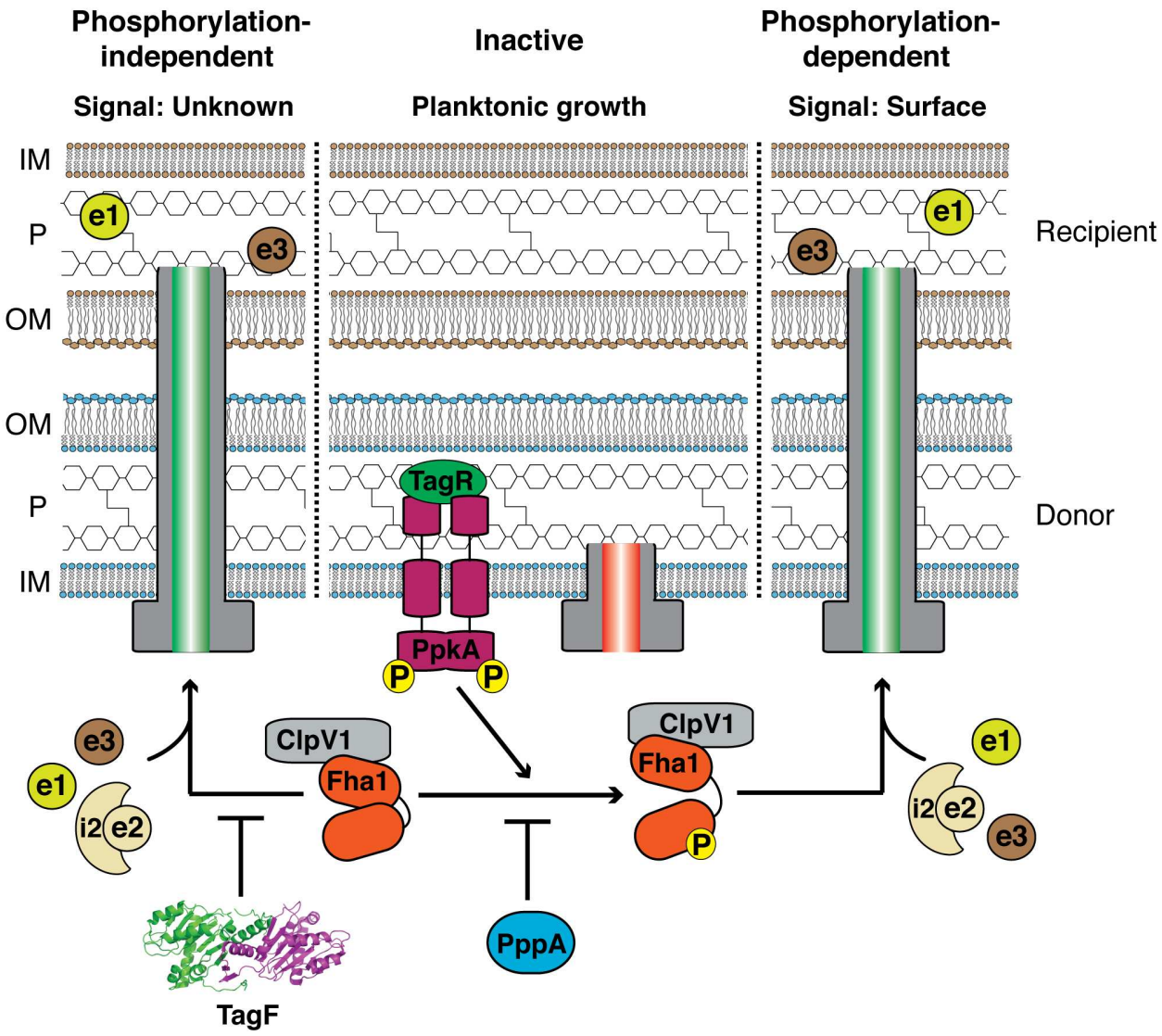


**Figure 2.8: Model of H1-T6SS posttranslational regulatory pathways.** The schematic depicts the interface between *P. aeruginosa* (donor, blue) and a competing Gram-negative bacterium (recipient, brown). Inner membrane (IM), outer membrane (OM), and periplasm (P) of the cells are shown. Emphasis is given to peptidoglycan (interconnected hexagon chains), the target of Tse1 and Tse3 (204). Based on data from this study and previous studies, we propose two pathways for H1-T6SS-activation. During planktonic growth, the H1-T6S apparatus is not extended (red tube) and Tse1-3 (e1-3) secretion is repressed. Upon surface growth, the TPP is stimulated (right). This leads to PpkA activation, *p*-Fha1 formation, ClpV1 recruitment, extension of the apparatus (green tube), and effector delivery into recipient bacterial cells. Relevant phosphorylation events are indicated (yellow spheres). The H1-T6SS can also be activated by derepression of TagF through an unknown signal (left). When TagF repression is relieved, non-phosphorylated Fha1 activates the apparatus by a mechanism also involving ClpV1 recruitment.

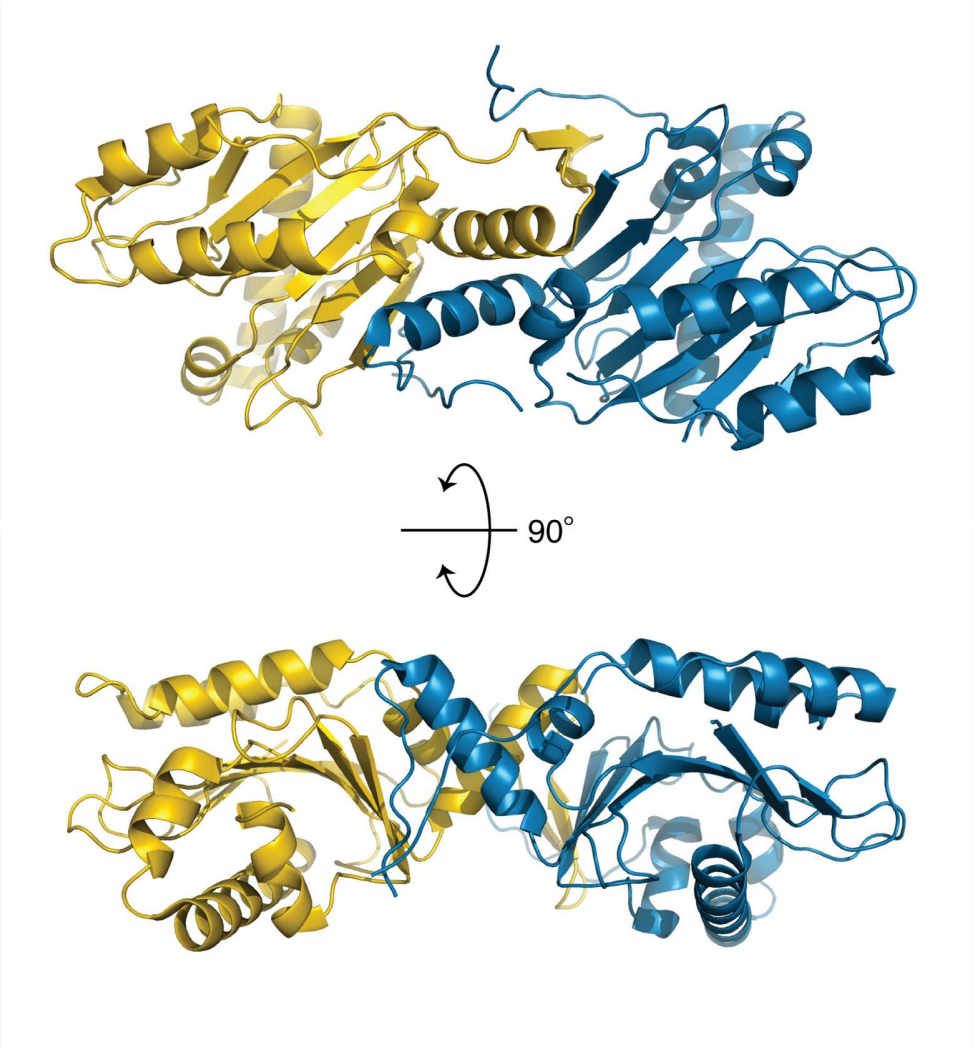


**Figure 2.9: Overview of the X-ray crystal structure of TagF.** Ribbon representation of the proposedTagF biological assembly. The two monomers, colored blue and yellow, are not related by crystallographic symmetry and appear to constitute a biologically relevant dimer. The two views show the dimer rotated ± 90° about the x-axis (accession code 2QNU; 2.05 Å resolution) (83). Images were generated using PyMOL (211).

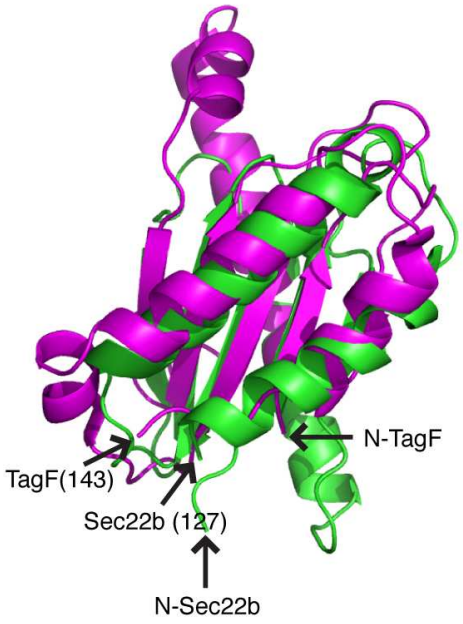


**Figure 2.10: Superimposition of the N-terminal domain of Sec22b (green, accession code 1IFQ, residues 1-127) with TagF** (magenta, accession code 2QNU, residues 1-143). The alignment is based on results obtained using DALI (112). For clarity, the structure of TagF is truncated at the region of overlap with Sec22b and monomerA of TagF is not shown. The positions of the N- and C-terminal residues of both structures are shown.

# CHAPTER III:

## An ABC transporter and an outer membrane lipoprotein participate in posttranslational activation of type VI secretion in *Pseudomonas aeruginosa*

Published as: Casabona, M.G*., Silverman J.M*., Sall K.M., Boyer F., Couté Y., Poirel J., Grunwald J., Mougous J.D., Elsen S., and Attree I. 2013.

*Environmental Microbiology*. 15(2): 471-86.

* Authors contributed equally to this work.

Note: JMS performed secretion assays, interbacterial competition experiments and Fha1 phosphorylation analysis. MGC conducted biochemical analyses and microscopy experiments.

**ABSTRACT**

*P. aeruginosa* is capable of injecting protein toxins into other bacterial cells through one of its three T6SSs. The activity of this T6SS is tightly regulated on the posttranslational level by phosphorylation-dependent and -independent pathways. The phosphorylation-dependent pathway consists of a Threonine kinase/phosphatase pair (PpkA/PppA) that acts on a forkhead domain-containing protein, Fha1, and a periplasmic protein, TagR, that positively regulates PpkA. In the present work, we biochemically and functionally characterize three additional proteins of the phosphorylation-dependent regulatory cascade that controls T6S activation: TagT, TagS and TagQ. We show that similar to TagR, these proteins act upstream of the PpkA/PppA checkpoint and influence phosphorylation of Fha1 and, apparatus assembly and effector export. Localization studies demonstrate that TagQ is an outer membrane lipoprotein and TagR is associated with the outer membrane. Consistent with their homology to lipoprotein outer membrane localization (Lol) components, TagT and TagS form a stable inner membrane complex with ATPase activity. However, we find that outer membrane association of T6SS lipoproteins TagQ and TssJ1, and TagR, is unaltered in a Δ*tagTS* background. Notably, we found that TagQ is indispensible for anchoring of TagR to the outer membrane fraction. As T6S-dependent fitness of *P. aeruginosa* requires TagT, S, R and Q, we conclude that these proteins likely participate in a trans-membrane signaling pathway that promotes H1-T6SS activity under optimal environmental conditions.

**INTRODUCTION**

Bacteria cope with their environment through an arsenal of secreted macromolecular products that are transported across the bacterial envelope by protein complexes called secretion systems.

Gram-negative bacteria possess six secretion machineries, each of divergent composition and function (21, 66). *P. aeruginosa*, an opportunistic human pathogen associated with a variety of acute and chronic diseases, possesses five of these, including the T3SS and T6SS (21). A defining feature of these two protein export machines is that they allow for the export of cargo proteins directly into eukaryotic and/or prokaryotic cells (54, 215). While the composition and mechanism of the T3SS has been studied in great detail (92, 160), the existence of T6SS has been described only recently and their function and composition are still largely unexplored.

T6SSs are encoded by genes organized in operons within genetic islands. In some instances, multiple T6SS are present in a given bacterial genome (27, 41, 84). Bioinformatic studies revealed that T6SSs are composed of 13 highly conserved core components and a set of additional proteins termed Tags (type six secretion-associated genes) (27, 218). Two core components are similar to IcmF and DotU of T4SSs (89, 154), and one protein, ClpV, belongs to a family of AAA+ ATPases (25). A hallmark of all T6SS is the presence of two conserved proteins, Hcp and VgrG. These proteins share sequence and structural homology with tail tube and spike proteins of bacteriophage, respectively (142, 166, 192, 194), and are proposed to form an injection device. Some specialized VgrG proteins possess C-terminal domains that contain eukaryotic cell effector activities. An example is VgrG-1 of *V. cholerae*, which can cross-link host actin (192).

HSI-I to III of *P. aeruginosa* encode three potential T6SSs. The H1-T6SS has been shown to be active in chronic *P. aeruginosa* infections, as sputum of chronically infected cystic fibrosis patients contains Hcp1 and the serum of these patients shows the presence of Hcp1-specific

antibodies (166). Furthermore, a mutation in HSI-I operons affected the survival of *P. aeruginosa* in a rat model of chronic respiratory infection (190). The H1-T6SS specifically exports at least three proteins, Tse1, Tse2 and Tse3. These proteins are important for fitness in interbacterial competition assays (113). While the target of Tse2 is not known, Tse1 and Tse3 are toxins targeting peptidoglycan of adjacent bacteria (204).

As with other secretion systems of *P. aeruginosa*, the H1-T6SS is finely regulated at several levels. Goodman *et al*. have shown that HSI-I operons are posttranscriptionally regulated by the Gac/Rsm pathway. Two sensor kinase/response regulator hybrid proteins, RetS and LadS, reciprocally regulate the H1-T6SS through this pathway (96, 165). A second level of regulation is exerted directly on H1-T6SS activity and depends on a set of accessory genes within HSI-I **(Figure 3.1)**. Among the proteins encoded by these genes are a trans-membrane threonine protein kinase, PpkA, a PP2C-type phosphatase, PppA, and a periplasmic protein, TagR, which promotes dimerization-induced activity of the kinase (115, 167). The cytoplasmic target of PpkA is a ForkheadAssociated domain (FHA)-harbouring protein, Fha1. Fha1 is in a complex with the ClpV1 ATPase, and upon phosphorylation of Fha1, effector export is triggered (115, 167). This regulatory pathway will be referred to hereafter as the TPP (222). Reminiscent of T3SS activity, the intoxication of target cells by T6S effectors requires close cell–cell contact (104, 186). Interestingly, the TPP is stimulated when *P. aeruginosa* is grown on a surface, as observed by increased levels of phosphorylated Fha1 and Hcp1 secretion (222). These findings suggest that the TPP responds to specific physiological stimuli. In addition to this pathway, TagF, a protein encoded upstream of *pppA*, has been reported to function as a negative posttranslational regulator of the H1-T6SS that acts independently of the TPP (222).

Three uncharacterized genes, *tagT*, *tagS* and *tagQ*, neighbour genes involved in the TPP. In the current study, we found that the proteins encoded by these genes act upstream of PpkA in the TPP and are required for efficient protein transport through the T6S machinery. We demonstrated that in a heterologous host, TagT and TagS form a membrane-bound complex with ATPase activity, features characteristic of bacterial ABC transporters. We also investigated the localization of TagQ and showed that its outer membrane localization requires a conserved cysteine within the lipo-box sequence. TagQ, but not TagTS, is required for association of the kinase activator, TagR, with the outer membrane fraction. These findings, together with *in silico* analysis of available genomes, illustrate the complexity and novelty of trans-membrane signaling that lead to tuning of H1-T6SS activity.

## RESULTS

**TagT, TagS and TagQ participate in posttranslational regulation of the H1-T6SS.** TagT, TagS and TagQ are non-conserved T6SS components (27) encoded within the HSI-I operon that contains each of the known posttranslational regulators of the system (*tagR*, *ppkA*, *pppA* and *tagF*) (115, 167, 222). Furthermore, conserved synteny of *tag* genes with *ppkA* and *pppA* in *Pseudomonas species*, *Pseudomonas fluorescens*, *Pseudomonas mendocina* and *Pseudomonas brassicacearum* (http://www.pseudomonas.com/), suggests their functional relationship **(Figure 3.1)**.

Our previous work on the H1-T6SS has shown that the basal activation of the system in wild-type cells is exceedingly low. Indeed, under planktonic conditions, the quantity of secreted Hcp1 is below standard detection levels. However, using more sensitive detection methods, we found

that basal Hcp1 secretion levels can be distinguished from background levels observed in an H1-T6SS-inactive strain (*ΔppkA*) **(Figure 3.2A)**. In this study, we utilize this basal level of Hcp1 secretion as a means to investigate genes involved in H1-T6SS activation. To evaluate the contribution of TagT, TagS and TagQ to T6S activity, Hcp1 secretion levels were assayed in strains with *tagT*, *tagS* or *tagQ* deletions. Secreted Hcp1 levels of these strains were compared with strains that abrogate Hcp1 secretion (Δ*ppkA* and Δ*tagR*). As shown in **Figure 3.2A**, individual isogenic PAO1 mutants (Δ*tagT*, Δ*tagS* and Δ*tagQ*) were impaired in Hcp1 export.

The H1-T6SS exports three low-molecular weight effectors encoded by genes outside of the HSI-I locus, Tse1, Tse2 and Tse3 (113). To determine the effect of *tagT*, *tagS* and *tagQ* genes on Tse export, we analysed secretion levels of Tse1 in the mutant strains. To detect Tse1, a chromosomal fusion of vesicular stomatitis virus G encoding sequence (VSV-G) to *tse1* (Tse1–V) was used (113). As in the case of Hcp1, the quantity of secreted Tse1–V was decreased in strains lacking *tagT*, *tagS* and *tagQ*. To gain information regarding the functional hierarchy of the Tag proteins relative to the TPP, we examined Hcp1 and Tse1 export in mutants prepared in the Δ*pppA* background. Strains lacking both the tag genes and *pppA* did not display a decrease in Hcp1 secretion levels **(Figure 3.2B)**, suggesting that these proteins represent regulatory accessory components that act upstream of the kinase/phosphatase checkpoint. Interestingly, the deletion of *tagS* in strains lacking *pppA* reproducibly resulted in higher levels of exported Hcp1, but not Tse1, relative to *pppA* and the other tag genes. Possible explanations for this finding are discussed below.

Phosphorylation of Fha1 requires PpkA and is promoted by growing bacteria on solid medium (222). To determine if TagT, TagS and TagQ affect phosphorylation of Fha1, we assayed phosphorylated Fha1 (*p*-Fha1) levels in tag deletion strains. A chromosomal *fha1*-VSV-G fusion was used and *p*-Fha1 levels were detected by electrophoretic mobility shift **(Figure 3.2C)**. Consistent with previous studies, we observed an increase in *p*-Fha1 levels in the wild-type background when grown on solid versus liquid media. Interestingly, individual tag deletion strains abrogated surface growth-dependent *p*-Fha1 levels. As expected, under liquid growth conditions, only low levels of *p*-Fha1 were detected in all strains containing PppA. Taken together with the secretion phenotypes observed, these results suggest that TagT, TagS and TagQ act upstream of PpkA in the TPP.

***tagT, S* and *Q* are required for T6S-dependent fitness.** Previous studies have shown that the TPP activates the H1-T6SS during surface growth and therefore is required for H1-T6S-dependent fitness against competing bacteria (222). We hypothesized that if TagT, S and Q act upstream of PpkA in the TPP, these proteins should contribute to H1-T6SS-dependent fitness. Using growth competition assays, we assessed the fitness of donor strains containing in-frame deletion of *tagT, S* or *Q* relative to a Tse2-sensitive recipient strain (Δ*tse2* Δ*tsi2*) **(Figure 3.2D)**. This experiment confirmed that *tagT, S* or *Q* are required for H1-T6SS-dependent fitness. As an additional control, we included a donor strain lacking TagR, a protein previously demonstrated to act upstream of PpkA in the TPP. This strain also displayed a loss of H1-T6SS-dependent fitness. Together with their involvement in promoting surface-dependent Fha1 phosphorylation, these findings support a critical role for TagT, S and Q in TPP activation during surface growth.

**TagT and TagS form a membrane-bound complex with ATPase activity.** TagT and TagS share sequence signatures with bacterial ABC transporters (61). The *tagT* gene encodes a protein of 26 kDa with Walker domains (Walker A and Walker B) and other conserved features of ATPases associated with ABC transporters as shown in **Figure 3.3A**. The *tagS* gene encodes a protein of 42 kDa, predicted to be an integral membrane protein with four hydrophobic trans-membrane helices (TMH) and a long periplasmic segment of 233 amino acids between TMH1 and TMH2. BLAST analysis showed high homology of TagS and TagT with membrane components of the lipoprotein outer membrane localization (Lol) complex (173), sharing 56.0%/38.5% and 40.0% similarity with LolE/LolC and LolD of P. aeruginosa, respectively (233) **(Figure 3.3A)**. Based on sequence homology, the predicted TagT protein belongs to a family of MecA/FtsE/SalX ATPases of bacterial ABC transporters (see also Discussion).

To investigate the mechanism by which TagT, S and Q regulate the H1-T6SS through the TPP, we purified the proteins and conducted biochemical analyses. Co-production of TagT and TagS resulted in formation of a stable protein complex associated with *E. coli* membranes that could be solubilized by a detergent and purified to homogeneity by affinity chromatography **(Figure 3.3B)**. As mentioned previously, TagT harbours all conserved signatures of classical ATPases. In order to test whether the TagTS complex is capable of ATP hydrolysis, the complex was incubated in the presence of ATP and magnesium and the formation of inorganic phosphate (Pi) was quantified by a malachite green method (240). Notably, the TagTS complex displayed significant ATPase activity varying, in three independent purifications, between 70 and 100 nmol Pi min−1 mg−1. The specific activities of the TagTS complex was consistent with activities of several bacterial ABC transporters reported to date (198, 239, 247). Moreover, the ATPase

activity of the complex was sensitive to orthovanadate **(Figure 3.3C)**, a small organic molecule that impedes ATP hydrolysis by interfering with binding of ATP to the Walker A motif (187). Finally, to confirm that ATP hydrolysis was due to the TagTS complex, we replaced a conserved amino acid within the Walker A motif of TagT (K/A: Lys 44 to Ala) and purified the complex **(Figure 3.3B)**. The K/A mutation abolished ATPase activity of the TagTS complex **(Figure 3.3C)**. In conclusion, these results clearly show that the TagTS complex possesses ATPase activity that is dependent on the conserved Walker A motif within the TagT ATPase.

**TagQ encodes an outer membrane lipoprotein.** The last gene of the operon, *tagQ*, encodes a 31.7 kDa protein with a stretch of hydrophobic and uncharged amino acids at the N-terminus. This sequence is characteristic of a signal peptide and conserved lipo-box with an invariable Cysteine, a sequence recognized by signal peptidase II **(Figure 3.4A)** (11). In order to study the localization of TagQ in *P. aeruginosa*, we created a fusion protein between TagQ and the red fluorescent protein mCherry, and examined its localization by confocal microscopy using green fluorescent protein (GFP)-expressing P. aeruginosa strains (GFP TagQ-mCherry). TagQ-mCherry was readily detected and localized around the periphery of bacterial cells **(Figure 3.4A)**. To gain information on the precise localization of TagQ, *P. aeruginosa* cells were treated with lysozyme to create spheroplasts, bacterial cells lacking the peptidoglycan layer. *P. aeruginosa* spheroplasts, while maintaining an intact internal membrane, appear to have a crescent-shaped external membrane as it begins to dissociate from the rest of the spheroplast (148). When *P. aeruginosa* GFP TagQ-mCherry was treated to obtain spheroplasts, the majority of cells retained mCherry fluorescence in the crescent-shaped labelling pattern particularly visible under xyz scan **(Figure 3.4A)**, strongly suggesting the association of TagQ with the outer

bacterial membrane. Lipid modifications occur at a conserved cysteine within a lipo-box sequence of lipoproteins and promote its association with membranes. To test the requirement for Cys30 in TagQ-mCherry localization, we created a mutant fusion protein, TagQΔCys-mCherry, and checked its localization **(Figure 3.4A)**. *P. aeruginosa* GFP TagQΔCys-mCherry cultures systematically showed a mixed population, with the majority of cells harbouring mCherry at the periphery and some cells displaying overlapping cytoplasmic GFP and mCherry. This result suggests that the absence of Cys30 affects the efficient transport of the protein across the inner membrane. The majority of spheroplasts obtained from TagQΔCys-mCherry P. aeruginosa lost outer membrane labeling, strongly suggesting that in most cases the protein had lost its lipid anchor and was released by lysozyme treatment **(Figure 3.4A)**. These observations were immuno-quantified by fractionation of membranes and periplasm of Δ*tagQ* strains ectopically expressing wild-type *tagQ* or *tagQΔCys* **(Figure 3.4B)**. The deletion of Cys30 resulted in partial processing of the protein, as two anti-TagQ-specific polypeptides were visualized in total bacterial extracts. In addition, while the majority of wild-type TagQ was found to be associated with membrane fractions, the majority of the mutated protein was recovered in periplasmic fractions, in concordance with confocal microscopy observations.

**The Lol-like TagTS complex is dispensable for OM localization of TagQ and TssJ1.** As the TagTS complex shows significant homology with lipoprotein recycling systems of *E. coli* and *P. aeruginosa*, we first hypothesized that this complex is involved in the transport of specific lipoproteins of the H1-T6SS. To compare membrane distribution of TagQ in different strains, we set up membrane fractionation experiments on discontinuous sucrose gradients coupled to immuno-detection. These experiments were performed using *P. aeruginosa* Δ*retS* background to

obtain higher expression of the whole HSI-I locus. The quality of separation between inner (IM) and outer membranes (OM) was systematically determined by measuring the activity of NADH oxidase and by Coomassie blue staining of SDS-PAGE gels of each recovered fraction. As shown in **Figure 3.4C**, in accordance with microscopy experiments, the majority of TagQ was found in OM fractions. In order to determine whether the Lol-like ABC transporter TagTS was involved in localization of TagQ, we fractionated membranes of Δ*retS* Δ*tagTS* in an identical manner and detected no significant difference of TagQ distribution between the two strains **(Figures 3.4C and 3.5)**. The second lipoprotein of the H1-T6SS is TssJ1 (PA0080). TssJ1 shares 50% similarity with OM lipoprotein SciN involved in assembly of the Sci-1 T6SS of enteroaggregative *E. coli* (7). To ascertain whether TssJ1 is targeted to the OM in *P. aeruginosa*, we constructed a fusion between TssJ1 and mCherry, and examined its localization by confocal microscopy (not shown) and by fractionation on discontinuous sucrose gradients. Similar to our findings with TagQ, TssJ1-mCherry associated with the OM and its localization was not significantly altered in the *tagTS* mutant **(Figure 3.6)**. Together these results show that the ABC transporter TagTS, despite its strong homology to the Lol system, does not participate in membrane targeting of two H1-T6SS-specific lipoproteins.

**TagQ is required for TagR association with the OM.** Preliminary nanoLC/LC mass spectrometry data performed on inner and outer membrane fractions (M.G. Casabona and Y. Couté, unpublished) indicated the presence of TagR, a positive regulator of the TPP, in OM fractions. This result was intriguing, as TagR is predicted to be a soluble protein and was shown to fractionate with the periplasm, wherefrom it promotes dimerization and activation of PpkA (115). To further address the localization of TagR, we raised anti-TagR antibodies and analysed

fractionated membranes from wild-type PAO1, confirming that at least one portion of TagR associated with outer membranes **(Figure 3.7)**. This association was significant, as a soluble periplasmic protein, DsbA, was not found in any of the membrane fractions (not shown). Whereas TagR OM localization was not altered in a *tagTS* mutant **(Figure 3.8)**, the absence of *tagQ* clearly influenced the distribution of TagR between inner and outer membrane fractions **(Figure 3.7)**. In accordance, a strain expressing *tagQ*ΔCys in trans, resulted in TagR mislocalization, demonstrating that OM-anchored TagQ is essential for OM localization of TagR. Of note, TagR was found dispensable for OM localization of the TagQ lipoprotein **(Figure 3.9)**.

**In silico genome wide analysis of TagTSR-like systems.** Participation of the TagTS complex in trans-membrane signalling involving a periplasmic protein TagR and an inner membrane-bound Ser/Thr kinase prompted us to perform in silico analysis of all available complete bacterial genomes to search for homologues of these proteins. Both TagT and TagS attributed COGs (COG1136-COG4591) are frequently adjacent to other ABC transporter-specific COGs involved in peptide and drug transport, specifically COG0845 and COG0577 which are membrane components of the AcrA and SalY family of multidrug efflux pumps and antimicrobial peptides transport systems, respectively. We found also two strong associations between COG1136-COG4591 tandem and regulatory partners. In 90 Firmicutes, ABC transporters are encoded adjacent to homologues of the OmpR family two-component regulatory system (COG0642 and COG0745). In addition, in 100 Enterobacteriaceae, ABC transporters are encoded upstream of NagC (COG1940), a transcriptional regulator involved in sugar transport. This observation suggests a more general functional relationship between the TagTS family of ABC transporters

with trans-membrane signalling and regulation. Finally, we examined the local organization of chromosomal regions encoding the ATPase component (TagT, COG1136), the predicted permease component (TagS, COG4591) and COG1262 (TagR) in all available microbial genomes. TagQ was excluded from this screen as it lacks an attributable COG number. As shown by a maximum likelihood tree **(Figure 3.10)**, tagT, S and R are predominately found within T6SS-encoding loci in Pseudomonas (*P. aeruginosa*, *Pseudomonas fulva*, *P. fluorescens*, *P. brassicacearum*). We found that in *Rhodobacter sphaeroides*, an α-proteobacterium that possess a T6SS locus with similar gene content of HSI-I, *tagT, S* and *R* are neighbouring genes coding for PpkA and PppA homologues. However, *tagT, S* and *R* are not exclusively found in bacterial genomes encoding T6SS, suggesting that these components may play a role in different cellular processes.

**DISCUSSION**

Our current study identified TagT, TagS and TagQ as new components of a posttranslational regulatory pathway that modulates the activity of the H1-T6SS of *P. aeruginosa*. We found that these components participate in a phosphorelay system that is stimulated by surface growth conditions. Phosphorelay systems are classical ways for bacteria to regulate adaptive cellular responses induced by external stimuli; however, to our knowledge, this is the first example of an ABC transporter complex, TagTS, participating in trans-membrane signalling that involves a Ser/Thr kinase-dependent phosphorylation pathway.

Some parallels can be made with a large family of ‘co-sensor’ ABC transporters that interact with membrane-integrated histidine kinases (HK) (235, 236). These proteins clearly play a

regulatory role in adaptive responses to certain environmental stimuli (236). This is well illustrated by the ABC transporter PstSCAB of *E. coli* that is linked to sensing inorganic phosphate in phosphate-limiting conditions. It has been proposed that the membrane components of this ABC transporter transmit the signal towards the membrane-integrated HK, PhoR, which signals to a transcriptional regulator (response regulator, RR) (158). A role for related systems in resistance against antimicrobial peptides was recently proposed (56, 67). For example, it has been experimentally demonstrated in *Staphylococcus aureus* that the detection of, and response to, antibiotic peptide bacitracin requires the interplay between two ABC transporters, BraD/BraE and VraD/VraE, and the HK/RR system BraS/BraR (109). Interestingly, our in silico analysis showed that genes encoding TagTS-like proteins (COG1136-COG4591) frequently co-occur with genes encoding proteins that participate in two component-regulatory systems. In addition, our in silico analysis highlights the association of TagTS-like proteins with NagC, a transcriptional regulator involved in the response to N-acetylglucosamine and peptidoglycan in *E. coli* and *P. aeruginosa* (130, 185), further implying their participation in signal recognition and transmission. It is worth noting that in at least one non-Pseudomonas T6SS, *Vibrio anguillarum*, an inner membrane polypeptide belonging to a major facilitator superfamily of transporters is required for regulating Hcp export and two additional periplasmic proteins contribute to this signalling (248).

The TagTS complex could be involved in export or import of a small molecule required for activating the H1-T6SS, or it may play a structural role by stabilizing other Tag proteins. Future experiments aim to determine whether TagT ATPase activity and a long periplasmic loop present in TagS are required for its role in signalling. The apparent conflicting effects on Hcp1 export

between Δ*pppA* Δ*tagS* versus Δ*pppA* Δ*tagTS* **(Figure 3.2)** suggest a possible second role for the integral inner membrane domain of TagS, independent of its ATPase partner, TagT. Interestingly, a long periplasmic loop present in TagS-related proteins, LolC and BraB, mediates the detection of cognate substrates, lipoproteins and bacitracin respectively, and it was proposed, for BraB, to interact through the inner membrane with the HK partner.

Outer membrane-localized TagQ is a top candidate for signal detection. The region from amino acids 68 to 114 of TagQ is annotated as PF05433, a family of proteins that include several Rickettsia genus specific 17 kDa surface antigens, annotated also as a conserved trans-membrane alpha-helical region containing glycine zipper motifs (http://pfam.sanger.ac.uk). There is rising evidence that OM lipoproteins play crucial roles in trans-membrane signaling in bacteria. A well-characterized example is the Rcs phosphorelay in *E. coli*, which reflects envelope stress response activated by peptidoglycan stress and antibiotics. In this complex system, RcsF, an OM lipoprotein, is proposed to transmit the signal to the IM-located HK sensor and allow further signal transduction from the cell envelope to the cytoplasm (79, 147).

What may be the link between IM TagTS, OM TagQ and the IM PpkA-kinase? The finding that some portion of TagR is also associated with the OM indicates that TagTS, TagR and TagQ may represent a unique complex participating in trans-membrane signaling. Taking into account the sequence predictions for TagR, its role in signal transduction, and our current findings, we hypothesize that TagR associates with membranes through interactions with other OM proteins, such as TagQ. The distribution of TagR between inner and outer membranes was clearly affected

by the absence of TagQ, leaving open the possibility that TagQ may correctly position TagR to interact with the kinase.

Finally, what is the nature of the signal(s) that activate the H1-T6SS? Silverman et al. discovered that surface growth of *P. aeruginosa* induces the TPP (222), and, here, we show that *tagQ*, *tagR*, *tagS* and *tagT* are important in surface-induced phosphorylation of Fha1. Moreover, using growth competition assays we showed that the fitness of Tag mutants was impaired. All together these results imply that the predicted ABC transporter, TagTS, and the OM lipoprotein TagQ are essential players in intrabacterial communication through H1-T6SS activity. The rapid detection of neighbouring cells may thus be essential to turning on the injection device.

Although we have no evidence yet demonstrating direct interactions between the four Tag proteins (except for TagT and TagS) and the kinase, PpkA, we propose a model **(Figure 3.11)** in which TagTS and TagQ participate in detection and transmission of an environmental signal to PpkA, by modulating either localization or conformation of the kinase activator TagR, leading to rapid response of «attacking» bacteria in highly competitive multi-species niches, such as infecting tissue. Our future work will aim at discovering the signal nature and deciphering the connections between Tag proteins and their link with other components of trans-membrane signaling in T6SS.

## MATERIALS AND METHODS

**Genetic constructions.** Genes of interest were PCR amplified using PAO1 genomic DNA as a template, cloned into pCR-Blunt II-TOPO (Invitrogen) and sequenced before cloning into final

destination vectors. The list of oligonucleotides with appropriate restriction sites is given in Table S1. For overexpression, *tagT* and *tagTS* were amplified and cloned into pETDuet-1. In the pETDuet-*tagTS* bicistronic vector, only *tagT* is fused to a histidine tag encoding sequence. For Hcp1 overexpression, the gene was cloned into pET52b giving Hcp1-Strep fusion. The *tagQ* gene was amplified so that it lacks the sequence encoding the first 29 amino acids and the predicted lipo-box (TagQΔ2-30). It was cloned into pET15b by fusing *tagQ* to a sequence encoding hexa-histidine tag on N-terminus. For TagR overproduction, the *tagR* gene was amplified and cloned into pET52b resulting into TagR-His10 protein. All fusions to mCherry were constructed using pJN105-derived plasmids, which contain an arabinose inducible promoter. The gene encoding mCherry was amplified and cloned into XbaI and SacI sites of pJN105 (175) giving pJN-mCherry. The DNA sequence containing the ribosome binding site of tagQ and the whole gene was cloned upstream of mCherry-encoding gene using EcoRI and XbaI sites, giving pJN-tagQ-mCherry. *tssJ1*-encoding sequence was amplified and cloned in the same manner to give pJN-*tssJ1*-mCherry. Site-directed mutagenesis (QuikChangeII Site-Directed Mutagenesis kit, Stratagene) was employed to generate TagTK/AS mutant and TagQΔCys, using pETDuet-*tagTS* and pJN-*tagQ*-mCherry as templates respectively. The TGA stop codon was introduced between TagQ and mCherry encoding sequence by site directed mutagenesis using pJN-*tagQ*-mCherry and pJN-*tagQ*ΔCys-mCherry. To constitutively express GFP, pX2-*gfp* (238) was transferred in mini-CTX1 (110)and inserted into the chromosome of *P. aeruginosa* strains as described. All replicative plasmids were introduced in *P. aeruginosa* strains by transformation. Constructs used to generate in-frame deletions of *tag* genes or a *tse1*-VSV-G chromosomal fusion were previously reported (222).

*P. aeruginosa* strains were grown in Luria-Bertani (LB) medium at 37°C supplemented with carbenicillin 100–250 µg ml−1, gentamycin 200 µg ml−1 and tetracycline 200 µg ml−1 when needed. *E. coli* strains were grown in LB medium at 37°C supplemented with ampicillin 100 µg ml−1, gentamycin 50 µg ml−1, kanamycin 25 µg ml−1,tetracycline 10 µg ml−1 as required.

**Fha1 phosphorylation assays.** Cellular samples of Fha1 from liquid and solid grown cultures were prepared and analysed as previously described (115, 167). Western blots were developed using chemiluminescent substrate (SuperSignal West Pico Substrate, Thermo Scientific) and imaged with a FluorChemQ (ProteinSimple). Densitometry was performed as previously described (222) using AlphaView®Q software (ProteinSimple). The percentage of phosphorylated Fha1 was determined by measure band intensity of phosphorylated and total Fha1 from three independent experiments. The values were normalized to Δ*ppkA*, which was set at 0% *p*-Fha1.

**Interbacterial growth competition assays and quantification.** Growth competition assays were performed as previously described (222). Each donor and recipient strain contained constitutively expressing yellow fluorescent protein (YFP) or cyan fluorescent protein (CFP) respectively. pUCP18-mini-Tn7 containing *yfp* or *cfp* (inserted at the neutral phage attachment site, attB) was used to construct these strains (136). The plasmids were introduced into *P. aeruginosa* via four-parental mating conjugation or electroporation (47). Vector backbones were not removed. To observe an H1-T6SS-dependent fitness advantage, Tse2 and Tsi2 were overexpressed in the donor strain. Donor strains harboured pPSV18::PA2702-PA2703 for constitutive expression of Tse2 and Tsi2, and recipient strains harboured the empty vector,

pPSV18 (201). Overnight cultures were mixed at a 1:1 ratio to a total density of approximately 1.0 × 108 cfu ml−1 in 1 ml of LB medium. Competitions were grown on 0.2 µM polycarbonate membranes on LB agar for 18 h at 37°C, or in 2 ml of LB with shaking. Cells were re-suspended in LB medium and spotted onto 1.0% agarose PBS pads and imaged as described (222). YFP and CFP filters were used to image the two cell populations. Assays were performed in triplicate. Three fields containing 100 to 200 cells were imaged for each competition. To determine the competitive index (the number of YFP positive cells to CFP positive cells), NIS-Elements computer-assisted morphometry was used to count YFP and CFP cells.

**TagTS expression and protein purification.** *E. coli* BL21(DE3) Star cells harbouring pETDuet-*tagTS* were grown in LB medium at 37°C and 200 r.p.m. At OD600 of 0.7, the expression of *tagT* and *tagS* was induced with 0.5 mM IPTG for 4 h. Cells were recovered by centrifugation and lysed in buffer containing 25 mM Tris-HCl, 500 mM NaCl, 10 mM imidazole, pH 8.0 and cocktail of protease inhibitors (PIC, Roche). The lysis was achieved by passage of cells through a Microfluidizer (M-100P, Microfluidics, USA) at constant pressure of 10 000 psi. After centrifugation at 200 000 g for 1 h, membranes were recovered in solubilization buffer containing 25 mM Tris-HCl, 500 mM NaCl, 2% n-dodecyl-β-D-maltopyranoside (DDM), 15% glycerol, pH 8.0 and PIC. The solubilization was performed in a glass beaker at 4°C for 1 h 30 min by agitation. The obtained suspension was further centrifuged at 200 000 g for 1 h. Solubilized material was loaded at 0.5 ml min−1 on HisTrapHP Ni2+-column previously equilibrated in solubilization buffer. The washes and elution was performed on AktaPurifier FPLC apparatus (GE Healthcare) with buffer A (25 mM Tris-HCl, 500 mM NaCl, 0.05% DDM, 15% glycerol, pH 8.0) and buffer B (25 mM Tris-HCl, 500 mM NaCl, 0.05% DDM, 15%

glycerol, 200 mM imidazole, pH 8.0). The washes were performed with 30 and 80 mM imidazole obtained by mixing buffers A and B, and elution was performed using buffer B. Fractions eluted from the column were analysed on SDS-PAGE and the gel was stained by Coomassie Brillant Blue R-250.

**ATPase activity and orthovanadate assay.** ATPase activity was quantified by measuring inorganic phosphate Pi by a malachite green method (240). The reaction mixture (100 µl) containing 0.5 mM ATP, 1 mM MgCl2 and 10 mM Tris-HCl, pH 7.5, and 1 µg of purified TagTS complex was incubated for 30 min at 37°C. When indicated, the orthovanadate was added to protein samples at indicated concentrations before the reaction. The reaction was stopped by adding 800 µl of malachite green solution. Malachite green solution was prepared 30 min in advance by mixing 3 vols of 0.045% malachite green with 1 vol. of 4.2% ammonium molybdate in 4 M HCl and 1/50 of volume of Triton X-100. Greenish colour resulting from precipitation of Pi was measured at 640 nm.

**Secretion assays.** Overnight cultures were diluted at $OD_{600}$ of 0.02 and incubated at 37°C with shaking up to mid-log phase, in the presence of antibiotics when needed. At this point, 250 µl of bacteria were harvested by centrifugation at 7000 g and re-suspended in 100 µl of loading buffer and stored at −20°C until use. Extracellular proteins were precipitated by a TCA-sarkosyl method (0.5% final volume of sarkosyl and 7.5% final volume of TCA) (46) after a double centrifugation of 1250 µl of culture and 1 h incubation on ice. Pellets were re-suspended in a final volume of 25 µl of loading buffer. Samples were then analysed by SDS-PAGE and immunoblotting.

**Proteomic analyses by mass spectrometry (MS).** Protein bands were manually excised from the gels and washed. Proteins were in-gel digested with trypsin (Promega, sequencing grade) and peptides extracted from gel slices (Shevchenko et al., 1996). The dried extracted peptides were re-suspended in 5% acetonitrile and 0.1% trifluoroacetic acid and analysed by online nanoLC-MS/MS (Ultimate 3000, Dionex and LTQ-Orbitrap XL, Thermo Fischer Scientific). The nanoLC method consisted in a 15 min gradient ranging from 5% to 40% acetronitrile in 0.1% formic acid at a flow rate of 300 nl min−1. Peptides were sampled on a 300 µm × 5 mm PepMap C18 precolumn and separated on a 75 µm × 150 mm RP column (PepMap C18, Dionex). MS and MS/MS data were acquired using Xcalibur (Thermo Fischer Scientific) and processed automatically using Mascot Daemon software (version 2.3, Matrix Science). Searches against the PAO1 database, SwissProt-Trembl_decoy (*E. coli* taxonomy) and contaminants databases (534637 sequences) were performed using an in-house version of Mascot 2.3. ESI-TRAP was chosen as the instrument, trypsin/P as the enzyme and two missed cleavages was allowed. Precursor and fragment mass error tolerances were set respectively at 10 ppm and 0.6 Da. Peptide modifications allowed during the search were: Carbamidomethyl (C, fixed), Deamidated (NQ, variable), Oxidation (M, variable) and Acetyl (Protein N-term, variable). The IRMa soft (Dupierris et al., 2009) was used to filter the results by query homology threshold $P < 0.01$ and a minimum of two peptides per protein.

**Spheroplast preparation and confocal microscopy.** Overnight cultures of *P. aeruginosa*-GFP strains producing TagQ-mCherry, TagQΔC-mCherry or TssJ1-mCherry fusion proteins were diluted at OD600 of 0.15 in 3 ml of LB. Cultures were incubated until mid-log phase of growth

in the presence of antibiotics and then induced for 1.5 h by 0.25% arabinose. At this point, cells were harvested and spheroplasts were created (117). Briefly, 1 ml of culture was centrifuged at 6000 g for 5 min. The pellet was re-suspended in TSE buffer (0.1 M Tris-acetate, 16% saccharose, 5 mM EDTA, pH 8.2) and lysozyme was added at a final concentration of 50 µg µl−1. Spheroplasts were incubated on ice and centrifuged at 1000 g for 5 min after the addition of $MgSO_4$ to a final concentration of 0.1 M. Finally, spheroplasts were re-suspended in TSM buffer (0.05 M Tris-acetate, 8% sucrose, 10 mM $MgSO_4$, pH 8.2). 1 ml culture of arabinose-induced bacteria was harvested by centrifugation at 7000 g for 5 min and re-suspended in 100 µl of LB.

Specimens were analysed by confocal laser scanning microscopy, using a Leica TCS-SP2 operating system (Manheim, Germany). GFP and mCherry fluorescences were excited and collected sequentially (400 Hz line by line) by using 488 nm for GFP and 543 nm for mCherry excitation. Fluorescence emissions were collected from 500 to 537 nm for GFP and from 557 to 625 nm for mCherry.

**Fractionation of *P. aeruginosa*.** Cultures of *P. aeruginosa* grown for 16 h were diluted to an OD600 of 0.15 in 30 ml of LB cultures with antibiotics when needed. Cultures were incubated with agitation until OD600 of 0.85 and at this point, 100 µl of cells were harvested by centrifugation as a total bacteria fraction. The rest of the cultures was centrifuged at 6000 g for 10 min. Pellets were washed with 10 ml of TMP buffer (10 mM Tris-HCl, 200 mM MgCl2, PIC) and re-centrifuged at 6000 g for 10 min. Pellets were re-suspended in 1 ml of TMP and incubated for 30 min at 300 r.p.m. and 23°C in the presence of 0.5 mg ml−1 lysozyme. Next, bacteria were

centrifuged at 8000 g for 15 min at 4°C, obtaining the periplasm fraction (supernatant) and spheroplasts (pellet). At this point, the proteins present in the periplasm fraction were precipitated (as described in Secretion assays). Spheroplasts were then re-suspended in 1 ml of TMP, recentrifuged and the pellet, recovered in 1 ml of TM buffer (30 mM Tris-HCl, 10 mM MgCl2, pH 8.0), was disrupted by sonication. Unbroken spheroplasts were eliminated by a low speed centrifugation and the supernatant was ultracentrifugated for 30 min at 100 000 g with a TLA120 rotor at 4°C to obtain the cytosolic fraction (supernatant) and the total membrane fraction (pellet). All fractions were re-suspended in loading buffer and heated at 100°C for 10 min before SDS-PAGE and immunoblotting analysis.

**Inner and outer membrane separation.** Inner and outer membranes of *P. aeruginosa* cells were separated by a discontinuous sucrose gradient as described (Viarre et al., 2009). Briefly, 500 ml cultures of *P. aeruginosa* at OD600 of 1 were harvested by centrifugation. In the case of PAO1 Δ*tagQ* + *tagQ*ΔCys, bacteria were grown with appropriate additives and induced by 0.01% arabinose at OD600 0.5. Pellets were re-suspended in 25 ml of 10 mM Tris-HCl, 20% sucrose, 10 mg ml−1 DNase, 10 mg ml−1 RNase, pH 7.4, and were disrupted by using a Microfluidizer at 15 000 psi. Unbroken cells were removed by 15 min centrifugation at 6000 g. Total membrane fraction was obtained by ultracentrifugation at 100 000 g and re-suspended in 500 µl of 20% sucrose containing PIC. The total membrane fraction was then applied at the top of a discontinuous sucrose gradient composed of 1.5 ml layers of 60%, 55%, 50%, 45%, 40%, 35% and 30% of sucrose in 10 mM Tris-HCl, 5 mM EDTA, pH 7.4 (from bottom to top). Sucrose gradients were centrifuged at 90 000 g at 4°C for 36–72 h, and 500 µl of fractions were collected from the top. All fractions were then characterized by SDS-PAGE, Western Blot

analysis and NADH oxidase activity. Antibodies against T2SS protein XcpY (163), kindly gifted by R. Voulhoux (CNRS, Marseille, France), were used as an inner membrane marker and porines visualized directly on Coomassie blue-stained SDS-PAGE as markers of the outer membrane. NADH oxidase activity was determined as described elsewhere by measuring the NADH consumption at 340 nm of 50 µl of each fraction (10).

**Hcp1, TagQ, TagR and Tse1 expression for antibody production.** The pET52b-*hcp1*, pET15b-*tagQ*Δ2-30 and pET15b-*tagR* expression vectors were introduced into E. coli BL21(DE3)Star. Expression was induced at OD600 of 0.7 by 0.5 mM IPTG and lasted for 4 h. Bacteria were lysed by the Microfluidizer at 10 000 psi and the proteins were purified on appropriate affinity columns using AktaPurifier (GE Healthcare). TagR-His10 was obtained by solubilization of inclusion bodies using 6 M guanidine. Antibodies were raised in guinea pig for Hcp1 (Eurogentec, Belgium) and in mouse for TagQ and TagR (Agro-Bio, France).The anti-Tse1 polyclonal rabbit antibody was raised against purified Tse1 (GenScript).

**Immunoblotting.** For Western blotting, antibodies were used at dilutions: anti-Hcp1 1:5000, anti-XcpY 1:1000, anti-TagQ 1:20000, anti-TagR 1:1000 and anti-Tse1 1:2000. Commercial antibodies anti-VSV-G (Sigma Aldrich) and anti-mCherry (Clontech) were used as recommended by the manufacturers. Secondary antibodies were anti-rabbit (Zymed), HRP-coupled anti-guinea pig (Invitrogen) and HRP-coupled anti-mouse (Sigma), all used at 1:5000 dilution. Western blots were developed by ECL Detection Kit (Amersham) or Millipore HRP Substrate.

**In silico bacterial genome scanning for *tagTSR*.** Annotated genomes were downloaded (September 2011) from the Genome Reviews ftp site (ftp://ftp.ebi.ac.uk/pub/databases/genome_reviews/) (Sterk et al., 2006) and http://www.pseudomonas.com/ for Pseudomonas genomes unavailable in Genome Reviews (250). Predicted protein sequences for all genomes were aligned with rpsblast (5) against the COG section of the CDD database (September 2011) (159). COG hits were considered positive if their alignment covered at least 30% of the COG PSSM and had an E-value ≤ 10−6. TagR and tagR-like sequences were aligned using MUSCLE (73). Based on this alignment, a maximum likelihood tree with 100 bootstrap replicates was computed using PhyML (98).

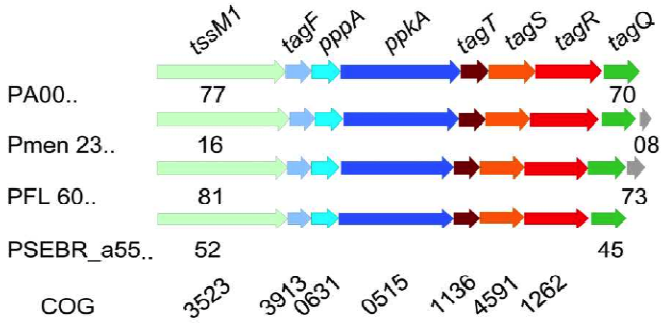


**Figure 3.1:** Organization of the *P. aeruginosa* (PA) HSI-I operon containing tag genes and comparison with *P. mendocina* ymp (Pmen), *P. fluorescens* (PFL) and *P. brassicacearum* (PSEBR). Orthologues are represented in the same colour. Gene and COG numbers are indicated.

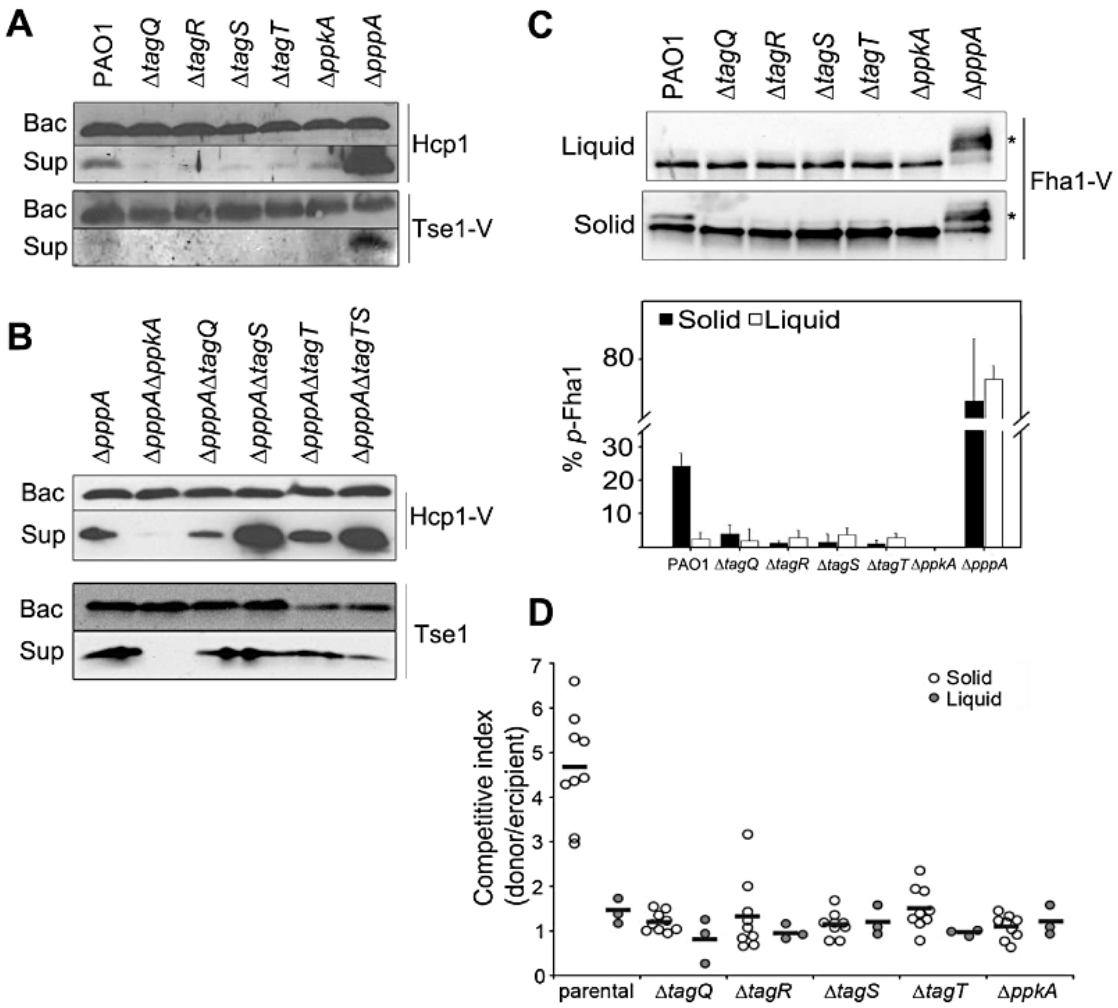


**Figure 3.2: TagT, TagS and TagQ are required for activation of the H1-T6SS.** (A) Analysis of Hcp1 (structural component) and Tse1 (effector) export from strains containing in-frame deletions of tag genes. (B) Cellular and secreted Hcp1 and Tse1 from strains lacking Δ*pppA* and indicated tag gene. (C) Western blot analysis of Fha1 from indicated strains grown either in liquid or on solid medium. The band corresponding to phosphorylated Fha1 (*p*-Fha1) is indicated by an asterisk. Lower panel corresponds to the quantification of *p*-Fha1. Experiments were performed in triplicate (black = solid grown, white = liquid grown). Bac: bacteria, sup: supernatant. (D) *P. aeruginosa* requires *tagT*, *S*, *R* and *Q* for an H1-T6SS-dependent fitness advantage against competing bacteria. The competitive index is plotted for competitions between each indicated donor strain and a H1-T6SS-susceptible recipient strain of *P. aeruginosa* (PAO1 Δ*tse2* Δ*tsi2*) (white = solid grown, gray = liquid grown).

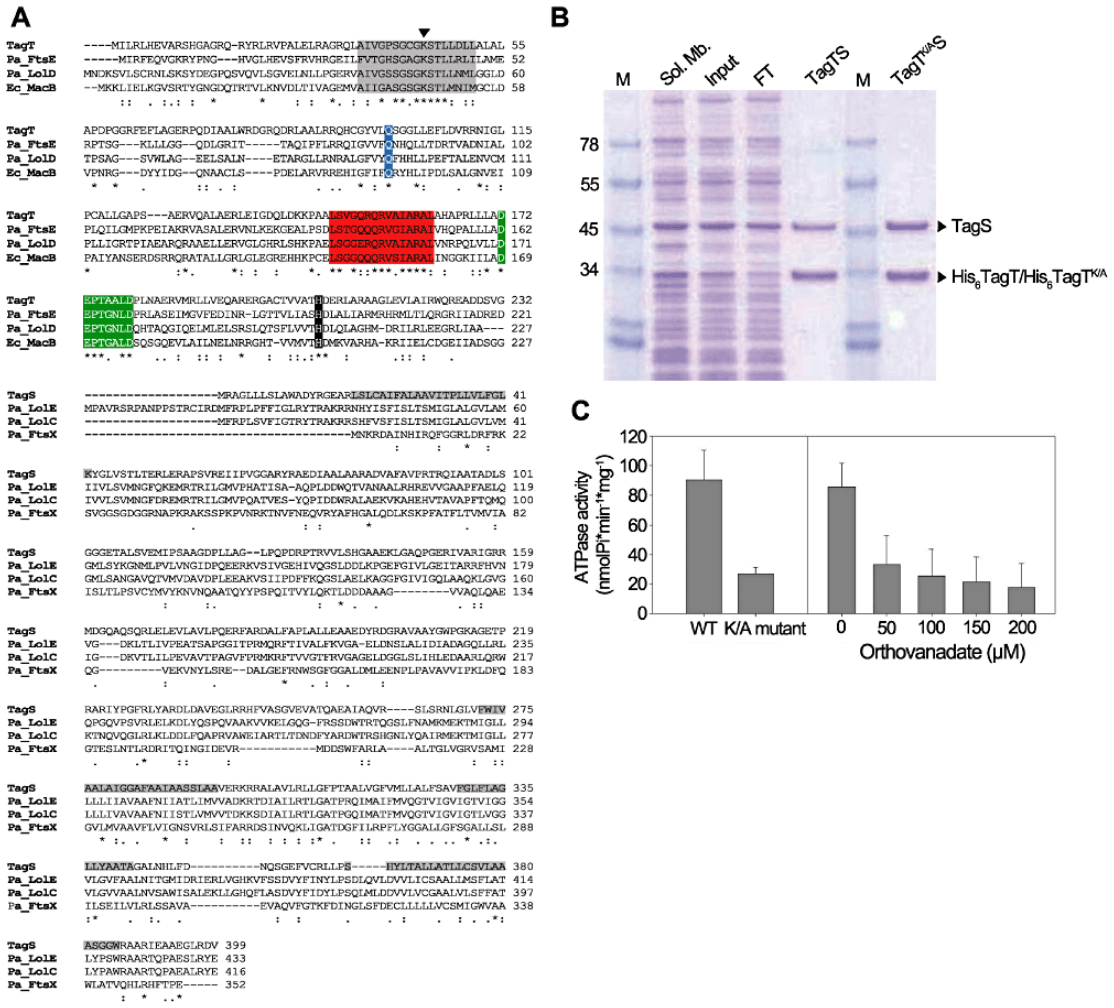


**Figure 3.3: TagT and TagS form a membrane-bound complex harbouring ATPase activity.** (A) Sequence alignment of TagT and TagS with ABC transporters of the same family in *P. aeruginosa* (Pa) and *E. coli* (Ec). Conserved features of TagT are highlighted in colours: Walker A domain (grey), 'Q' motif (blue), ABC transporter signature (red), Walker B motif (green) and 'H' signature (black). The arrow indicates the conserved Lys residue mutated in the $TagT^{K/A}S$ mutant. TagS TMHs are shown in grey background. (B) SDS-PAGE analysis of different fractions obtained during $His_6$-TagTS expression, solubilization and purification. M: molecular weight marker (kDa); Sol. mb: detergent-solubilized membranes; FT: flow through; TagTS: wild-type complex eluted with 200 mM imidazole; $TagT^{K/A}S$: Walker A mutant eluted with 200 mM imidazole. (C) Fractions collected in 200 mM imidazole elution step were analysed for ATPase activity by malachite green assay. The ATPase activity of the wild-type complex was inhibited by orthovanadate in a dose-dependent manner. Analysis by Maria Guillermina Casabona.

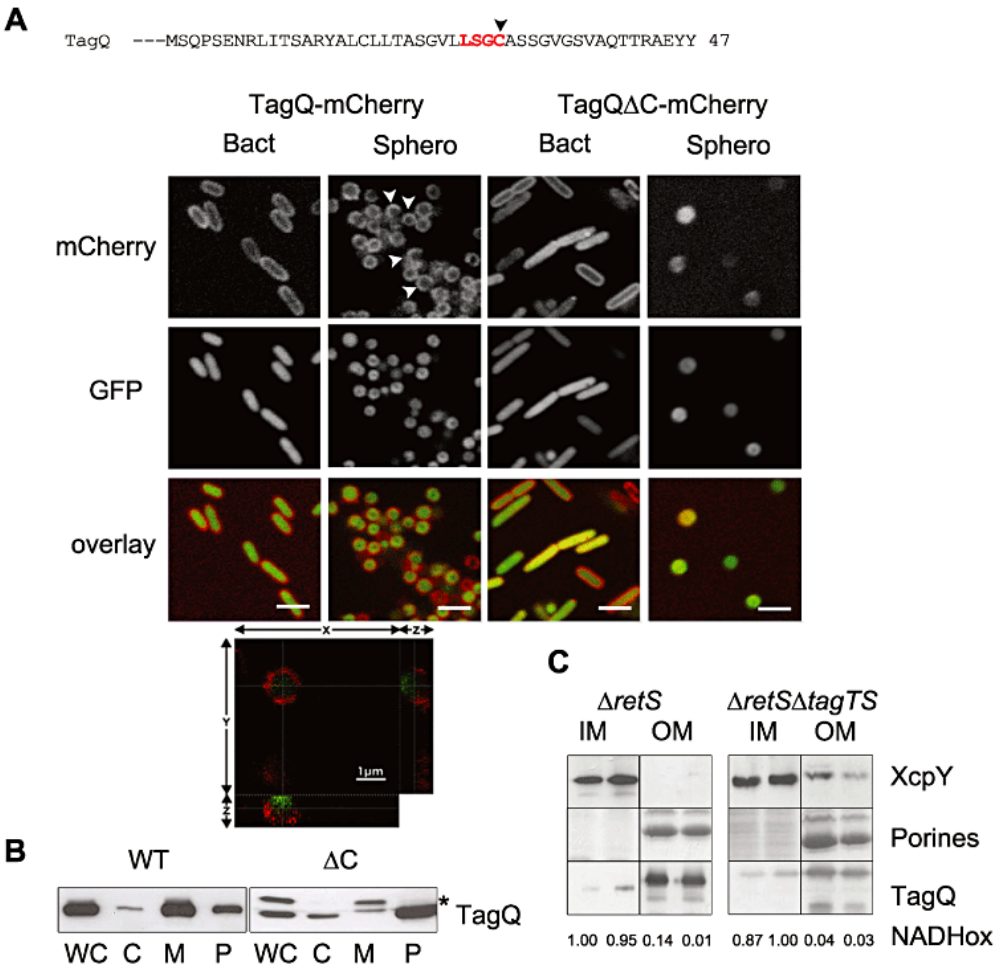


**Figure 3.4: TagQ is an outer membrane lipoprotein that localizes independent of TagTS.** (A) The N-terminal sequence and lipo-box (in red) of TagQ is shown. An arrow indicates the mutated cysteine. Confocal microscopy images of PAO1Δ*retS*-GFP producing TagQ-mCherry or TagQΔCys-mCherry. TagQ-mCherry is localized at the bacterial periphery. White arrows on spheroplast images indicate the crescent-shape labelling of the OM. The bar represents 2 µm. Bact: bacteria; Sphero: spheroplasts. The confocal image in XYZ confirms the presence of the protein in the OM. (B) Subcellular fractionation of PAO1 Δ*tagQ* complemented with a plasmid encoding TagQ (WT) or TagQΔCys (ΔC). Whole cells (WC), cytosol (C), membranes (M) and periplasm (P) were analysed by Western blot using specific antibodies against TagQ. ΔCys mutation results in partial processing of the protein (indicated with an asterisk) and its accumulation in the periplasm. (C) Discontinuous sucrose gradient separation of inner and outer membranes in PAO1Δ*retS* and PAO1 Δ*retS*Δ*tagTS*. Fractions were characterized by NADH oxidase (NADHox) activity, SDS-PAGE and Western blotting using anti-TagQ antibodies. NADH oxidase activity is represented relative to the fraction with the highest level activity (noted as 1.0). XcpY was used as an IM marker and porines visualized in Coomassie blue stained gels as an OM marker. The representative IM and OM fractions are indicated. The analysis of the whole gradient is shown in Figure 3.5. Analysis by Maria Guillermina Casabona.

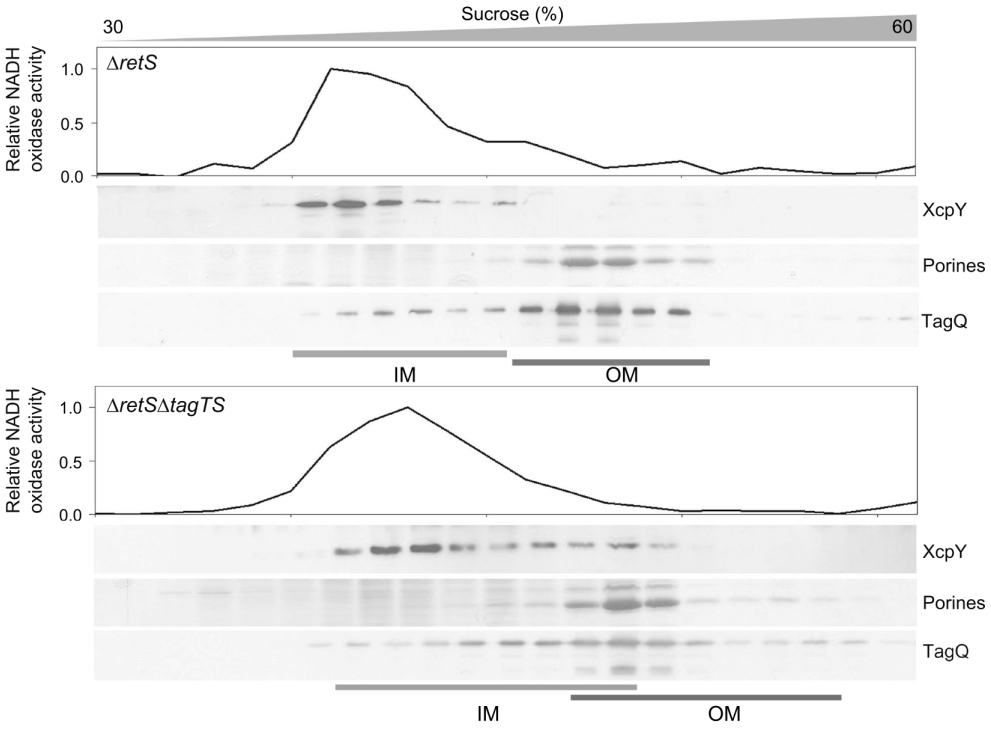


**Figure 3.5: TagQ localization to the OM is not influenced by TagTS**. Complete analysis of discontinuous sucrose gradients of PAO1Δ*retS*and PAO1Δ*retS* Δ*tagTS* are shown. NADH oxidase activity and XcpY are used as IM markers, and porines are used as OM markers. TagQ was detected using specific antibodies. Note that the NADH oxidase activity is represented relative to the fraction of highest activity. IM and OM are indicated. Analysis by Maria Guillermina Casabona.

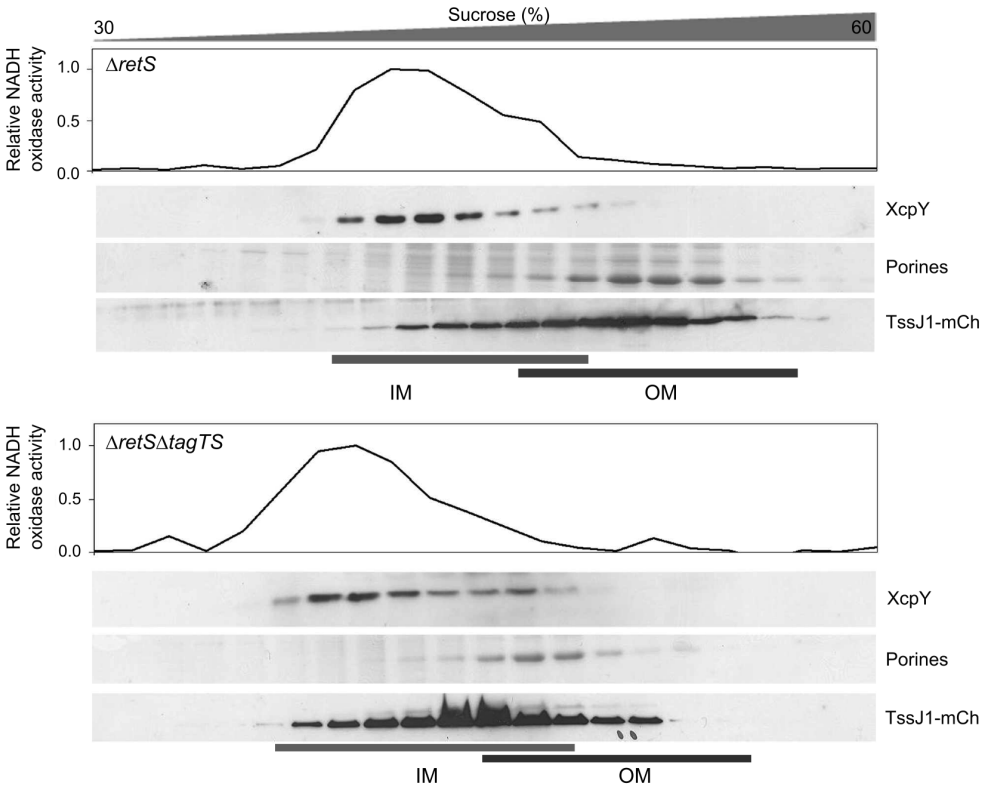


**Figure 3.6:** The TagTS complex does not influence TssJ1-mCherry localization to the outer membrane. Discontinuous sucrose gradient separation of TssJ1-mCherry in PAO1Δ*retS* and PAO1Δ*retS* Δ*tagTS* strains. NADH oxidase activity and controls were as described in Figure 3.5. Fusion protein TssJ1-mCherry was detected by anti-mCherry antibodies. Analysis by Maria Guillermina Casabona.

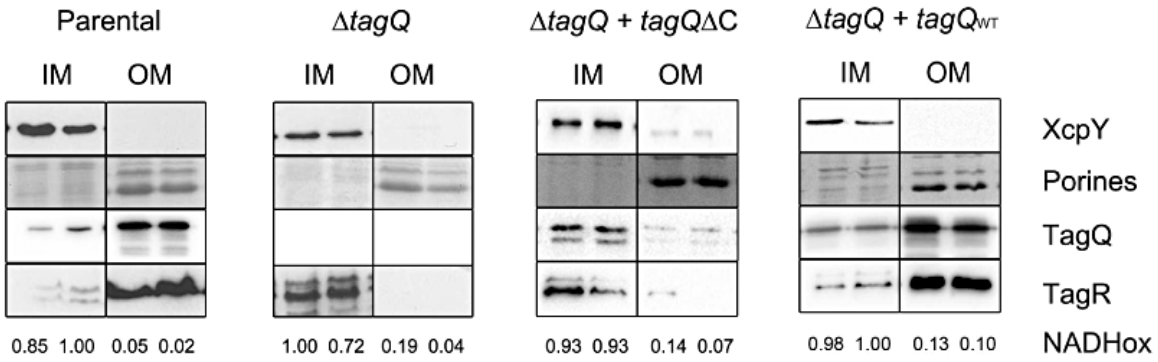


**Figure 3.7: Outer membrane localized TagQ is required for outer membrane anchoring of TagR.** Membrane separations and analysis were performed as described in Figure 3.4C. Strains used were: PAO1 (parental), PAO1 Δ*tagQ* and PAO1 Δ*tagQ* expressing either TagQ ΔCys or TagQ WT. Only the representative IM and OM fractions are shown. TagR and TagQ were detected by specific antibodies. Analysis by Maria Guillermina Casabona.

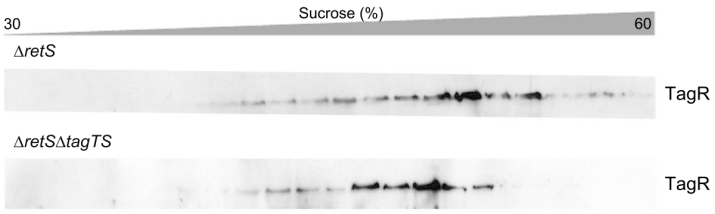


**Figure 3.8. TagTS does not influence TagR localization to the OM.** Discontinuous sucrose gradient separations shown in Figure 3.5 were further analysed using anti-TagR antibodies, showing that TagR is localized to the OM both in PAO1Δ*retS* and PAO1Δ*retS* Δ*tagTS*. Analysis by Maria Guillermina Casabona.

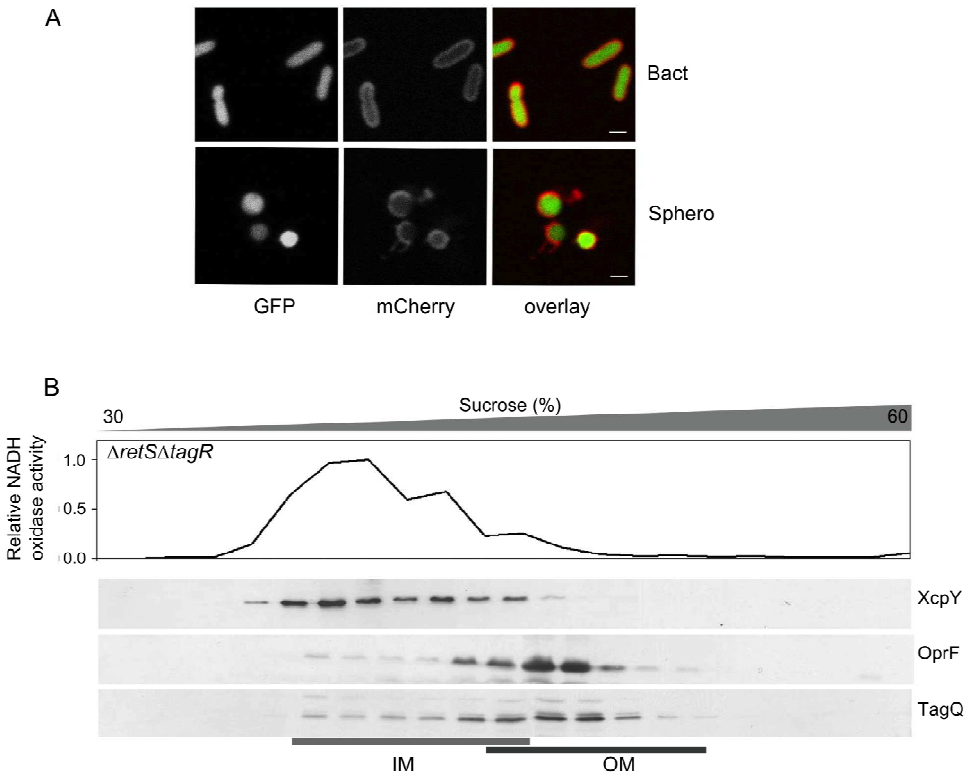


**Figure 3.9: TagR does not play a role in the OM localization of TagQ.**
(A) Confocal microscopy analysis of PAO1Δ*retS*Δ*tagR* expressing GFP and harbouring TagQ-mCherry. White arrows show the OM of *P. aeruginosa* that remains partially attached to spheroplasts after lysozyme treatment (see text for details). Bact: bacteria, Sphero: spheroplasts. The bar represents 1 µm. (B) Discontinuous sucrose gradient separation of the IM and OM of PAO1Δ*retS* Δ*tagR*. Analysis by Maria Guillermina Casabona.

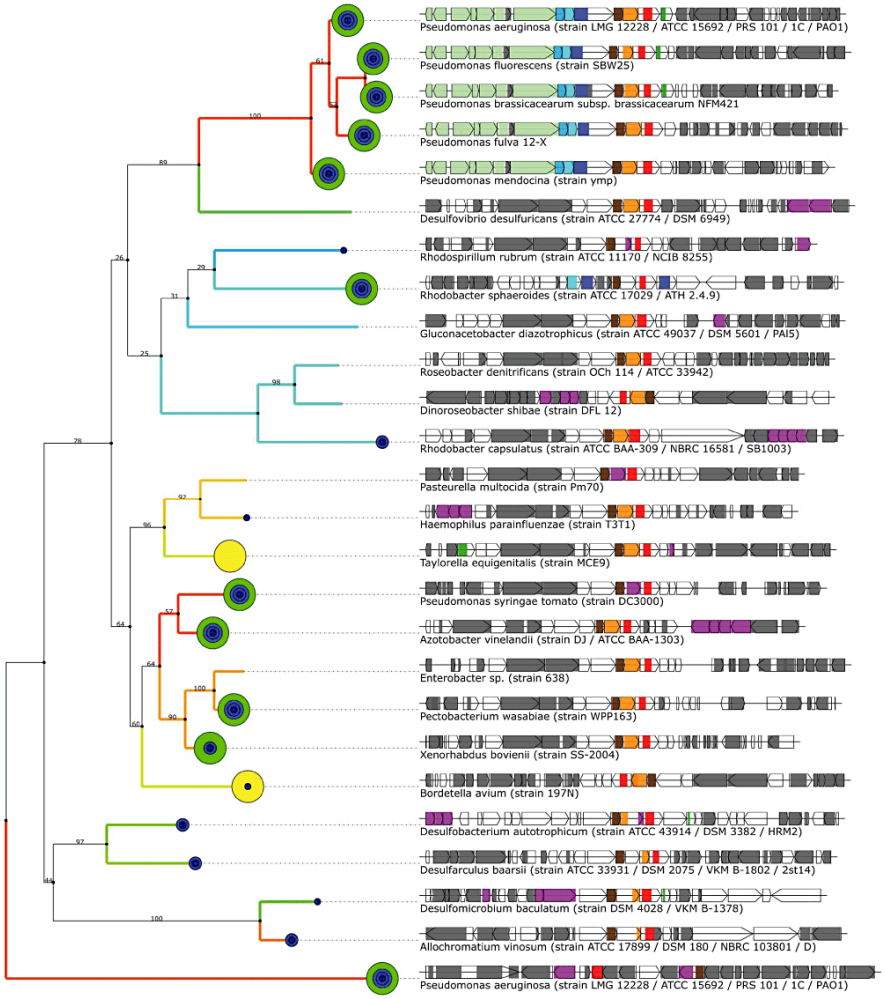


**Figure 3.10: In silico analysis of *tagTSR*-like genes.** Maximum likelihood tree of TagR and TagR-like proteins (matching COG1262) with genomic context of the associated genes, together with the periplasmic PvdO protein of *P. aeruginosa* involved in pyoverdine maturation (Yeterian et al., 2010) (and its genomic context) used as outgroup. Green and yellow circles indicate genomes with complete or incomplete T6SS respectively. Inside of circles, blue points indicate the presence of *pppA*/*ppkA*/*fha1*. Coloured boxes represent hits on the COG database; colours are according to Figure 3.1, except for purple boxes representing hits on ABC transporter related COGs.

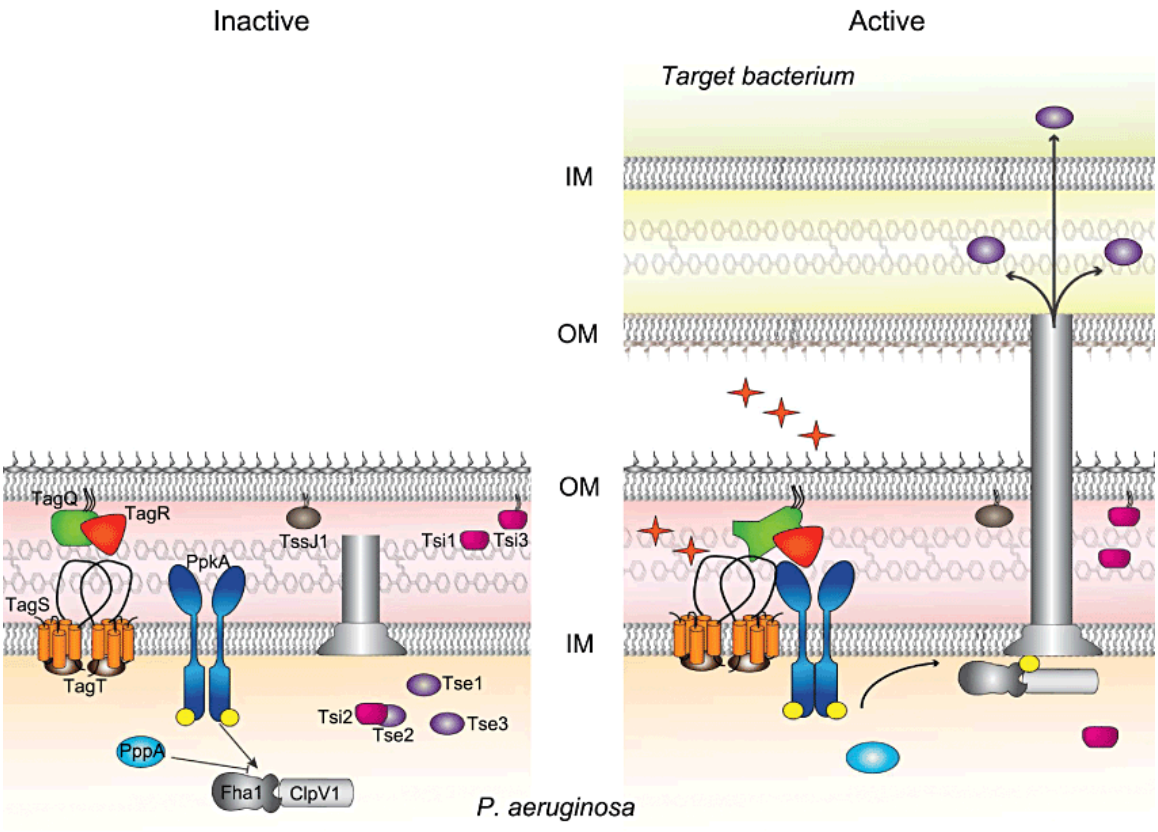


**Figure 3.11: Model for trans-membrane signaling leading to H1-T6SS activation.** The H1-T6S machinery is represented as a single tunnel. Tse1–3 are T6S exported effectors. Molecular players biochemically characterized in this study are: TagQ (OM lipoprotein, Pseudomonas specific), TagS and TagT (ABC transporter), TagR (OM associated protein) and TssJ1 (conserved OM lipoprotein). The Ser/Thr kinase, PpkA, and the phosphatase, PppA, as well as the phosphorylation target protein Fha1, are represented. A putative signal is designated by red stars. Proteins are represented using the same colour code as the ORFs in Figure 3.1, and yellow spheres indicate phosphorylation. IM and OM of *P. aeruginosa* and the target bacterium are shown.

# CHAPTER IV.

## Haemolysin co-regulated protein is an export receptor and chaperone for type VI secretion substrates

Submitted as: Silverman J.M., Agnello D.M., Zheng H., Andrews B.T., Li M., Catalano C.E., Gonen T., and Mougous J.D. Haemolysin Co-regulated Protein is an Exported Receptor and Chaperone of Type VI Secretion Substrates.

**ABSTRACT**

Secretion systems require high fidelity mechanisms to discriminate substrates amongst the vast cytoplasmic pool of proteins. Factors mediating substrate recognition by the type VI secretion system (T6SS) of Gram-negative bacteria, a widespread pathway that translocates effector proteins into target bacterial cells, have not been defined. We report that haemolysin co-regulated protein (Hcp), a ring-shaped hexamer secreted by all characterized T6SSs, binds specifically to cognate effector molecules. Electron microscopy analysis of an Hcp–effector complex from *Pseudomonas aeruginosa* revealed the effector bound to the inner surface of Hcp. Further studies demonstrated that interaction with the Hcp pore is a general requirement for secretion of diverse effectors encompassing several enzymatic classes. Though previous models depict Hcp as a static conduit, our data indicate it is a chaperone and receptor of substrates. These unique functions of a secreted protein highlight fundamental differences between the export mechanism of T6 and other characterized secretory pathways.

## INTRODUCTION

Bacteria possess discrete pathways for delivering proteins to their surroundings. A diversity of secretion systems facilitates the necessary heterogeneity in size, structure and function within the proteins exported by these cells (72). For example, the type V secretion system can export exceptionally large proteins, such as filamentous adhesins, to the cell surface or the extracellular milieu (60, 244), whereas types III, IV and VII systems exhibit the ability to directly translocate proteins into host cells (1, 89, 91, 120). Of the thousands of proteins present in a cell, each secretion system acts with extraordinary fidelity to specifically recognize and release a distinct subset of substrates.

Substrate selection can be affected by several factors, including signal sequences, chaperones and receptors. For example, type III secretion system (T3SS) substrates are recruited to the secretory apparatus in complex with specialized chaperones (3, 227). A T3S-associated ATPase then engages the substrate by binding its N-terminal export signal, releasing it from the chaperone and driving substrate unfolding and translocation through the apparatus. Similar mechanisms appear to drive substrate recognition and export by the T4S pathway (35, 232). While the factors involved in substrate selection for T3SSs and T4SSs are in part defined, comparatively little is known about this process in a related, but more recently described pathway, the type VI secretion system (T6SS).

The T6SS is a widely distributed protein translocation pathway that is able to directly target bacterial and eukaryotic cells (40). The core T6 machinery consists of 13 essential subunits, encoded within large gene clusters on bacterial chromosomes (27). While a T6SS ultrastructure

has not been determined, X-ray crystallographic and protein–protein interaction data suggest that an envelope-spanning assembly and a bacteriophage-like complex make up much of the secretory machinery (42). The bacteriophage-like complex consists of TssB (type six secretion B), TssC, Hcp (haemolysin co-regulated protein) and VgrG (valine-glycine repeat protein G). Visualization of *Vibrio cholerae* cells by fluorescence microscopy showed that TssB and TssC form a dynamic filamentous complex within the cytoplasm; switching between extended and contracted states while remaining anchored at the inner membrane (14). Hcp and VgrG are secreted components of the T6SS with significant structural homology to T4 bacteriophage tail tube (gp19) and tail spike proteins (gp5–gp27), respectively. By analogy to contractile bacteriophage, TssB and TssC are proposed to form a sheath enclosing a tube composed of Hcp, with VgrG localized at the tip to allow membrane breaching (125, 127). In this model, contraction of the TssB/C complex is thought to drive Hcp and VgrG out of the cell, allowing effector delivery though the Hcp tubule. While this model is conceivable, certain aspects of it lack experimental support. Most glaringly, Hcp and VgrG have not been shown to associate with each other or the TssB/C filament (14, 127).

Hcp is a central component of the bacteriophage-like model of T6S-dependent intercellular effector transport. Studies have demonstrated that this universally and abundantly T6S-exported protein is essential for both the assembly of the T6S apparatus and the export of its effectors (113, 166, 192). Nevertheless, the precise function of Hcp in the T6SS has not been addressed. The supposition that Hcp forms a channel through which small or partially unfolded proteins transit derives from X-ray crystal structures of the protein solved from several bacterial species. In all cases, the protein adopts a homohexameric ring structure with a ~40 Å internal diameter;

furthermore, these rings stack to form a tubular structure within the crystal lattice (124, 166, 179). However, Hcp tubes have only been observed under crystallographic conditions, or when stabilized *in vitro* with engineered disulfide bonds between ring subunits (12). Also, since both stacking arrangements (head-to-head or head-to-tail) are found in Hcp X-ray crystal structures, the physiological significance of its tubule form is uncertain.

The Hcp secretion island I (HSI-I)-encoded T6SS (H1-T6SS) of *P. aeruginosa* is a model system for understanding the substrates, apparatus dynamics, and interbacterial interactions mediated by T6 (13, 48, 113, 204). The H1-T6SS delivers at least three toxic effectors, Tse1-3 (type VI secretion exported 1-3), into target bacterial cells. Tse1 and Tse3 are translocated into the periplasm of target cells where they degrade peptidoglycan and cause cell lysis using amidase and muramidase activity, respectively (204). The precise molecular target of Tse2 is not yet known; however, this effector induces stasis and acts in the cytoplasm of recipient cells. Structure prediction algorithms indicate that Tse2 may function as a nuclease (149). As the bacterial targeting activities of the H1-T6SS are also directed at kin, *P. aeruginosa* requires immunity proteins, Tsi1-3 (type VI secretion immunity 1-3), encoded alongside their cognate effector in bicistrons. *P. aeruginosa* harbors two additional T6SSs, the H2- and H3-T6SSs. Interestingly, these systems appear to export non-overlapping sets of effectors, though the factors mediating effector discrimination have not been elucidated (205).

In this study, we report that Hcp is a chaperone and receptor of T6S effectors. Focusing on Tse2, we show that a direct and highly specific interaction with the pore of its cognate Hcp, Hcp1 of the H1-T6SS, is required for the stability and export of the protein. We further demonstrate that

effectors with unrelated sequences, Tse1 and Tse3, also require direct interactions with the pore of Hcp1 for secretion. Certain amino acid substitutions within the Hcp1 pore differentially affect the secretion of the three Tse proteins, indicating the capacity of Hcp1 to bind diverse proteins via distinct epitopes. Finally, we probe the generality of our results and find that specific interactions between T6S effectors and cognate Hcp proteins occur in diverse bacteria. Overall, our findings reveal a new paradigm for substrate recognition by a complex bacterial protein translocation machine.

## RESULTS

### Hcp1 Stabilizes Tse2 Posttranslationally

In the course of investigating factors that influence effector transport through the H1-T6SS of *P. aeruginosa*, we observed that strains lacking *hcp1* displayed markedly reduced intracellular levels of Tse2 (Figure 1A). We conducted this, and subsequent studies in the Δ*retS* background, which is frequently employed for the study of the H1-T6SS (13, 99, 166). The inactivation of *retS* overrides the requirement for cell–surface contact for T6S activation, and it results in elevated expression of both the H1-T6SS and its effectors, facilitating their detection via Western blot (113, 222). Deletions of other essential T6SS components including *clpV1*, *tssM1*, *tssE1*, and the functionally redundant *vgrG1* and *vgrG4* genes, did not lead to reduced Tse2 levels, indicating this phenotype is specific to the loss of *hcp1* (Figure 1A). To measure more conclusively the effect of Hcp1 on overall Tse2 levels, we probed the consequences of *hcp1* deletion in the Δ*tssM1* background. The *tssM1* gene encodes a core component of the secretory system; its deletion abrogates apparatus assembly and effector export (81, 166). Tse2 levels were also strongly reduced in the Δ*hcp1* Δ*tssM1* background, suggesting that Hcp1 is required for

maintenance of intracellular Tse2 (Figure 1B). We also examined whether the levels of Tse1 and Tse3 are sensitive to the presence of Hcp1. Though not as dramatic as the effect on Tse2, we detected a significant reduction of intracellular Tse1 and Tse3 upon deletion of *hcp1* from the Δ*tssM1* background (Figure 1B). The effects of Δ*hcp1* on all effectors could be partially (Tse2) or fully (Tse1 and Tse3) genetically complemented.

As an alternative approach for probing the influence of Hcp1 on effector levels, we used the ClpXP targeted degradation system to specifically deplete the protein from *P. aeruginosa* (43, 162). To accomplish this, we generated a *P. aeruginosa* strain wherein the native *hcp1* open reading frame was modified to include a C-terminal fusion to the *ssrA*-like sequence, DAS+4 (Hcp1–D4). Consistent with our deletion studies, depletion of Hcp1–D4 resulted in a concomitant precipitous drop in cellular Tse2 levels (Figure 1C). Tse1 levels similarly decreased as observed in the Δ*hcp1* background, while Tse3 levels were not visibly affected by Hcp1 depletion. The cellular half-life of Tse3 may be too long to observe the relatively minor effect of Hcp1 during the 90 minute depletion assay (Figures 1B and 1C). Together, these data demonstrate that the Hcp1 protein is essential for the maintenance of intracellular Tse2 levels. Though Tse1 and Tse3 levels are measurably influenced by *hcp1* deletion, significant intracellular accumulation of these effectors occurs independent of the protein. To investigate the mechanism underlying the influence of Hcp1 on H1-T6S effectors, we initially focused on Tse2, where a highly distinct Hcp1-dependent phenotype was observed.

**Hcp1 Interacts Directly with Tse2**

The dramatically lowered abundance of Tse2 in the absence of Hcp1 suggests that Hcp1 – acting directly or indirectly – plays a critical role either in regulating *tse2* expression or stabilizing Tse2 posttranslationally. To test the former, we generated *tse2* expression reporter strains containing a chromosomally-integrated construct consisting of the predicted *tse2* promoter followed by an open reading frame consisting of the first 8 codons of *tse2* fused to *lacZ*. Though the activity of the reporter increased as expected in the Δ*retS* background, a known posttranscriptional regulator of *tse2*, its activity was insensitive to the deletion of *hcp1* (Figure 2A) (28). Unable to implicate Hcp1 in a regulatory capacity, we probed for a physical interaction between the proteins using a co-immunoprecipitation (co-IP) assay. Interestingly, Tse2 specifically precipitated with Hcp1, suggesting a physical association between this effector and Hcp1 might underlie the Hcp1 requirement for Tse2 stability (Figure 2B). To test whether the observed interaction requires other T6S-associated factors, we next performed co-IP experiments from T6SS$^-$ *E. coli* strains co-expressing C-terminally hexahistidine-tagged *hcp1* (*hcp1-his*$_6$) and a vesicular stomatitis virus glycoprotein (VSV-G) epitope-tagged non-toxic allele of *tse2* (*tse2*$^{NT}$*–V*). In this heterologous host, the accumulation of Tse2 remained dependent upon the presence of Hcp1 (Figure 2C). Furthermore, co-expressed Tse2$^{NT}$–V and Hcp1 associated tightly. To rule out nonspecific mechanisms that could explain our *E. coli* data, we tested the activity of another Hcp protein from *P. aeruginosa*, Hcp2, which does not participate in the H1-T6SS. Despite expression equivalent to or in excess of Hcp1, Hcp2 did not stabilize or interact with Tse2. From these data, we conclude that a direct interaction between Hcp1 and Tse2 likely promotes Tse2 stability.

**Tse2 Interacts with the Inner Surface of Hcp1 Rings**

X-ray crystallographic and electron microscopic (EM) studies of Hcp proteins, including Hcp1, have consistently observed the protein in a hexameric ring configuration (124, 142, 166, 179). Using sedimentation velocity analytical ultracentrifugation at low Hcp1 concentrations (10.3-3.2 μM), we further confirmed this quaternary state as the single detectable species in solution (Figure S1). These observations, taken together with the large hydrophobic interface observed between Hcp protomers, argue that the hexameric assembly is the relevant physiological state of Hcp proteins.

The Hcp1 hexamer reveals several potential protein–protein interaction surfaces. Sequence analysis of Hcp homologs shows that residues on the "top" and "bottom" faces of Hcp rings are highly conserved and may be important for ring–ring interactions (Figure S2) (166). Thus, we reasoned that Tse2 likely interacts with either the inside or outside face of the Hcp1 ring. To define the regions of Hcp1 involved in Tse2 interaction, we pursued a site-directed mutagenesis approach, targeting all residues with more than 60% solvent accessibility located on the inner or outer surface of the Hcp1 ring. To this end, we mutated 34 positions; non-polar or small side chain amino acids were substituted with glutamine, and those with a polar or large side chain with alanine. The relative affect of each Hcp1 point mutation on Tse2 stability was determined by co-expression of the *hcp1* alleles with *tse2–V* in *E. coli*. We found that approximately half of the mutations localized to the inside surface of Hcp1 exhibit 1% or less Tse2 stabilization relative to wild-type Hcp1 (Figures 3A, 3B and S3), whereas all Hcp1 variants with substitutions mappings to the outer surface of the ring displayed substantial Tse2-stabilization activity (1.0-100%). Interestingly, the majority of substitutions that destabilize Tse2 over 100-fold map together within a discrete patch inside the Hcp1 ring (Figure 3B).

The ring shape of Hcp1 is readily discernable by negative stain transmission electron microscopy (TEM). Therefore, we reasoned that Hcp1 rings bound to Tse2 might be distinguished by TEM as "filled" particles. TEM analysis of approximately 3,000 randomly selected purified Hcp1–V–$Tse2^{NT}$–$His_6$ single particles showed that filled class averages constituted a significant fraction of total Hcp1 particles (Figures 3C, 3D and S4). In contrast, no class averages appeared filled in the control sample. The low fraction of filled rings observed in the Hcp1–Tse2 sample is likely explained by Tse2 degradation and precipitation during preparation (149, 260). Visualization of the Tse2–Hcp1 complex provides direct evidence that Tse2 interacts with the inner surface of Hcp1 rings.

**Tse2 Secretion Requires Interaction with Hcp1**

Motivated by our *in vitro* findings, we next sought to determine the influence of the interaction between Tse2 and the inner surface of Hcp1 on Tse2 stability and secretion *in vivo*. Using allelic exchange, we generated a *P. aeruginosa* strain encoding $Hcp1^{S31Q}$ at the native *hcp1* locus. We selected this mutant from those identified by our *in vitro* studies, as this amino acid resides within the inner surface patch and strongly disrupts interaction with Tse2 via a relatively conservative substitution (small polar to large polar). Western blot analyses showed that although $Hcp1^{S31Q}$ is produced and secreted at levels comparable to the wild-type, strains bearing this mutation do not support Tse2 accumulation (Figure 4A). Furthermore, using interbacterial competition assays, we found that the $hcp1^{S31Q}$ background displays a marked defect in Tse2-dependent fitness (Figure 4B). The effects on H1-T6SS function appeared specific, as the levels of export and interbacterial delivery of Tse1 and Tse3 were not significantly impacted in the

*hcp1*$^{S31Q}$ background (Figures 4A and 4C). Overall these data demonstrate that Tse2 stability requires interaction with the inner surface of the Hcp1 ring.

Since Tse2 does not accumulate to detectable levels in *hcp1*$^{S31Q}$, we could not explicitly measure the requirement of interaction with Hcp1 for Tse2 secretion. However, a previous report from our laboratory demonstrated that over-expressed Tse2 can be detected in *P. aeruginosa* backgrounds lacking *hcp1* (113). Therefore, to overcome the Tse2 detection limit, we monitored the export of Tse2–V expressed with high induction from the *lac*UV5 promoter in the *hcp1*$^{S31Q}$ background. Western blot analysis confirmed that the Tse2–V protein is highly over-produced relative to endogenous Tse2 and that it is secreted in an Hcp1-dependent manner (Figure 4D). Interestingly, we found that despite intracellular accumulation, Tse2–V is not exported in the *hcp1*$^{S31Q}$ background. Thus, taken together with our observation that H1-T6SS function is generally preserved in the *hcp1*$^{S31Q}$ background, we conclude that interaction with Hcp1 is required both for the stabilization and export of Tse2.

**Recognition of Tse2-like Effectors by Hcp is General**

To determine the generality of our findings concerning *P. aeruginosa* Tse2 and Hcp1, we sought to identify and characterize functionally analogous proteins in other bacterial species. Protein BLAST analyses revealed Tse2 homologs within several T6SS$^{+}$ Gram-negative bacteria, including *Methylomonas methanica, Shewanella fridigimarina, Burkholderia ambifaria* and *Pseudoalteromonas sp*. (Figure 5A). Sequence alignments of the homologs highlighted the conservation of several motifs, including a putative aspartic acid-containing nuclease-related catalytic site (Asp63 in Tse2) identified using protein structure prediction algorithms (Figure S5)

(149). As additional evidence of the functional relationship between Tse2 and its homologs, we found each homolog encoded in an apparent bicistron with a smaller gene encoding a protein with attributes similar to Tsi2, including length (Tsi2, 77; homologs, 75-79 amino acids) and an acidic pI (Tsi2, 3.9; homologs, 4.0-4.5) (Figure 5A).

Confident we had identified bona fide Tse2 and Tsi2-related proteins, we selected *M. methanica* Tse2 ($Tse2^{MM}$), which shares 71% identity with *P. aeruginosa* Tse2, for more detailed analyses. The genome of *M. methanica* contains a single T6S gene cluster and encodes a single clear homolog of *P. aeruginosa* Hcp1, $Hcp1^{MM}$, making $Tse2^{MM}$ well suited for our study. To first establish that the *M. methanica tse2 tsi2* pair is functionally orthologous to *P. aeruginosa tse2 tsi2*, we conducted toxicity studies in *E. coli*. Similar to *tse2*, expression of $tse2^{MM}$ in *E. coli* caused a dramatic drop in recovered c.f.u. (Figure 5B). Moreover, this toxicity was observed for $Tse2^{MM(D63N)}$, and it was inhibited by co-expression with $tsi2^{MM}$.

We next tested whether $Tse2^{MM}$, like Tse2, interacts with the Hcp1 homolog, $Hcp1^{MM}$, encoded within the putative T6SS of *M. methanica*. Indeed, we found $Tse2^{MM}$ interacts directly with $Hcp1^{MM}$ and, additionally, requires $Hcp1^{MM}$ for intracellular accumulation (Figure 5C). Interestingly, we found that $Tse2^{MM}$ also interacts with and is stabilized by *P. aeruginosa* Hcp1, and likewise for the *P. aeruginosa* Tse2–$Hcp1^{MM}$ pair (Figures 5C and 5D). The specificity of these interactions is underscored by the observation that neither Tse2 nor $Tse2^{MM}$ interact with Hcp1 from *Pseudomonas protegens* ($Hcp1^{PP}$), despite the fact that this Hcp1 homolog is nearly equally divergent from *P. aeruginosa* Hcp1 as $Hcp1^{MM}$ ($Hcp1^{PP}$, 76%; $Hcp1^{MM}$, 77%). Notably, $Hcp1^{PP}$ is encoded within an HSI-I-like gene cluster, yet *P. protegens* does not have a Tse2

homolog encoded within its genome. Finally, consistent with the hypothesis that interaction with Hcp is a key determinant for export via the T6S pathway, we observed efficient release of Tse2$^{MM}$ via the H1-T6SS (Figure 5E).

**Amidase and Muramidase T6S Effector Classes Recognize Cognate Hcp Proteins**

In the course of studying the behavior of Hcp1 point mutants in *P. aeruginosa*, we observed that while the effects of Hcp1$^{S31Q}$ are limited to Tse2, other Tse2-destabilizing Hcp1 pore substitutions also reduce the export of Tse1 and Tse3 (Figure 6A). These Hcp1 variants are themselves secreted, suggesting their effect on Tse1 and Tse3 export is not a consequence of misfolding or a failure to be recognized by the secretory apparatus. Moreover, certain substitutions exhibited differential effects on the secretion of Tse1 and Tse3. For example, Hcp1$^{L28A}$ inhibits Tse3 secretion, but not that of Tse1. On the contrary, Hcp1$^{S115Q}$ strongly affects both Tse1 and Tse3 secretion. Together with our observation that Tse1 and Tse3 display decreased abundance in strains lacking Hcp1 (Figure 1B), our findings led us to hypothesize that non-Tse2-type effectors also engage in specific interactions with the inner surface of the Hcp1 pore, and that these are required for H1-T6SS-dependent secretion.

To determine whether Hcp1 directly interacts with Tse1 and Tse3, we performed co-IP assays using proteins co-expressed in *E. coli*. As a means of linking potential interactions to the secretion phenotypes observed, we utilized the secretion defective *hcp1*$^{S115Q}$ pore substitution mutant in addition to wild-type *hcp1*. Interbacterial competition assays confirmed this mutation functionally disrupts Tse1- and Tse3-dependent intoxication (Figure S6). While Tse1 and Tse3 did not efficiently co-IP with Hcp1$^{S115Q}$, both proteins were detected in association with the wild-

type protein (Figures 6B and 6C). From these data, we conclude that interaction with the inner surface of Hcp1 is a common requirement for the secretion of the three known H1-T6SS effectors. The observation that Hcp1 substitutions can have variable effects on the Tse proteins suggests that, consistent with their divergent sequences, the proteins each form a unique network of interactions with Hcp1.

Bioinformatic work conducted by our laboratory has found evidence of a non-random association between *hcp* genes and predicted T6S amidase effectors (Tae) (Figure S7) (206). Based on this observed genetic link, our finding that direct interactions between Tse1-3 and Hcp1 are required for secretion, and the results of a prior study demonstrating the interaction of a putative *Edwardsiella tarda* T6S effector with an Hcp homolog (258), we posited that the recognition of effectors by cognate Hcp proteins might be a general determinant of substrate selectivity by the T6SS. As a first step toward validating this model, we selected two predicted cognate Tae–Hcp pairs based on genetic linkage (*Salmonella enterica* serovar Typhi Tae2) or homology to Tse1 (*Burkholderia phytofirmans* Tae1). As predicted, both effectors bound cognate, but not non-cognate Hcp proteins (Figures 6D and 6E). In total, our data suggest that the interaction between effectors and cognate Hcp proteins is a general phenomenon that is likely to – at least in part – define the particular effectors transported through a given T6SS.

**DISCUSSION**

We have identified Hcp as a critical gatekeeper protein of the T6SS. As a chaperone, a substrate receptor, and a secreted protein itself, the multipurpose nature of Hcp grants it a unique position among secretory system-associated proteins (Figure 7). This implies that the mechanism of

substrate export by the T6SS is fundamentally different from other characterized secretion systems. Arguably, T3S and T4S, which both translocate macromolecules in a concerted fashion into target cells, are the most analogous secretion pathways to the T6SS (54, 89). Indeed, T6S and T4S share two homologous proteins, TssL (DotU) and TssM (IcmF) (27). In light of this relatedness, it is interesting that effector recognition by the T6SS occurs via a principally different process than these related pathways, which both utilize ATPases to directly engage substrates and provide the energy necessary for export (3, 50). The fact that the T6S pathway does not appear to directly link effector recognition to energizing secretion may be explained by its putative bacteriophage origins (125). The energy driving unidirectional protein transport in the T6S pathway is thought to be stored in a filamentous structure composed of TssB/C, which contracts and is then recycled by a ClpB-like AAA+ family ATPase, ClpV (14, 25).

Prior models of the T6SS depict Hcp as a passive conduit for effectors (14, 26, 223). However, our data suggest that Hcp associates with effectors, protects them from proteolysis, and likely traffics with effectors during transport (Figure 7). Stoichiometric, or near stoichiometric, release of Hcp hexamers with effectors reconciles the massive accumulation of Hcp in the culture supernatants of T6S-activated strains (166, 189, 193, 253). Whether effectors in complex with Hcp are folded cannot be definitively established from our data. The structures of several amidase effectors indicate the proteins are of a size that could be accommodated within the Hcp pore (48, 68). However, based on the instability of effectors in the absence of cognate Hcp proteins, we speculate they do not adopt their final folded configuration until, or accompanying, release from Hcp. It is of note that intra-molecular disulfide bonds have been observed in the structures of amidase effectors. The failure of these bonds to form in the cytoplasm could explain

the instability of the proteins in this compartment, while their formation in the periplasm could drive release from Hcp. Interestingly, Tse2 lacks cysteine residues and ultimately accesses the cytoplasm of the recipient. In this case, interaction with the outer face of the inner membrane, or a receptor associated with the membrane, might drive effector release. It is also possible that the T6S apparatus remodels or modifies proteins during export to disrupt Hcp–substrate interactions.

Our data suggest that interactions with the pore of Hcp are, broadly, a critical determinant for the secretion of T6 effectors. However, we posit that other mechanisms may facilitate the recognition and export of disparate effector classes. Rather than a genetic linkage with *hcp* genes, Tle (type VI secretion lipase effector) and Rhs (recombination hot spot) effectors are encoded in association with *vgrG* genes (132, 205). VgrG proteins often facilitate intercellular T6S-dependent delivery of effectors present as C-terminal fusion to their structural domain (30, 192, 230). It is conceivable that Tle and Rhs effectors, which are considerably larger than Tse-type effectors, might gain access to recipient cells by non-covalently associating with VgrG proteins. A Tle protein from *V. cholerae* was found in the immunoprecipitate of a VgrG protein, however the genetically linked VgrG tested was not tested (69).

While we have delineated a critical step in the process of effector secretion by the T6SS, many aspects of the overall structure–function model for the system remain untested. Hcp has so far not been shown to associate with the TssB/C sheath-like complex. If Hcp and TssB/C interact as predicted, this step would presumably follow formation of the Hcp–substrate complex. However, there is some evidence suggesting that Hcp may not interact with TssB/C. For instance, Hcp proteins bearing large C-terminal fusions have been identified (22, 180). It is difficult to envision

how these much larger proteins would be accommodated inside the TssB/C structure. Also, Hcp has so far not been observed to co-purify in isolations of the TssB/C complex (14). In either case, it remains almost entirely unresolved how Hcp–substrate complexes cross the inner and outer bacterial membranes. An envelope-spanning complex consisting of integral inner membrane proteins and an outer membrane lipoprotein has been identified, however the ultrastructure of this novel complex awaits visualization (81). Interestingly, Hcp has been shown to form a complex with two integral membrane proteins of the envelope-spanning complex, TssL and TssM (156). The ATPase activity of TssM aids in the formation of this complex, thus an effector–Hcp–TssM–TssL complex might represent an important intermediate in the T6S process.

Immunity to Tse2 is provided by the Tsi2 protein, a small acidic cytoplasmic protein that directly binds and inactivates the toxin. The current study adds previously unrecognized complexity to the subject of effector immunity, particularly cytoplasmic effectors like Tse2 that interact with cognate proteins prior to export. Based on the studies reported herein and the observation that Tsi2 is an essential gene, it is apparent that significant Tse2 immunity is not provided by Hcp1 (113, 121). It is conceivable that Tsi2 interacts with Tse2 in the context of Tse2–Hcp1 complexes, however we did not detect this complex and favor the hypothesis that Tsi2 functions by scavenging free Tse2, including endogenous Tse2 and Tse2 delivered by other *P. aeruginosa* cells in trans.

Our discovery that effectors interact with the pore of Hcp may have implications for the identification of novel T6S substrates. The discovery of effectors by virtue of interaction with

cognate Hcp proteins stands to overcome several difficulties encountered in such efforts. For instance, this method would not depend upon effector export, which is often repressed under *in vitro* culturing conditions (223). Our findings may also guide efforts to engineer non-native substrate export into the T6S pathway. This approach could provide new ways to modulate the outcome of interbacterial interactions.

## MATERIALS AND METHODS

**Bacterial Strains, Plasmids and Growth Conditions.** All *P. aeruginosa* strains were derived from the sequenced strain PAO1. Genomic DNA from *M. methanica* MC09, *S.* Typhi Ty2, *P. protegens* Pf-5 and *P. aeruginosa* PAO1 was used to amplify effector, immunity and *hcp* genes (23, 65, 183, 229). *E. coli* strains DH5α, SM10 and BL21 were used for plasmid maintenance, conjugative transfer and gene expression, respectively. *P. aeruginosa* was grown in Luria-Bertani (LB) media at 37°C supplemented with 30 μg/uL gentamicin, 25 μg/mL irgasan, 100 μg/mL tetracyclin, 5% sucrose and 0.5 mM IPTG as required. Plasmids used in this study are described and referenced in Table S1. In-frame deletions, chromosomal fusions and chromosomal point mutations were generated as previously described using the pEXG2 suicide vector (166, 200). Quikchange (Stratagene) or Kunkel based methods were used for site-directed mutagenesis of *hcp* and *tse2* homologs (135).

**Preparation of Proteins and Western Blot Analysis.** Cell associated fractions from *P. aeruginosa* were prepared from 2 mL cultures grown to mid-log phase. Harvested pellets were resuspended in 100 μL Buffer 1 (0.5 M NaCl, 50 mM Tris pH 7.5 and 10% glycerol) and mixed 1:2 with SDS-PAGE sample loading buffer (125 mM Tris, pH6.8, 2% (w/v) 2-mercaptoethanol, 20% (v/v) glycerol, 0.001% (w/v) bromophenol blue and 4% (w/v) SDS).

Western blot analyses of protein samples were performed as previously described using rabbit α-VSV-G (1:5000, Sigma) or rabbit α-Tse2, α-Tse1, α-Tse3 (diluted 1:2000) and detected with α-rabbit horseradish peroxidase-conjugated secondary antibodies (Sigma) (113). Mouse α-$His_6$ (Life Tein) or mouse α-RNA polymerase β-subunit antibodies (1:2000, Neoclone) were used to

detect $His_6$–tagged proteins or RNAP, respectively. Western blots were developed using chemiluminescent substrate (SuperSignal West Pico Substrate, Thermo Scientific) and imaged with a FluorChemQ (ProteinSimple).

**Hcp1 Depletion Assays.** A controllable protein degradation system dependent on the ClpXP protease was used to deplete Hcp1 from *P. aeruginosa* cells. This system was originally developed for use in *E. coli*, but has been optimized for use in *P. aeruginosa* (44, 162). We generated *P. aeruginosa* strains lacking the native *sspB* gene, and with *hcp1* fused to a chromosomally encoded C-terminal degradation tag, DAS+4 (Hcp1-D4). SspB recognizes proteins containing D4 and delivers them to ClpXP for degradation. For controllable degradation of Hcp1-D4, we introduced a plasmid with inducible expression of *sspB*. Strains were sub-inoculated from overnight cultures at 1:1000 in LB. At mid-log phase, cultures were induced with 100 μM of IPTG. Protein samples were prepared after 90 minutes of *sspB* expression. Sample loading for SDS/PAGE and Western blot analysis was corrected for based on final $OD_{600}$.

**β-Galactosidase Assay.** β-Galactosidase assays were performed as described previously with minor modifications. A chromosomal integration vector (mini-CTX-*lacZ*) carrying a fusion of *lacZ* to the putative promoter region and first eight codon of *tse2* was used to generate strains for analysis. The plasmid was introduced into *P. aeruginosa* by conjugation (110). Overnight cultures were diluted 1:1000 in LB with 50 mM MOPS pH 7 and grown to mid-log phase. Cells were permeabilized with chloroform (15% chloroform) and assayed using the Tropix Galacon-

Plus reagents (Tropix, Bedford, MA). Values were normalized to the $OD_{600}$ for each strain. β-galactosidase assays were performed in triplicate.

**Co-Immunoprecipitation Assays.** For *P. aeruginosa* co-IP assays, overnight cultures were diluted 1:1000 into 100 mL of LB. At an $OD_{600}$ of 0.7, cells were harvested by centrifugation at 4,000 x g for 15 minutes. Pellets were resuspended in 2 mL of Buffer 2 (50 mM Tris HCl pH 7.5, 150 mM NaCl, 2% glycerol) supplemented with 1 mg/mL lysozyme. The resuspension was sonicated 3 times and centrifuged at 4°C for 30 minutes at 16,000 x g. Lysates were applied to 30 μL of anti-VSV-G agarose beads (Sigma) and incubated with rotation for 1 hour at 4°C. Beads were washed 3 times in 10 mL of Buffer 2 and resuspended in 30 μL of loading dye. Samples were analyzed by SDS-PAGE and Western blotting.

For *E. coli* co-IP assays with Tse2 homologs and Hcp, cells were grown to an $OD_{600}$ of 0.6 and induced with appropriate reagent for four hours. Cultures were harvested and pellets were resuspended in 2 mL LIB (low imidazole buffer, 50 mM Tris HCl pH 7.5, 500 mM NaCl, 10% glycerol, 30 mM Imidazole) and 1 mg/mL lysozyme and sonicated 3 times. Nontoxic alleles of *tse2* from *P. aeruginosa* contained mutations encoding substitutions T79A S80A (149) and *M. methanica* contained mutations encoding D63N. Clarified lysates were applied to 30 μL of Nickel-NTA sepharose beads and incubated by rotation for 1 hour at 4°C. Beads were washed 3 times in 10 mL LIB and resuspsended in 30 μL of loading dye. The same procedure was used for *E. coli* co-IP assays with Hcp homologs and Tse1, Tse3, $Tae2^{TY}$ or $Tae1^{BP}$ with the exception that pellets were resuspended in 2 mL of Buffer 3 (50 mM Tris HCl pH 7.5, 100 mM NaCl, 2%

glycerol, 50 mM Imidazole, 0.1% Triton X-100) with 1 mg/mL lysozyme and Nickel-NTA sepharose beads were washed 5 times in 10 mL of Buffer 3.

**Sedimentation Velocity Analytical Ultracentrifugation.** Sedimentation velocity (SV) experiments were performed using Hcp1 purified as previously described (12). SV Experiments were performed in 20 mM Phosphate, pH 7.5, 150 mM NaCl, and 2% glycerol (v/v). Data were collected using a Beckman XL-A analytical ultracentrifuge (Beckman Instruments, Inc., Fullerton, CA) using 12 mm Epon charcoal two sector centerpieces at 50,000 rpm and 10°C. Absorbance data were collected at 230 nm, using a spacing of 0.001 cm, with two average measurements in continuous scan mode; scans were collected every 7 minutes. The raw data were analyzed using the SedFit data analysis suite (212) using c(s) with one discrete component.

**Tse2 Stability Assays with Hcp1 Point Mutants.** *E. coli* BL21 plysS with plasmids containing each *hcp1* allele (pET29b) and $tse2^{NT}$ (pSCRhaB2-CV) were co-transformed into *E. coli*. Overnight cultures were sub-inoculated (1:1000) into 3 mL of 2xYT and grown to an $OD_{600}$ of 0.6. Cultures were induced with 0.1% rhamnose and 10 μM IPTG and harvested after 4 hours. 300 μl from each sample were centrifuged at 16,000 x g and resuspended in 30 μL Buffer 1 and 30 μL of SDS-PAGE loading dye, boiled and analyzed by Western blot. Densitometry was performed using AlphaView®Q software (ProteinSimple). The percentage of total accumulated Tse2 was determined by the following equation: (([Tse2*]/[Tse2])/ ([Hcp1*]/[Hcp1]))*100, where Tse2* = Tse2 accumulated in the presence of each Hcp1 point mutation (Hcp1*).

**Secretion Assays.** Overnight cultures of *P. aeruginosa* strains were used to inoculate 2 ml of LB (1:1000) supplemented with 0.5 mM IPTG. Cultures were grown at 37°C with shaking to mid-log phase and cell and supernatant fractions were processed as previously described (113).

**Interbacterial Competitions Assays.** Competition assays between *P. aeruginosa* strains were performed as previously described with minor variations (113, 204). Recipient strains contained *lacZ* inserted at the neutral phage attachment site (attTn7). For both Tse2 and Tse1/Tse3 dependent competitions assays, donor and recipient strains were mixed at a 1:1 ratio and 5 μL of the mixture were spotted on a 0.2 μM nitrocellulose membrane on LB low salt (LB-LS) 3% agar and grown at 37°C or inoculated into 2 mL of LB-LS and grown at 37°C with shaking. Competitions were harvested at 6 hours for assays with Δ*tse2* Δ*tsi2* recipients and 12 hours for assays with Δ*tse1* Δ*tsi1* Δ*tse3* Δ*tsi3* recipients. The competitive index was determined from plate counts of the initial and final time points. Statistical significance was determined using ANOVA and Tukey's *post hoc* test.

**Purification of Tse2-Hcp1 Complex for Transmission Electron Microscopy.** The Tse2-Hcp1 complex was purified from *E. coli* using a two-step affinity chromatography method. Two liters of *E. coli* BL21 cells containing plysS, pET29b::$tse2^{NT}$-$His_6$ and pPSV35::*hcp1*-VSV-G were grown to an $OD_{600}$ of 0.6 in 2xYT and induced with 100 μM IPTG for four hours at 37°C. Cells were harvested and resuspended in mLIB and 1 mg/mL lysozyme and lysed by sonication followed by a 1 hour centrifugation step at 16,000 x g. Clarified lysates were purified by elution from a metal-chelating affinity column. Eluted fractions were subjected to an addition

purification step by immune-affinity chromatography with anti-VSV-G conjugated agarose beads. Samples were eluted with 100 μg/mL VSV-G peptide.

**Single Particle Electron Microscopy of Hcp Rings and Hcp1-Tse2 Complex.** Hcp1 rings purified from *E. coli* were negatively stained by 0.75% uranyl formate as described previously (178). Images were collected on a transmission electron microscope T12 (FEI) at room temperature under 120 kV, and recorded at a magnification of 67,000× on a 4k × 4k Gatan CCD rendering a final pixel size of 1.65 Å on the specimen level. 2872 particles were selected and windowed into 120 × 120 pixel images using WEB (87). Projection averages of Hcp rings were generated after several cycles of reference-free multivariate statistical analysis using SPIDER (87). Among all the particles analyzed, 2770 were classified as intact ring-shape, and the rest were deformed. 6-fold symmetry was applied to the representative projection averages using command proc2d in EMAN (153). The same procedure was applied to the *E. coli* purified Hcp1–V/Tse2–$His_6$ complex. In this case, 3250 particles were selected and classified. Among them, 725 particles were un-filled rings, 2373 were filled rings and the remaining were deformed.

***E. coli* Toxicity Measurements.** *E. coli* BL21 plysS strains containing expression plasmids for *tse2* wild type or catalytic point mutants from *P. aeruginosa* or *M. methanica* (pSCRhaB2), and immunity homologs (pPSV39-CV) or empty vector were diluted in LB from overnight cultures to $10^6$ at 10 fold dilutions. 5 μl of each dilution were spotted onto LB agar plates containing appropriate antibiotics and 0.05% rhamnose and 100 μM IPTG. Photographs were take after overnight growth at 37°C.

**Software.** Protein sequences were obtained from NCBI (http://www.ncbi.nlm.nih.gov/). Full-length sequence alignments were prepared with Geneious software using the MUSCLE algorithm (73). Molecular graphics were generated using Pymol (www.pymol.org) (211).

**ACKNOWLEDGEMENTS**

The authors wish to thank Colin Murrell for providing *M. methanica* genomic DNA, Simon Dove for sharing the *sspB* knockout and expression constructs, Michele LeRoux and Brook Peterson for critical review of the manuscript, Alistair Russell for assistance with bioinformatics, and Spencer Anthony-Cahill, Peter Brzovic, Rachel Klevit, and members of the Mougous laboratory for helpful discussions. The Catalano laboratory is supported by National Institutes of Health Grant GM088186 and National Science Foundation Grant MCB-1158107. The Gonen laboratory is supported by the Howard Hughes Medical Institute. Work in the Mougous laboratory was funded by a grant from the NIH (AI080609). J.M.S. was supported by Public Health Service National Research Service Award T32 GM07270 from NIGMS and by a Helen Riaboff Whiteley Fellowship from the Department of Microbiology. J.D.M. holds an Investigator in the Pathogenesis of Infectious Disease Award from the Burroughs Wellcome Fund.

**Table 4.1. Plasmids Used in This Study**

| Plasmid name | Relevant features | Reference |
|---|---|---|
| pEXG2 | Allelic replacement vector containing *sacB* | (200) |
| pPSV35-CV | Expression vector with *lacI*, *lacUV5* promoter, C-terminal VSV-G tag | (115, 200) |
| pPSV39-CV | Derived from pPSV35-CV, lacking a cryptic start codon of the alpha fragment | (200) |
| pSCRhab2 | Expression vector with *PrhaB* | (37) |
| Mini-CTX-*lacZ* | miniCTX with *lacZ* translational reporter fusion | (110) |
| pPSV38-CV::PA4427 | For inducible expression of *sspB* | (43) |
| pSCRhab2-CV::PA2702 | Rhamnose inducible expression of *tse2* for toxicity assays | (113) |
| Mini-CTX-P*tse2–lacZ* | Chromosomal integration vector for *tse2-lacZ* reporter | This study |
| pSCRhab2-CV::PA2702 T79A S80A | Rhamnose inducible expression of non-toxic Tse2 | This study |
| pSCRhab2-CV::PA2702 D63N | Non-toxic *tse2* for co-IP and toxicity assays | This study |
| pSCRhab2-CV::metme3457 D53N | Non-toxic $tse2^{MM}$ for co-IP and toxicity assays | This study |
| pSCRhab2-CV::metme3457 | $tse2^{MM}$ for toxicity assays | This study |
| pET29b::PA0085 | $hcp1\text{-}his_6$ for stability assays, co-IPs, template for point mutants | (12) |
| pET29b::PFL6089 | $hcp^{PP}\text{-}his_6$ for co-IPs | This study |
| pET29b::metme0853 | $hcp^{MM}\text{-}his_6$ for coIPs | This study |
| pET29b::t2584 | $hcp^{TY}\text{-}his_6$ for coIPs | This study |
| pET29b::bphty4915 | $hcp^{BP}\text{-}his_6$ for coIPs | This study |
| pET29b::PA1512 | $hcp^{2}\text{-}his_6$ for coIPs | This study |
| pEXG2::PA0085 L28A | For generating chromosomal *hcp1* L28A point mutant | This study |
| pEXG2::PA0085 S31Q | For generating chromosomal *hcp1* S31Q point mutant | This study |
| pEXG2::PA0085 A29Q | For generating chromosomal *hcp1* A29Q point mutant | This study |
| pEXG2::PA0085 S35Q | For generating chromosomal *hcp1* S35Q point mutant | This study |
| pEXG2::PA0085 M42A | For generating chromosomal *hcp1* M42A point mutant | This study |
| pEXG2::PA0085 T59Q | For generating chromosomal *hcp1* T59Q point mutant | This study |
| pEXG2::PA0085 S115Q | For generating chromosomal *hcp1* S115Q point mutant | This study |
| pEXG2::PA0085 T122Q | For generating chromosomal *hcp1* T122Q point mutant | This study |
| pEXG2::PA0085 N124A | For generating chromosomal *hcp1* N124A point mutant | This study |
| pET29b::PA2702 T79A S80A | $tse2^{NT}$ for Hcp1-Tse2 purification | This study |
| pPSV35-CV::PA0085 | *hcp1* for Hcp1-Tse2 purification | This study |
| pPSV39-CV::PA2703 | *tsi2* for toxicity assays | This study |
| pPSV39-CV::metme3456 | $tsi2^{MM}$ for toxicity assays | This study |
| pPSV35-CV::t2586 | $tae2^{TY}$, amidase effector form *S.* Typhi TY2, for co-IP | (206) |
| pPSV39-CV::metme3457 D63N | Non-toxic $tse2^{MM}$ for expression in *P. aeruginosa* | This study |
| pPSV35-CV::bphty5187 | $tae1^{BP}$, amidase effector from *B. phytofirmans*, for co-IP | (206) |
| pPSV35-CV::PA3484 | *tse3*, for co-IP | (113) |
| pPSV35-CV::PA1844 | *Tse1*, for co-IP | (113) |

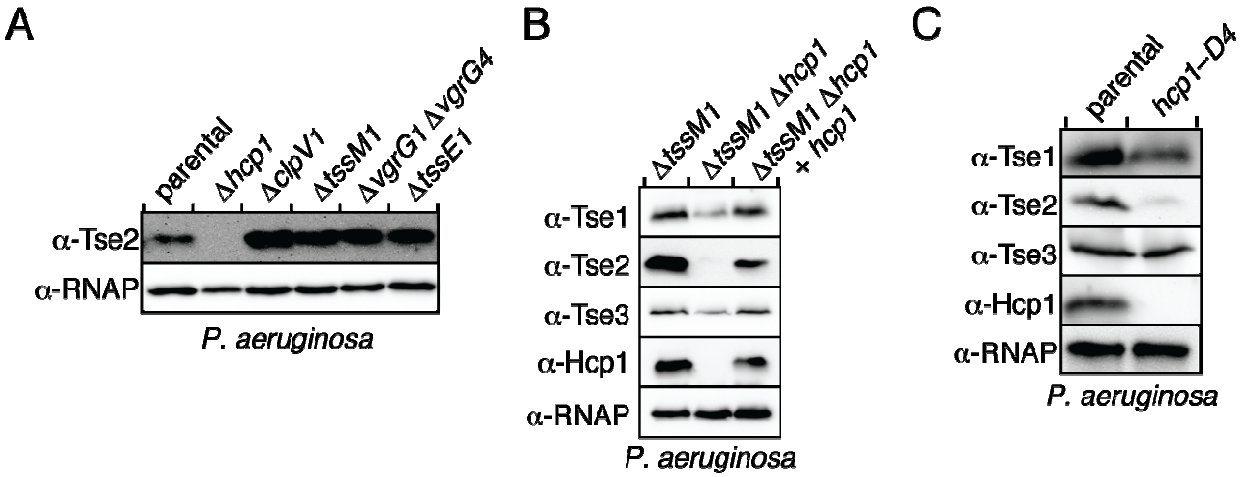


**Figure 4.1: Tse2 Requires Hcp1 for Intracellular Accumulation.** (A and B) Western blot analysis of intracellular levels of H1-T6S effectors (Tse1, Tse2 and Tse3) in the indicated *P. aeruginosa* backgrounds. RNA polymerase (RNAP) is included as a loading control. Unless otherwise indicated, the parental background in this and all subsequent figures is Δ*retS*. (C) Western blot analysis of intracellular Hcp1 and H1-T6S effector levels in a ClpXP-dependent Hcp1 depletion assay. Samples were processed 90 minutes after induced *sspB* expression in *P. aeruginosa* strains lacking the native *sspB* gene and containing wild-type *hcp1* or *hcp1–D4*.

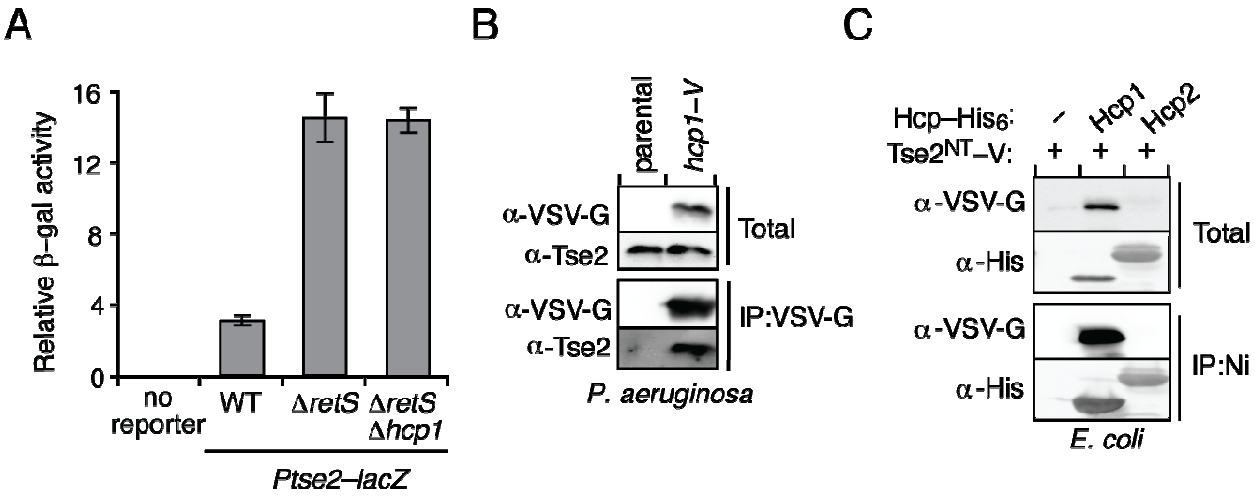


**Figure 4.2: Hcp1 Interacts Directly with Tse2.** (A) Relative levels of β-galactosidase activity from the indicated *P. aeruginosa* strains containing a chromosomally-integrated *lacZ* reporter fused to the promoter region and first eight codons of *tse2* (*Ptse2–lacZ*). Error bars represent standard deviation based on three independent replicates. (B) Western blot analysis of Tse2 from total and bead-associated fractions of an anti-VSV-G immunoprecipitation from *P. aeruginosa* strains encoding Hcp1 or ectopically expressing Hcp1. (C) Immunoblot detecting total and bead-associated fractions of a nickel-NTA precipitation assay from *E. coli* expressing a nontoxic, VSV-G epitope-tagged allele of *tse2* (*tse2*$^{NT}$*–V* (T79A S80A)) with empty vector (–) or a plasmid containing the indicated *hcp* (*hcp1* or *hcp2*) homolog fused to a $His_6$ tag.

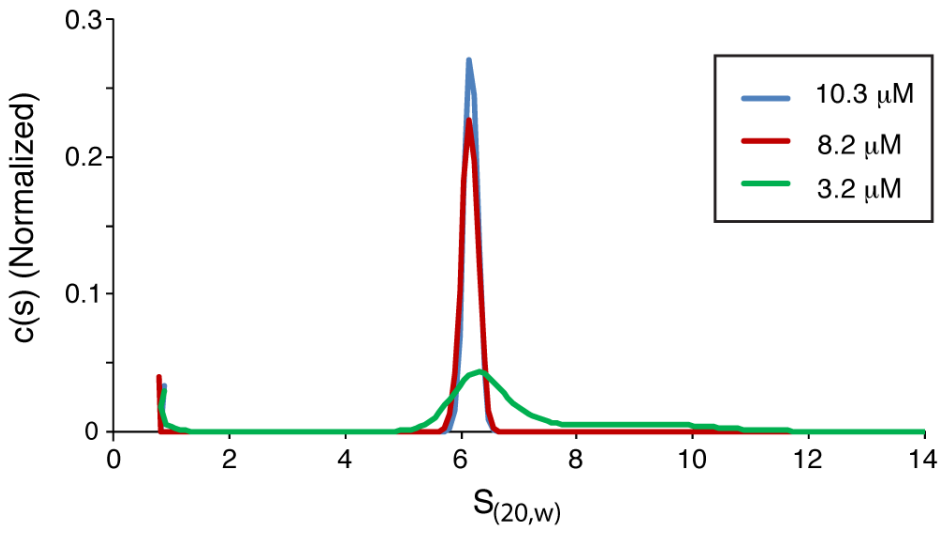


**Figure 4.3: Hcp exists as a hexamer above 3.2 μM.** Sedimentation velocity analytical ultracentrifugation (SV-AUC) data was analyzed with SedFit (see experimental procedures). A c(s) analysis shows a homogenous species consistent with Hcp hexamer at concentrations between 3.2 μM and 10.3 μM. Some apparent heterogeneity in the 6.1S species at 3.2 μM is due to low signal-noise at low concentration.

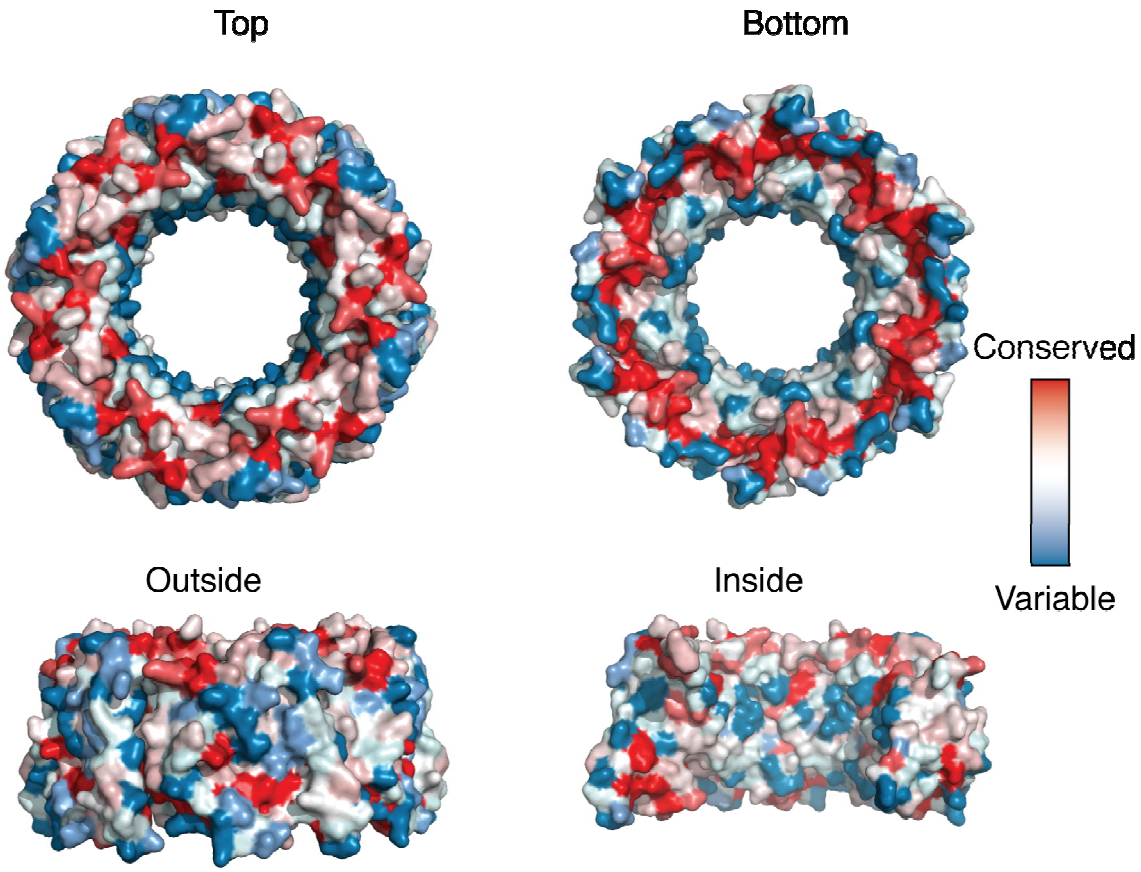


**Figure 4.4: Sequence Conservation Analysis of Hcp1.** Surface representation of Hcp1 (PDB: 1Y12) amino acid conservation, where highly conserved residues are colored in red and highly variable residues are colored in blue. A multiple sequence alignment of 100 Hcp proteins was obtained using BLink (http://www.ncbi.nlm.nih.gov). Sequence conservation values were generated using ConSurf (http://consurf.tau.ac.il).

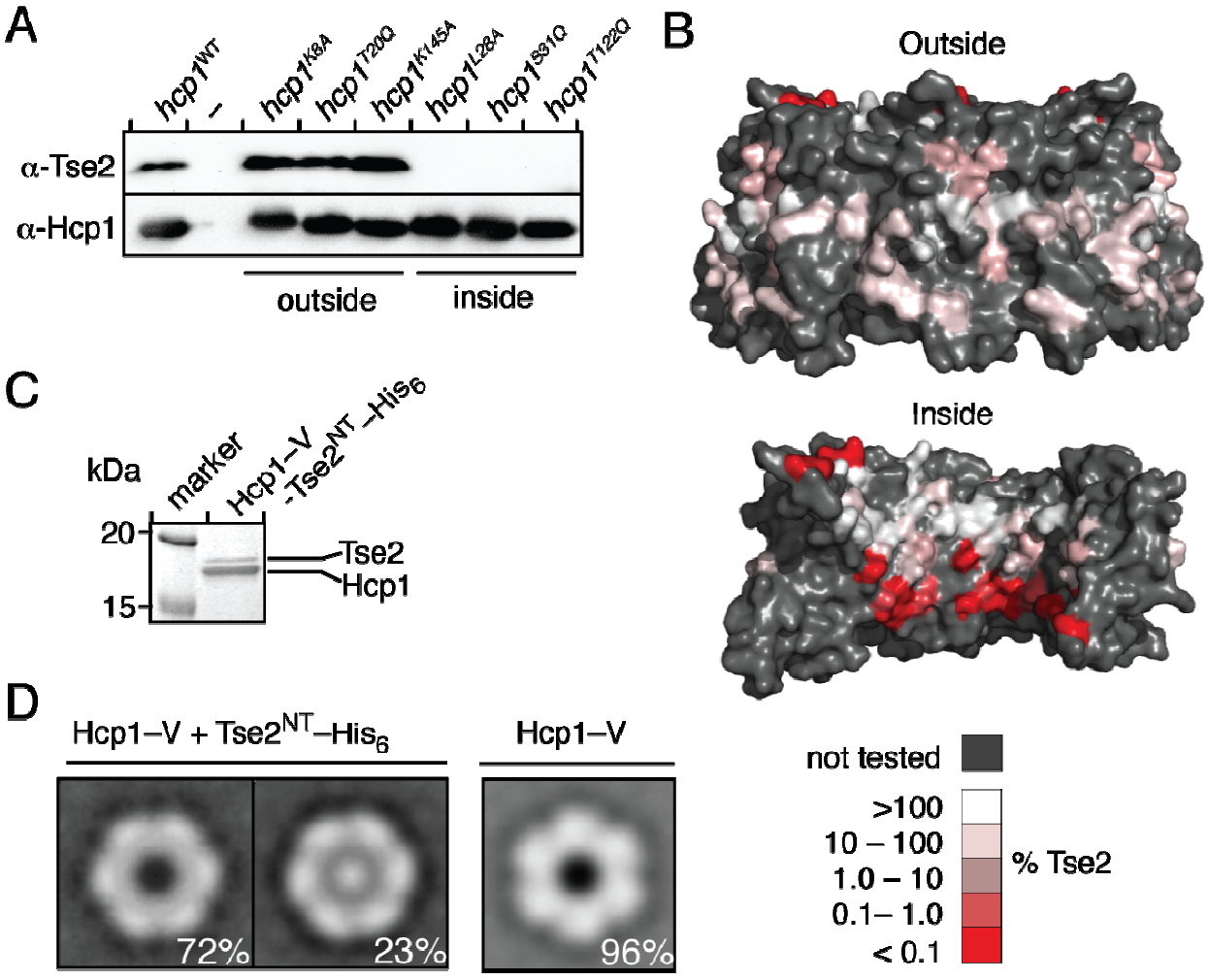


**Figure 4.5: Tse2 binds to the pore of the Hcp1 ring.** (A) Representative Western blots showing the effect of the indicated Hcp1 amino acid substitutions on intracellular levels of $Tse2^{NT}$ in *E. coli*. The localization of the substitutions to the inside or outside surface of the Hcp1 ring is noted. (B) Surface representation of the Hcp1 ring colored to reflect Tse2 stabilization activity of each variant tested (white-red =100%-0.01%, gray = not tested). The lower image depicts a cutaway view of the Hcp1 hexamer. Levels of Tse2 were calculated based on the ratio of band intensity of $Tse2^{NT}$ and Hcp1 point mutants, normalized to Tse2 and wild-type Hcp1 (Figure S2). (C) Coomassie-stained SDS-PAGE gel of co-purified $Tse2^{NT}$–$His_6$ and Hcp1–V. (D) Class averages with applied six-fold symmetry from analysis of transmission electron micrographs of $Tse2^{NT}$–$His_6$ -Hcp1–V and a Hcp1–V-only control. The percentage of particles represented by each class average is indicated in the corresponding frame.

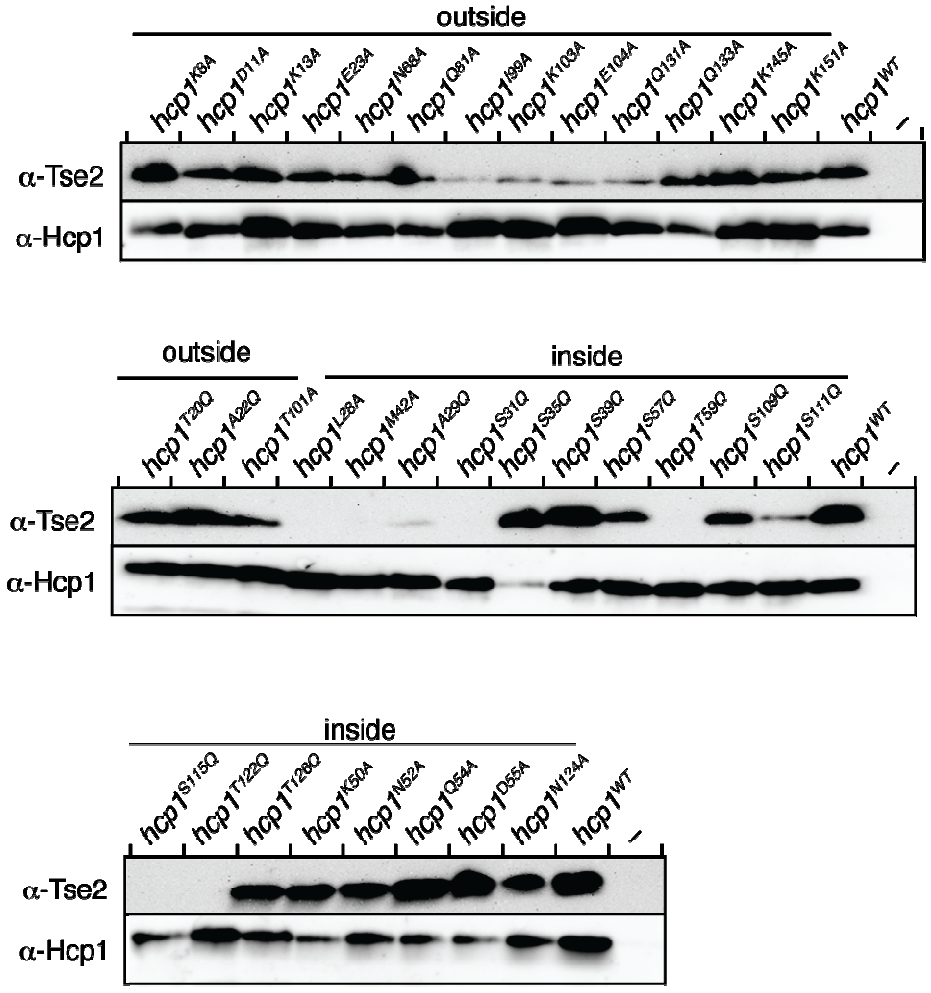


**Figure 4.6: Analysis of Tse2 stabilization by Hcp1 point mutants.** Related to Figure 3A and 3B. Western blot results showing the effect of each Hcp1 point mutant on intracellular levels of $Tse2^{NT}$. The Hcp1 point mutations are located on the inside or outside surface of Hcp1 rings as indicated. Each *hcp1* point mutant was co-expressed with a nontoxic allele of *tse2* (T79A S80A) in *E. coli*.

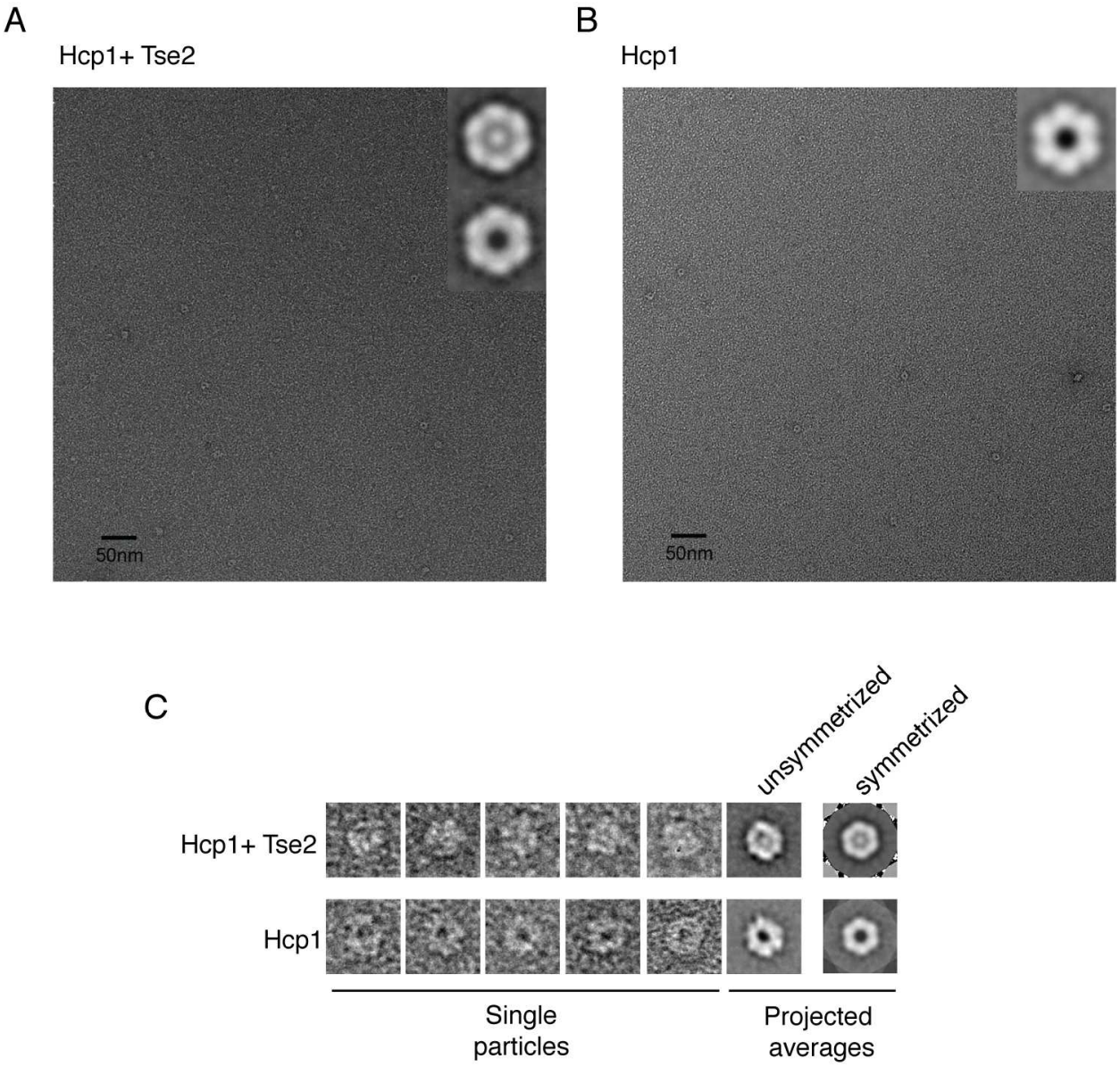


**Figure 4.7: Representative transmission electron micrographs of Hcp and the Hcp1-Tse2 complexes.** Full frame transmission electron micrographs from purified Tse2–$His_6$ -Hcp1–V (A) and Hcp1–V-only (B) samples. Class averages with applied six-fold symmetry for each sample are shown in the upper right hand corner. (C) Single particles, projected asymmetric average and symmetry applied average from Hcp1 and Hcp1–Tse2 samples.

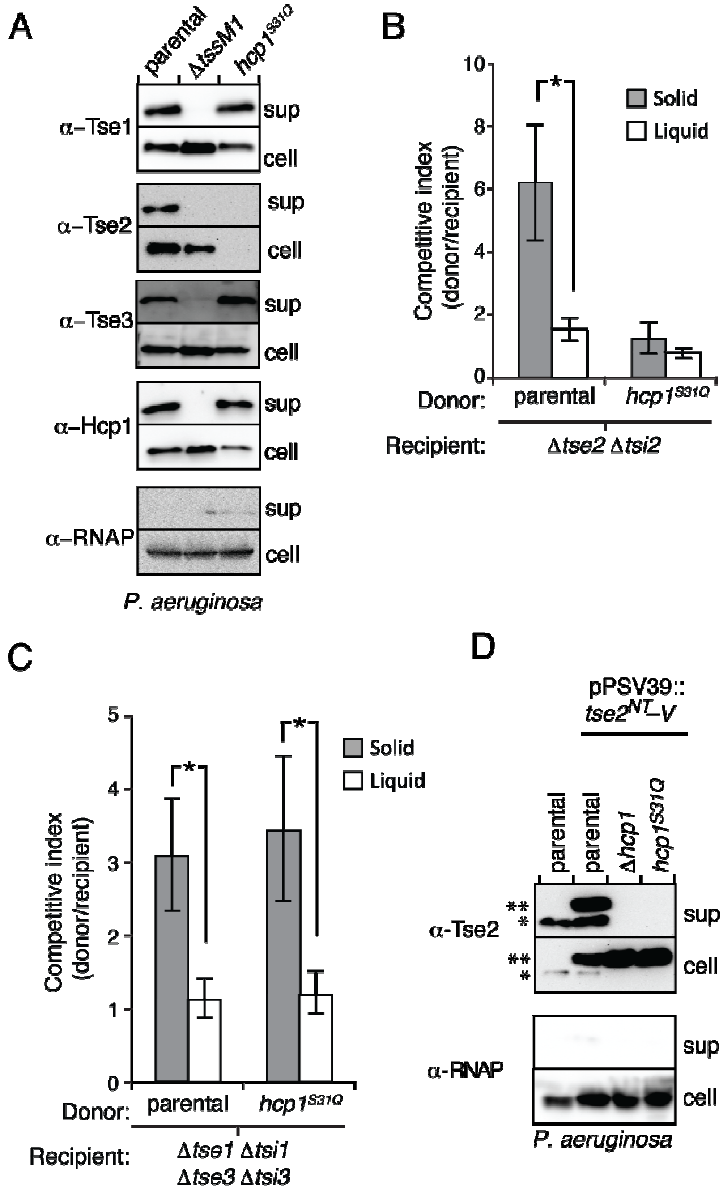


**Figure 4.8: Tse2 requires interaction with Hcp1 for secretion. (**(A) Western blot analysis of cell and supernatant fractions of Hcp1 and H1-T6S effectors in *P. aeruginosa* strains harboring wild-type *hcp1* or *hcp1*$^{S31Q}$. Equally exposed α-RNA polymerase (RNAP) blots of equivalent fractions of total cell and supernatant (sup) samples are included as loading and cytoplasmic leakage controls in this and subsequent secretion assays. (B and C) Outcome of growth competition experiments between *P. aeruginosa* donor strains (parental or *hcp1*$^{S31Q}$) and a Tse2-susceptible (Δ*tse2* Δ*tsi2*) (B) or a Tse1- and Tse3-susceptible recipient strain (Δ*tse1* Δ*tsi1* Δ*tse3* Δ*tsi3*) (C) on solid (gray) or liquid (white) media. The competitive index is calculated as the change (final/initial) in ratio of donor to recipient c.f.u. Error bars represent standard deviation based on four replicates. Asterisks denote statistical significance using ANOVA and Tukey's *post hoc* test between the indicated conditions ($P < 0.001$). (D) Western blot analysis of cell and supernatant-associated fractions of chromosomal, endogenous Tse2 (one asterisk) and ectopically expressed Tse2$^{NT}$–V (two asterisks) in the indicated *P. aeruginosa* strains.

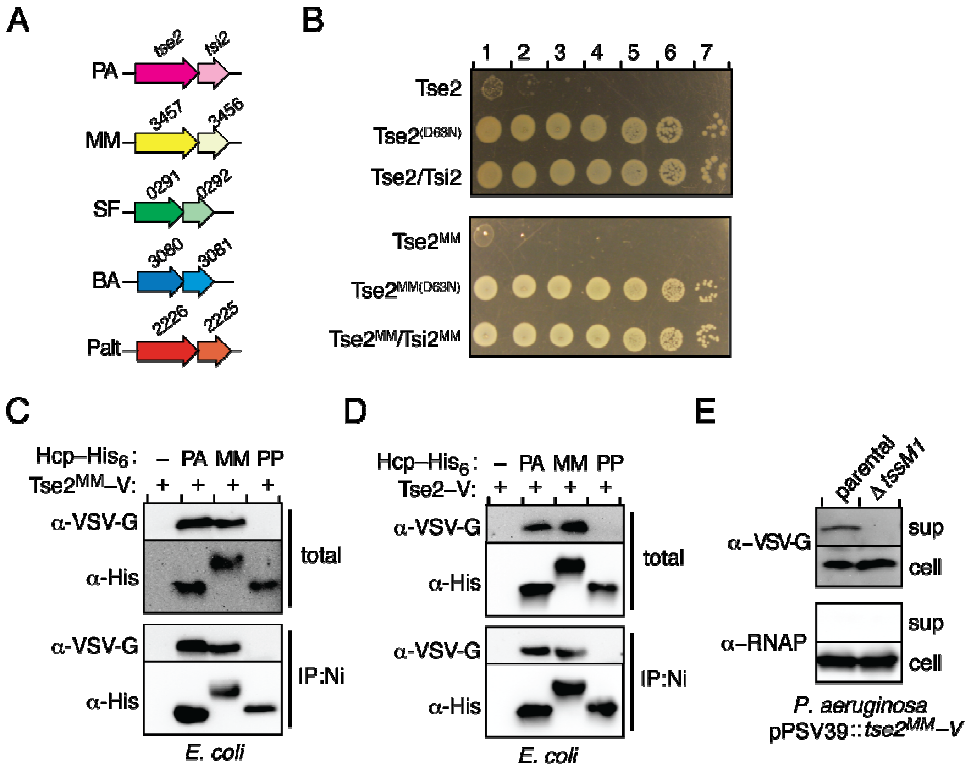


**Figure 4.9: Stabilization by cognate Hcp is a general feature of Tse2-like effectors.** (A) Genomic organization of *tse2* and *tsi2* homologs from *P. aeruginosa* (PA) *M. methanica* (MM), *S. frigidimarina* (SF), *B. ambifaria* (BA) and *Pseudoalteromonas* sp. (Palt). Abbreviated locus tag numbers are indicated for *tse2* (darker shade) and *tsi2* (lighter shade) homologs from each organism. (B) Growth of *E. coli* containing plasmids with inducible expression of *tse2* or *tsi2* homologs from *P. aeruginosa* (upper panel) or *M. methanica* (lower panel). Serial ten-fold dilutions are indicated by numbers. (C and D) Western blot results of co-IP assays from *E. coli* co-expressing *hcp–his*$_6$ homologs from *P. aeruginosa* (PA), *M. methanica* (MM) or *P. protegens* (PP) with *tse2*$^{(D63N)}$*–V* (mutation denoted with asterisk) from *M. methanica* (C) or *P. aeruginosa* (D). (E) Analysis of cell and supernatant-associated fractions of the indicated *P. aeruginosa* strains expressing Tse2$^{MM}$–V ectopically.

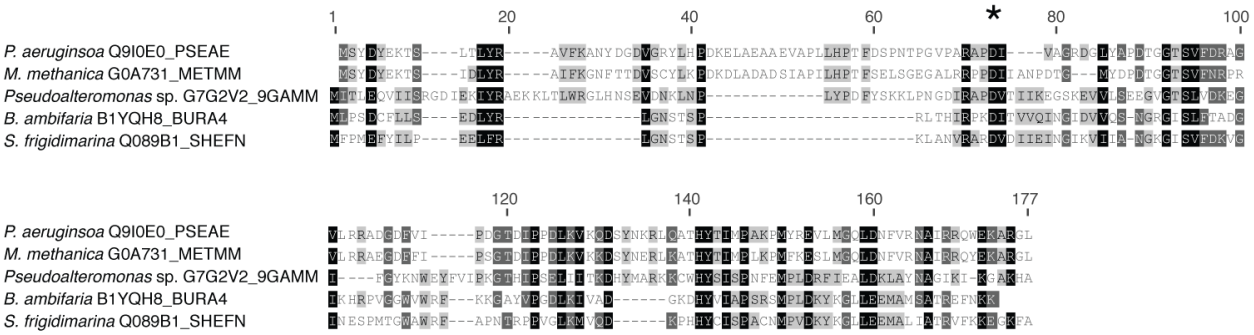


**Figure 4.10: Sequence alignment of Tse2 homologs.** Full-length sequences were aligned using Geneious software with the MUSCLE algorithm. The organism name and SWISS-PROT protein identification code are indicated for each Tse2 homolog. Individual residues are shaded according to their similarity with residues at that position for all sequences (darker=greater similarity). The conserved aspartic acid located within a putative catalytic motif is noted with asterisk.

‘

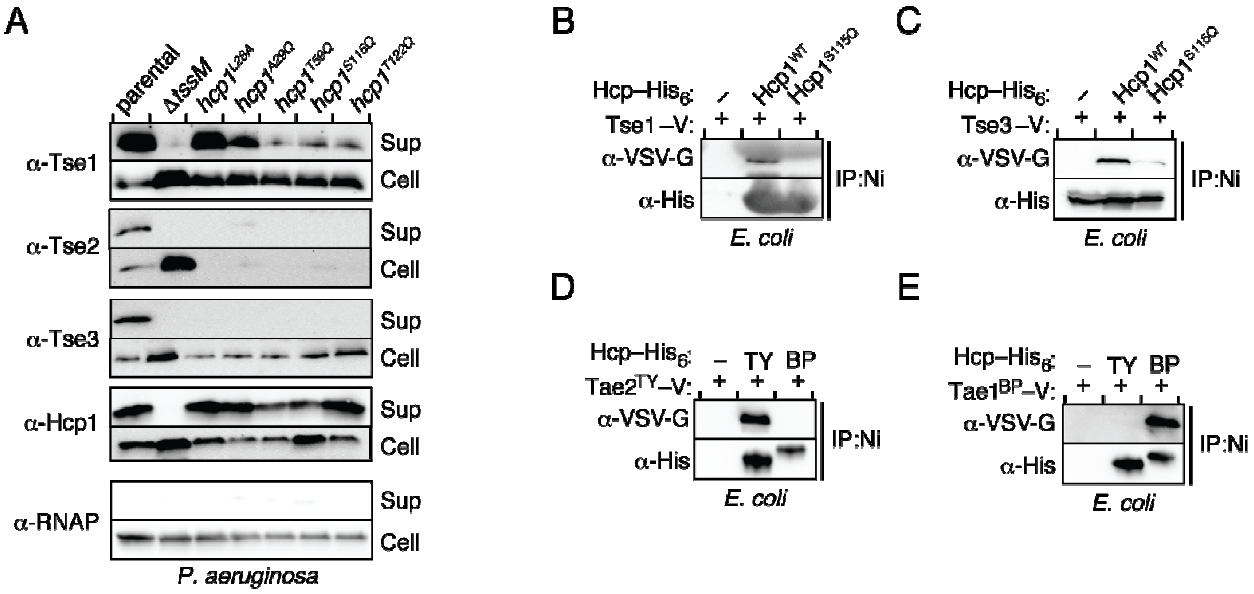


**Figure 4.11: Binding to the pore of cognate Hcp proteins is required for export of effectors with amidase and muramidase activities.** (A) Western blot analysis of cell and supernatant fractions of Hcp1 and H1-T6S effectors in *P. aeruginosa* strains wherein the native *hcp1* allele is substituted with the indicated mutant. (B and C) Western blot analysis of bead-associated fractions of a co-IP from *E. coli* co-expressing the indicated *hcp–his*$_6$ alleles with Tse1–V (B) or Tse3–V (C). (D and E) Immunoblot detecting bead-associated fractions of a co-IP from *E. coli* co-expressing *hcp–his*$_6$ homologs (TY, *S.* Typhi; BP, *B. phytofirmans*) and *tae2*$^{TY}$*–V* (D) or *tae1*$^{BP}$*–V* (E).

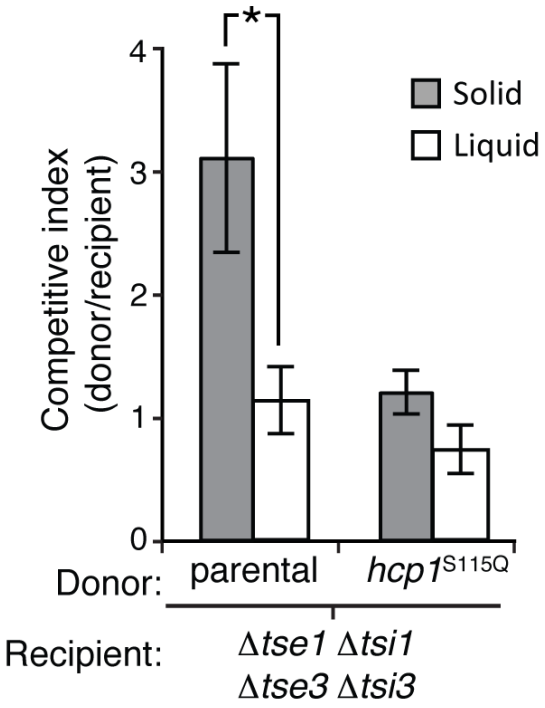


**Figure 4.12. Hcp1$^{S115Q}$ disrupts Tse1- and Tse3-dependent intoxication.** Outcome of growth competition experiments between *P. aeruginosa* donor strains (parental or *hcp1*$^{S115Q}$) and a Tse1- and Tse3-susceptible recipient strain (Δ*tse1* Δ*tsi1* Δ*tse3* Δ*tsi3*) (C) on solid (gray) or liquid (white) media. The competitive index is calculated as the change (final/initial) in ratio of donor to recipient c.f.u. Error bars represent standard deviation based on four replicates. Asterisks denote statistical significance using ANOVA and Tukey's *post hoc* test between the indicated conditions ($P < 0.001$).

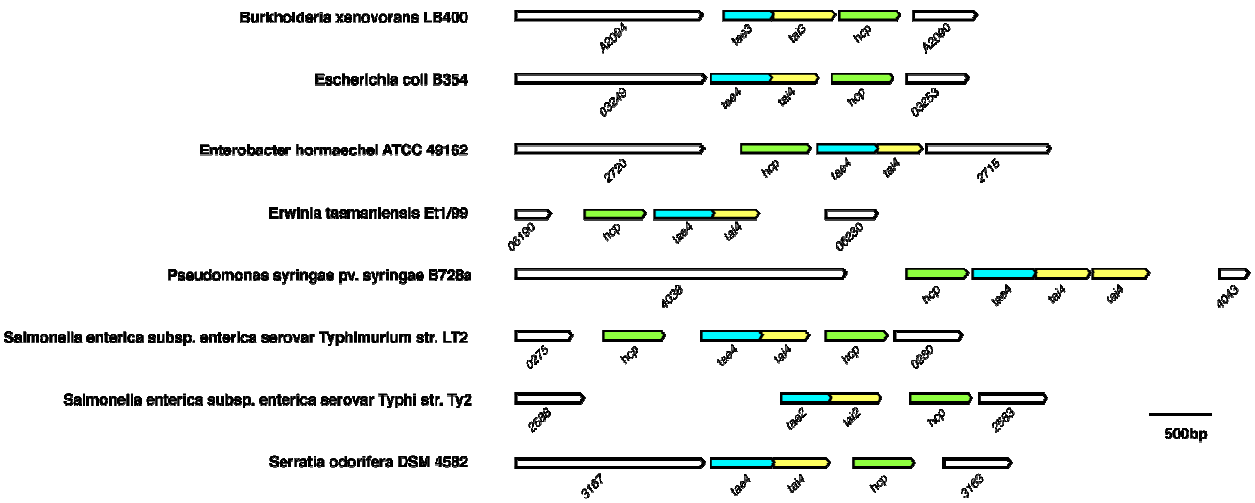


**Figure 4.13: Examples of genetically linked *hcp* and T6S amidase effector–immunity genes.** Schematic representing the genomic organization of a selection of non-orthologous *hcp* and T6S amidase effector–immunity (*tae–tai*) pairs. Genes colored in green encode Hcp proteins, while those colored in cyan or yellow encode Tae or Tai, respectively. Locus tags are provided for each gene.

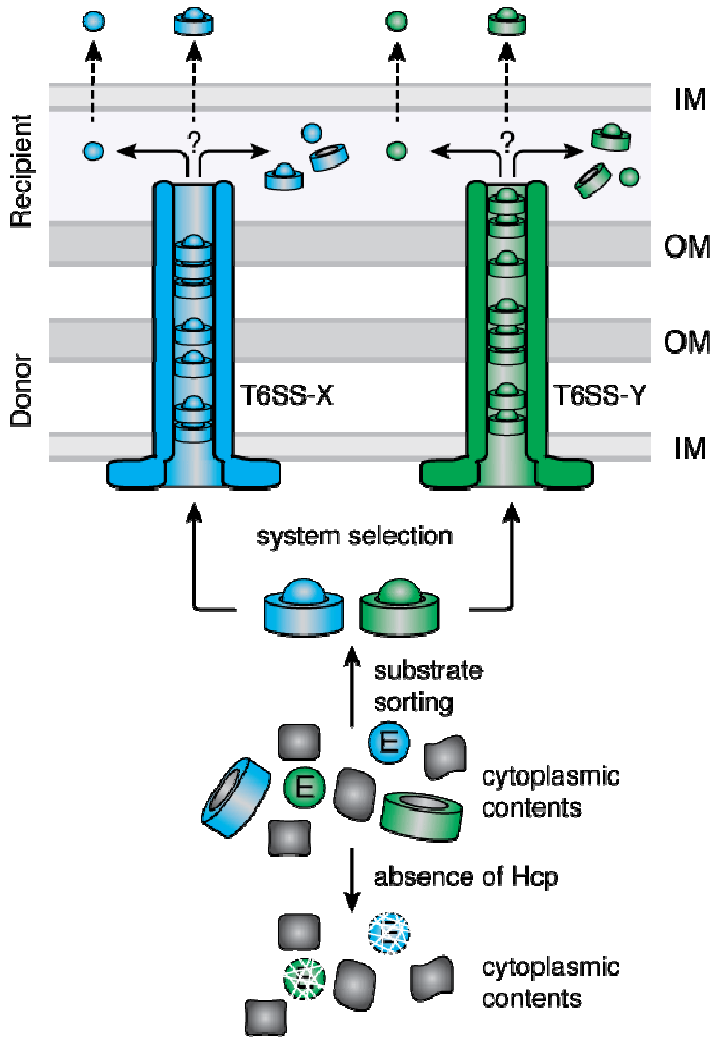


**Figure 4.14: Model depicting the role of Hcp in T6S effector recognition and export.** The schematic depicts the junction between two Gram-negative bacterial cells (OM, outer membrane; IM, inner membrane), a donor cell, harboring two T6SSs T6SS-X (blue) and T6SS-Y (green), and a recipient cell that is targeted by these systems. T6S effectors ($E_x$, $E_y$) are sorted from the cytoplasmic pool of proteins via interactions with cognate Hcp proteins ($H_x$, $H_y$). Interaction with Hcp prevents effector degradation. Hcp–effector complexes are recognized and transported through the appropriate T6SS via an unknown mechanism. Once the complex reaches the recipient cell, it may be either translocated into the periplasm intact, or the effector may dissociate from Hcp prior to periplasmic delivery. Likewise, effectors destined for the cytoplasm may be transported in complex or in isolation.

# CHAPTER V:

## Conclusions and future directions

The T6SS is a contact-dependent secretory pathway found abundantly in Gram-negative bacteria. This pathway delivers effector molecules into eukaryotic and prokaryotic cells, and in some cases, possesses dual functions – targeting both cell types (113, 157, 192, 216). The apparent versatility of the T6SS, and the distribution of this system among both pathogens and non-pathogens, is consistent with its role as a virulence factor and as a mediator of interbacterial interactions (215). The interbacterial targeting functions of T6SSs also has the potential to be a virulence determinant. Recent studies have found that the diverse and dynamic community of microorganisms that are directly associated with humans can have an impact on disease outcome (114). A candidate genetically encoded mechanism underlying this phenomenon is the T6SS. The findings from this thesis work, in combination with the continually expanding body of literature, have broadened our understanding of the T6SS and have laid the foundation for further studies that could potentially elucidate its role in the environment.

In this thesis work, I have characterized posttranslational regulators that control H1-T6SS activity in *P. aeruginosa*. Two distinct pathways – the phosphorylation-dependent and phosphorylation-independent pathways – that activate the H1-T6SS by promoting the assembly of the H1-T6S apparatus and initiating effector export have been elucidated (40, 115, 167, 222). Several components of the phosphorylation-dependent pathway, PpkA, PppA, Fha1 and TagR, were initially identified and characterized by Mougous and colleagues (115, 167). These proteins modulate the phosphorylated state of Fha1, wherein phosphorylated Fha1 triggers apparatus assembly and effector export. In this pathway, stimulated PpkA phosphorylates Fha1, while PppA antagonizes this process through phosphatase activity. The periplasmic localized protein,

TagR, acts as a co-receptor for PpkA by promoting Fha1 phosphorylation through PpkA dimerization and autophosphorylation.

The thesis work has added new dimensions to the phosphorylation-dependent pathway, also known as the TPP. First, this work has provided evidence that surface growth posttranslationally triggers H1-T6S activation via the TPP (222). Specifically, Fha1 phosphorylation is enhanced under these growth conditions, which, interestingly, are conditions that also promote T6S-dependent effector delivery through close cell-to-cell contact. These findings are consistent with the hypothesis that the H1-T6SS plays a role in sessile bacterial communities, which are often associated with chronic infection (55). Identification of specific signaling molecule, or a physiological change, that stimulates the TPP during surface-associated growth could provide important insights into the physiologically relevant function of the T6SS.

This thesis work has also resulted in the identification of additional HSI-I-encoded accessory proteins that participate in the TPP: TagQ, TagS and TagT (40). These proteins are positive regulators of the TPP, acting upstream of PppA and PpkA. TagQ, TagS and TagT stimulate the TPP upon surface-associated growth. In collaboration with Ina Attree's group, we found that TagS and TagT form a complex at the inner membrane. TagT exhibits ATPase activity; however, it is not yet known how this activity contributes to T6SS function. Through biochemical analyses, TagQ was characterized as an outer membrane lipoprotein. Together, these proteins promote phosphorylation-dependent activation of the H1-T6SS.

In addition to the TPP, a second posttranslational H1-T6SS regulatory pathway was identified from this work (222). An HSI-I encoded accessory protein, TagF, mediates this pathway by repressing H1-T6SS activation independent of the TPP. Although derepression of the H1-T6SS by TagF requires the presence of Fha1, Fha1 phosphorylation is dispensable. Furthermore, surface growth is not an environmental cue for this pathway. A physiological signal for the TagF-mediated pathway remains to be identified. The finding that two independent pathways posttranslationally modulate H1-T6SS activity indicates that this complex secretory pathway is under tight control. The TPP and TagF-mediated pathway may be important to initiate efficient effector export under suitable environmental conditions.

While the proteins involved in the TPP and TagF-dependent pathway are encoded within the HSI-I gene cluster, I found that they are dispensable for T6S function and are thus true accessory proteins. Consistent with their role in regulation is the observation that homologs of these genes are found in approximately 30% of sequenced T6S gene clusters (27). The distribution of these homologs suggests that a portion of T6SS may employ a common mechanism to regulate the activity of the secretory system.

Lastly, this thesis work has revealed that Hcp is a T6S receptor and chaperone for effectors. Hcp forms a homohexameric ring with a 40 Å pore that has long been hypothesized to assemble into a tube and serve as a static conduit for effector transit. In contrast to this model for effector secretion, this work demonstrated that T6S-effectors specifically and stably bind to the inner pore of the Hcp ring. These interactions are essential for effector secretion through the H1-T6SS. Together, these findings indicate that substrate specificity is likely governed by Hcp-dependent

effector interactions. Furthermore, this work has revealed that Hcp and effectors are likely co-secreted as a stable complex, rather than Hcp serving as a channel for effectors to pass through transiently.

The identification of two posttranslational pathways that regulate H1-T6S activity and the discovery of a T6S-specific effector receptor and chaperone contributes significantly to the growing body of data that shapes our understanding of this complex secretory system. Many questions remain regarding the signals and pathways that regulate the H1-T6SS and the mechanism of effector secretion. Several of these unanswered questions are discussed below.

*What are the environmental signals that stimulate activation of the T6SS?*

Previous studies have demonstrated that the T6SS directly transfers effectors into target cells in a cell contact-dependent manner (113, 204, 216). In this thesis work, a physiologically relevant trigger for posttranslational activation of the T6SS – surface associated growth – was identified. Together, these findings suggest that physiological changes that occur during surface growth may directly or indirectly stimulate the T6SS. Determining the specific signal that is involved in this process may provide further insight into when and where T6S-dependent interactions take place in the environment.

A candidate signaling molecule that may be involved in surface growth-dependent stimulation of the H1-T6SS via the TPP is the secondary messenger molecule c-di-GMP. In *P. aeruginosa*, as well as other Gram-negative bacterial species, c-di-GMP plays a key role, both directly and

indirectly, in regulating the transition of cells from planktonic to sessile growth, and vice versa (106). A correlation between increased c-di-GMP levels, induced by a mutation in a global regulator, *retS*, and elevated H1-T6S expression was previously reported (165). Nevertheless, this study did not examine the regulatory level at which c-di-GMP influences T6S expression, or whether this observation was direct or indirect. A link between c-di-GMP and T6S regulation has also been suggested in *Vibrio alginolyticus*, where a *pppA* homolog appears to modulate c-di-GMP levels (219). Specifically, deletion of *pppA* induced pleiotrophic effects on various cellular processes, including the production of c-di-GMP. Although the molecular mechanism for this observation was not investigated, it suggests a possible interaction between PppA and c-di-GMP.

To determine whether components of the TPP or TagF-mediated pathways directly interact with c-di-GMP, several approaches can be employed. For example, *in vitro* or *in vivo* c-di-GMP binding assays have been developed to identify c-di-GMP–protein interactions (108, 140). In addition, a FRET-based reporter can be engineered to the protein of interest to determine *in vivo* interactions with c-di-GMP or other small molecules (49). Previous studies have shown that c-di-GMP binding proteins frequently undergo conformational changes upon c-di-GMP binding. A protein of interest could be modified with dual fluorescence, for example YFP fused to the N-terminus and CFP fused to the C-terminus, and then monitored for conformational changes. A binding event can be detected when the orientation of both fluorescent proteins changes, resulting in a shift in FRET efficiency.

*Defining the full repertoire of protein effectors and other substrates of the T6SS.*

Characterizing the activities exhibited by secretion system substrates has aided in the discovery of functions for secretory pathways. For example, the identification of T6S substrates of the H1-T6SS in *P. aeruginosa* revealed its bacterial targeting function (204). While substrates have been identified for a variety of T6SSs, there are many examples of T6SSs wherein no substrates have been discovered. Previous studies have successfully identified T6S substrates through global analysis of secreted proteins from *P. aeruginosa* and *B. thailandensis* (113, 206). These approaches are not necessarily saturating. Two independent reports have found that *P. aeruginsoa* strains lacking the three previously identified effectors still display a partial T6S-dependent fitness advantage (69, 144). These findings suggest that unidentified effectors may be responsible for the phenotype. More exhaustive studies are required in order to fully define the substrates of this system.

Various high-throughput genetic screens could facilitate the identification of new effectors. Using transposon mutagenesis and high-throughput sequencing, T6S immunity genes were identified in *V. cholerae* and led to the discovery of T6S effectors (69). Similar to previously identified T6S-effectors–immunity pairs, the genes discovered in this screen were essential in the presence of the adjacently encoded T6S-effector, which also displayed antibacterial activity. This approach can be applied to various species where T6S substrates are yet to be identified.

In addition to previous studies that identified effectors through secretome analysis, determining the intracellular proteome could aid in the identification of new T6S effectors. This idea is based on findings from this thesis work that demonstrated stability of effectors is fully or partially dependent on Hcp. The intracellular proteome could be compared between a wild-type bacterial

strain and a strain containing a deletion of *hcp*. Relative changes in protein levels between these strains could reveal putative T6S effectors.

*What are the sequence or structural motifs of effectors that permit recognition by the T6SS?*

The surprising role for Hcp as a T6S-specific chaperone and receptor for substrates has raised new questions about the mechanism of substrate selectivity. This work has demonstrated that the inner surface of the Hcp ring is a binding site for effectors. Future studies will aim to dissect the sequences or structural motifs present within effectors that mediate these interactions. Substrate truncation analysis is a basic method that has been successfully employed to identify the minimal secretion signal for other secretory pathways. For T6S-substrates, 5-10 AA truncations can be generated sequentially, starting at the N-terminus or C-terminus. These truncated substrates can be subjected to protein-protein interaction analysis with Hcp *in vitro* and can be analysed for T6S-dependent secretion efficiency *in vivo.* These studies may reveal a common sequence motif, which, in turn, could facilitate the identification of addition substrates of the T6SS. However, due to the low sequence homology among H1-T6S substrates, it is more likely that effectors share a common tertiary structure that could mediate interactions with Hcp. Therefore, a more complex approach may be required to determine the recognition mechanism, possibly through the use of the structural information that is available for T6S-effectors.

In conclusion, this work contributes to the rapidly growing and fascinating field of contact-dependent mechanisms that bacteria utilize to mediate interactions with their environment. In

addition, these studies have broadened our general understanding of the diversity of mechanisms that facilitate protein export.

## REFERENCES


1. **Abdallah, A. M., N. C. Gey van Pittius, P. A. Champion, J. Cox, J. Luirink, C. M. Vandenbroucke-Grauls, B. J. Appelmelk, and W. Bitter.** 2007. Type VII secretion--mycobacteria show the way. Nature Reviews Microbiology **5:**883-891.
2. **Ackermann, H. W.** 1998. Tailed bacteriophages: the order caudovirales. Advances in Virus Research **51:**135-201.
3. **Akeda, Y., and J. E. Galan.** 2005. Chaperone release and unfolding of substrates in type III secretion. Nature **437:**911-915.
4. **Aksyuk, A. A., P. G. Leiman, L. P. Kurochkina, M. M. Shneider, V. A. Kostyuchenko, V. V. Mesyanzhinov, and M. G. Rossmann.** 2009. The tail sheath structure of bacteriophage T4: a molecular machine for infecting bacteria. The EMBO Journal **28:**821-829.
5. **Altschul, S. F., T. L. Madden, A. A. Schaffer, J. Zhang, Z. Zhang, W. Miller, and D. J. Lipman.** 1997. Gapped BLAST and PSI-BLAST: a new generation of protein database search programs. Nucleic Acids Research **25:**3389-3402.
6. **Alvarez-Martinez, C. E., and P. J. Christie.** 2009. Biological diversity of prokaryotic type IV secretion systems. Microbiology and Molecular Biology Reviews **73:**775-808.
7. **Aschtgen, M. S., C. S. Bernard, S. De Bentzmann, R. Lloubes, and E. Cascales.** 2008. SciN is an outer membrane lipoprotein required for Type VI secretion in enteroaggregative *Escherichia coli*. Journal of Bacteriology **190:**7523-7531.
8. **Aschtgen, M. S., M. Gavioli, A. Dessen, R. Lloubes, and E. Cascales.** 2010. The SciZ protein anchors the enteroaggregative *Escherichia coli* Type VI secretion system to the cell wall. Molecular Microbiology **75:**886-899.
9. **Aschtgen, M. S., M. S. Thomas, and E. Cascales.** 2010. Anchoring the type VI secretion system to the peptidoglycan: TssL, TagL, TagP... what else? Virulence **1:**535-540.
10. **Aubert, D., D. K. MacDonald, and M. A. Valvano.** 2010. BcsKC is an essential protein for the type VI secretion system activity in *Burkholderia cenocepacia* that forms an outer membrane complex with BcsLB. The Journal of Biological Chemistry **285:**35988-35998.
11. **Babu, M. M., M. L. Priya, A. T. Selvan, M. Madera, J. Gough, L. Aravind, and K. Sankaran.** 2006. A database of bacterial lipoproteins (DOLOP) with functional assignments to predicted lipoproteins. Journal of Bacteriology **188:**2761-2773.
12. **Ballister, E. R., A. H. Lai, R. N. Zuckermann, Y. Cheng, and J. D. Mougous.** 2008. In vitro self-assembly of tailorable nanotubes from a simple protein building block. Proceedings of the National Academy of Sciences **105:**3733-3738.
13. **Basler, M., and J. J. Mekalanos.** 2012. Type 6 Secretion Dynamics Within and Between Bacterial Cells. Science **337:**815.
14. **Basler, M., M. Pilhofer, G. P. Henderson, G. J. Jensen, and J. J. Mekalanos.** 2012. Type VI secretion requires a dynamic contractile phage tail-like structure. Nature **483:**182-186.
15. **Baynham, P. J., D. M. Ramsey, B. V. Gvozdyev, E. M. Cordonnier, and D. J. Wozniak.** 2006. The *Pseudomonas aeruginosa* ribbon-helix-helix DNA-binding protein

AlgZ (AmrZ) controls twitching motility and biogenesis of type IV pili. Journal of Bacteriology **188:**132-140.

16. **Bernard, C. S., Y. R. Brunet, M. Gavioli, R. Lloubes, and E. Cascales.** 2011. Regulation of type VI secretion gene clusters by sigma54 and cognate enhancer binding proteins. Journal of Bacteriology **193:**2158-2167.
17. **Bernard, C. S., Y. R. Brunet, E. Gueguen, and E. Cascales.** 2010. Nooks and Crannies in type VI secretion regulation. Journal of Bacteriology **192:**3850-3860.
18. **Bingle, L. E., C. M. Bailey, and M. J. Pallen.** 2008. Type VI secretion: a beginner's guide. Current Opinion in Microbiology **11:**3-8.
19. **Birtalan, S. C., R. M. Phillips, and P. Ghosh.** 2002. Three-dimensional secretion signals in chaperone-effector complexes of bacterial pathogens. Molecular Cell **9:**971-980.
20. **Bladergroen, M. R., K. Badelt, and H. P. Spaink.** 2003. Infection-blocking genes of a symbiotic *Rhizobium leguminosarum* strain that are involved in temperature-dependent protein secretion. Molecular Plant-Microbe Interactions **16:**53-64.
21. **Bleves, S., V. Viarre, R. Salacha, G. P. Michel, A. Filloux, and R. Voulhoux.** 2010. Protein secretion systems in *Pseudomonas aeruginosa*: A wealth of pathogenic weapons. International Journal of Medical Microbiology **300:**534-543.
22. **Blondel, C. J., J. C. Jimenez, I. Contreras, and C. A. Santiviago.** 2009. Comparative genomic analysis uncovers 3 novel loci encoding type six secretion systems differentially distributed in *Salmonella* serotypes. BMC Genomics **10:**354.
23. **Boden, R., M. Cunliffe, J. Scanlan, H. Moussard, K. D. Kits, M. G. Klotz, M. S. Jetten, S. Vuilleumier, J. Han, L. Peters, N. Mikhailova, H. Teshima, R. Tapia, N. Kyrpides, N. Ivanova, I. Pagani, J. F. Cheng, L. Goodwin, C. Han, L. Hauser, M. L. Land, A. Lapidus, S. Lucas, S. Pitluck, T. Woyke, L. Stein, and J. C. Murrell.** 2011. Complete genome sequence of the aerobic marine methanotroph *Methylomonas methanica* MC09. Journal of Bacteriology **193:**7001-7002.
24. **Boehm, A., M. Kaiser, H. Li, C. Spangler, C. A. Kasper, M. Ackermann, V. Kaever, V. Sourjik, V. Roth, and U. Jenal.** 2010. Second messenger-mediated adjustment of bacterial swimming velocity. Cell **141:**107-116.
25. **Bonemann, G., A. Pietrosiuk, A. Diemand, H. Zentgraf, and A. Mogk.** 2009. Remodelling of VipA/VipB tubules by ClpV-mediated threading is crucial for type VI protein secretion. The EMBO Journal **28:**315-325.
26. **Bonemann, G., A. Pietrosiuk, and A. Mogk.** 2010. Tubules and donuts: a type VI secretion story. Molecular Microbiology **76:**815-821.
27. **Boyer, F., G. Fichant, J. Berthod, Y. Vandenbrouck, and I. Attree.** 2009. Dissecting the bacterial type VI secretion system by a genome wide in silico analysis: what can be learned from available microbial genomic resources? BMC Genomics **10:**104.
28. **Brencic, A., and S. Lory.** 2009. Determination of the regulon and identification of novel mRNA targets of *Pseudomonas aeruginosa* RsmA. Molecular Microbiology **72:**612-632.
29. **Brencic, A., K. A. McFarland, H. R. McManus, S. Castang, I. Mogno, S. L. Dove, and S. Lory.** 2009. The GacS/GacA signal transduction system of *Pseudomonas aeruginosa* acts exclusively through its control over the transcription of the RsmY and RsmZ regulatory small RNAs. Molecular Microbiology **73:**434-445.

30. **Brooks, T. M., D. Unterweger, V. Bachmann, B. Kostiuk, and S. Pukatzki.** 2013. Lytic activity of the Vibrio cholerae type VI secretion toxin VgrG-3 is inhibited by the antitoxin TsaB. The Journal of Biological Chemistry **288:**7618-7625.
31. **Brunet, Y. R., C. S. Bernard, M. Gavioli, R. Lloubes, and E. Cascales.** 2011. An epigenetic switch involving overlapping fur and DNA methylation optimizes expression of a type VI secretion gene cluster. PLoS Genetics **7:**e1002205.
32. **Brunet, Y. R., L. Espinosa, S. Harchouni, T. Mignot, and E. Cascales.** 2013. Imaging type VI secretion-mediated bacterial killing. Cell Reports **3:**36-41.
33. **Burrowes, E., C. Baysse, C. Adams, and F. O'Gara.** 2006. Influence of the regulatory protein RsmA on cellular functions in *Pseudomonas aeruginosa* PAO1, as revealed by transcriptome analysis. Microbiology **152:**405-418.
34. **Calderwood, S. B., and J. J. Mekalanos.** 1987. Iron regulation of Shiga-like toxin expression in *Escherichia coli* is mediated by the fur locus. Journal of Bacteriology **169:**4759-4764.
35. **Cambronne, E. D., and C. R. Roy.** 2007. The *Legionella pneumophila* IcmSW complex interacts with multiple Dot/Icm effectors to facilitate type IV translocation. PLoS Pathogens **3:**e188.
36. **Campoy, S., M. Jara, N. Busquets, A. M. de Rozas, I. Badiola, and J. Barbe.** 2002. Intracellular cyclic AMP concentration is decreased in *Salmonella* typhimurium fur mutants. Microbiology **148:**1039-1048.
37. **Cardona, S. T., and M. A. Valvano.** 2005. An expression vector containing a rhamnose-inducible promoter provides tightly regulated gene expression in Burkholderia cenocepacia. Plasmid **54:**219-228.
38. **Carpenter, B. M., J. M. Whitmire, and D. S. Merrell.** 2009. This is not your mother's repressor: the complex role of fur in pathogenesis. Infection and Immunity **77:**2590-2601.
39. **Carruthers, M. D., P. A. Nicholson, E. N. Tracy, and R. S. Munson, Jr.** 2013. *Acinetobacter baumannii* Utilizes a Type VI Secretion System for Bacterial Competition. PLoS One **8:**e59388.
40. **Casabona, M. G., J. M. Silverman, K. M. Sall, F. Boyer, Y. Coute, J. Poirel, D. Grunwald, J. D. Mougous, S. Elsen, and I. Attree.** 2013. An ABC transporter and an outer membrane lipoprotein participate in posttranslational activation of type VI secretion in *Pseudomonas aeruginosa*. Environmental Microbiology **15:**471-486.
41. **Cascales, E.** 2008. The type VI secretion toolkit. EMBO Reports **9:**735-741.
42. **Cascales, E., and C. Cambillau.** 2012. Structural biology of type VI secretion systems. Philosophical Transactions of the Royal Society B: Biological Sciences **1592:**1102-1111.
43. **Castang, S., and S. L. Dove.** 2012. Basis for the essentiality of H-NS family members in *Pseudomonas aeruginosa*. Journal of Bacteriology **194:**5101-5109.
44. **Castang, S., H. R. McManus, K. H. Turner, and S. L. Dove.** 2008. H-NS family members function coordinately in an opportunistic pathogen. Proceedings of the National Academy of Sciences **105:**18947-18952.
45. **Chakraborty, S., J. Sivaraman, K. Y. Leung, and Y. K. Mok.** 2011. Two-component PhoB-PhoR regulatory system and ferric uptake regulator sense phosphate and iron to control virulence genes in type III and VI secretion systems of *Edwardsiella tarda*. The Journal of Biological Chemistry **286:**39417-39430.

46. **Chevallet, M., H. Diemer, A. Van Dorssealer, C. Villiers, and T. Rabilloud.** 2007. Toward a better analysis of secreted proteins: the example of the myeloid cells secretome. Proteomics **7:**1757-1770.
47. **Choi, K. H., and H. P. Schweizer.** 2006. mini-Tn7 insertion in bacteria with single attTn7 sites: example *Pseudomonas aeruginosa*. Nature Protocols **1:**153-161.
48. **Chou, S., N. K. Bui, A. B. Russell, K. W. Lexa, T. E. Gardiner, M. LeRoux, W. Vollmer, and J. D. Mougous.** 2012. Structure of a peptidoglycan amidase effector targeted to Gram-negative bacteria by the type VI secretion system. Cell Reports **1:**656-664.
49. **Christen, M., H. D. Kulasekara, B. Christen, B. R. Kulasekara, L. R. Hoffman, and S. I. Miller.** 2010. Asymmetrical distribution of the second messenger c-di-GMP upon bacterial cell division. Science **328:**1295-1297.
50. **Christie, P. J., K. Atmakuri, V. Krishnamoorthy, S. Jakubowski, and E. Cascales.** 2005. Biogenesis, architecture, and function of bacterial type iv secretion systems. Annual Review of Microbiology **59:**451-485.
51. **Christie, P. J., and J. P. Vogel.** 2000. Bacterial type IV secretion: conjugation systems adapted to deliver effector molecules to host cells. Trends in Microbiology **8:**354-360.
52. **Colvin, K. M., V. D. Gordon, K. Murakami, B. R. Borlee, D. J. Wozniak, G. C. Wong, and M. R. Parsek.** 2011. The pel polysaccharide can serve a structural and protective role in the biofilm matrix of *Pseudomonas aeruginosa*. PLoS Pathogens **7:**e1001264.
53. **Corbett, M., S. Virtue, K. Bell, P. Birch, T. Burr, L. Hyman, K. Lilley, S. Poock, I. Toth, and G. Salmond.** 2005. Identification of a new quorum-sensing-controlled virulence factor in *Erwinia carotovora subsp. atroseptica* secreted via the type II targeting pathway. Molecular Plant-Microbe Interactions **18:**334-342.
54. **Cornelis, G. R.** 2006. The type III secretion injectisome. Nature Reviews Microbiology **4:**811-825.
55. **Costerton, J. W., P. S. Stewart, and E. P. Greenberg.** 1999. Bacterial biofilms: a common cause of persistent infections. Science **284:**1318-1322.
56. **Coumes-Florens, S., C. Brochier-Armanet, A. Guiseppi, F. Denizot, and M. Foglino.** 2011. A new highly conserved antibiotic sensing/resistance pathway in firmicutes involves an ABC transporter interplaying with a signal transduction system. PLoS One **6:**e15951.
57. **Cover, T. L., and S. R. Blanke.** 2005. *Helicobacter pylori* VacA, a paradigm for toxin multifunctionality. Nature Reviews Microbiology **3:**320-332.
58. **D'Argenio, D. A., M. Wu, L. R. Hoffman, H. D. Kulasekara, E. Deziel, E. E. Smith, H. Nguyen, R. K. Ernst, T. J. Larson Freeman, D. H. Spencer, M. Brittnacher, H. S. Hayden, S. Selgrade, M. Klausen, D. R. Goodlett, J. L. Burns, B. W. Ramsey, and S. I. Miller.** 2007. Growth phenotypes of *Pseudomonas aeruginosa lasR* mutants adapted to the airways of cystic fibrosis patients. Molecular Microbiology **64:**512-533.
59. **Das, S., A. Chakrabortty, R. Banerjee, and K. Chaudhuri.** 2002. Involvement of in vivo induced icmF gene of *Vibrio cholerae* in motility, adherence to epithelial cells, and conjugation frequency. Biochemical and Biophysics Research Communications **295:**922-928.
60. **Dautin, N., and H. D. Bernstein.** 2007. Protein secretion in Gram-negative bacteria via the autotransporter pathway. Annual Review of Microbiology **61:**89-112.

61. **Davidson, A. L., E. Dassa, C. Orelle, and J. Chen.** 2008. Structure, function, and evolution of bacterial ATP-binding cassette systems. Microbiology and Molecular Biology Reviews **72:**317-364.
62. **De Maayer, P., S. N. Venter, T. Kamber, B. Duffy, T. A. Coutinho, and T. H. Smits.** 2011. Comparative genomics of the Type VI secretion systems of *Pantoea* and *Erwinia* species reveals the presence of putative effector islands that may be translocated by the VgrG and Hcp proteins. BMC Genomics **12:**576.
63. **de Pace, F., J. Boldrin de Paiva, G. Nakazato, M. Lancellotti, M. P. Sircili, E. Guedes Stehling, W. Dias da Silveira, and V. Sperandio.** 2011. Characterization of IcmF of the type VI secretion system in an avian pathogenic *Escherichia coli* (APEC) strain. Microbiology **157:**2954-2962.
64. **Deane, J. E., P. Abrusci, S. Johnson, and S. M. Lea.** 2010. Timing is everything: the regulation of type III secretion. Cell and Molecular Life Sciences **67:**1065-1075.
65. **Deng, W., S. R. Liou, G. Plunkett, 3rd, G. F. Mayhew, D. J. Rose, V. Burland, V. Kodoyianni, D. C. Schwartz, and F. R. Blattner.** 2003. Comparative genomics of *Salmonella enterica* serovar Typhi strains Ty2 and CT18. Journal of Bacteriology **185:**2330-2337.
66. **Desvaux, M., M. Hebraud, R. Talon, and I. R. Henderson.** 2009. Secretion and subcellular localizations of bacterial proteins: a semantic awareness issue. Trends in Microbiology **17:**139-145.
67. **Dintner, S., A. Staron, E. Berchtold, T. Petri, T. Mascher, and S. Gebhard.** 2011. Coevolution of ABC transporters and two-component regulatory systems as resistance modules against antimicrobial peptides in Firmicutes Bacteria. Journal of Bacteriology **193:**3851-3862.
68. **Dong, C., H. Zhang, Z. Q. Gao, W. J. Wang, Z. She, G. F. Liu, Y. Q. Shen, X. D. Su, and Y. H. Dong.** 2013. Structural insights into the inhibition of type VI effector Tae3 by its immunity protein Tai3. Biochemical Journal PMID: 23730712.
69. **Dong, T. G., B. T. Ho, D. R. Yoder-Himes, and J. J. Mekalanos.** 2013. Identification of T6SS-dependent effector and immunity proteins by Tn-seq in *Vibrio cholerae*. Proceedings of the National Academy of Sciences **110:**2623-2628.
70. **Dubuis, C., and D. Haas.** 2007. Cross-species GacA-controlled induction of antibiosis in pseudomonads. Applied and Environmental Microbiology **73:**650-654.
71. **Dudley, E. G., N. R. Thomson, J. Parkhill, N. P. Morin, and J. P. Nataro.** 2006. Proteomic and microarray characterization of the AggR regulon identifies a pheU pathogenicity island in enteroaggregative *Escherichia coli*. Molecular Microbiology **61:**1267-1282.
72. **Economou, A., P. J. Christie, R. C. Fernandez, T. Palmer, G. V. Plano, and A. P. Pugsley.** 2006. Secretion by numbers: Protein traffic in prokaryotes. Molecular Microbiology **62:**308-319.
73. **Edgar, R. C.** 2004. MUSCLE: multiple sequence alignment with high accuracy and high throughput. Nucleic Acids Research **32:**1792-1797.
74. **Ellermeier, J. R., and J. M. Slauch.** 2008. Fur regulates expression of the Salmonella pathogenicity island 1 type III secretion system through HilD. Journal of Bacteriology **190:**476-486.
75. **English, G., K. Trunk, V. A. Rao, V. Srikannathasan, W. N. Hunter, and S. J. Coulthurst.** 2012. New secreted toxins and immunity proteins encoded within the Type

VI secretion system gene cluster of *Serratia marcescens*. Molecular Microbiology **8:**921-936.
76. **Enos-Berlage, J. L., Z. T. Guvener, C. E. Keenan, and L. L. McCarter.** 2005. Genetic determinants of biofilm development of opaque and translucent *Vibrio parahaemolyticus*. Molecular Microbiology **55:**1160-1182.
77. **Enright, A. J., I. Iliopoulos, N. C. Kyrpides, and C. A. Ouzounis.** 1999. Protein interaction maps for complete genomes based on gene fusion events. Nature **402:**86-90.
78. **Fang, X., and M. Gomelsky.** 2010. A post-translational, c-di-GMP-dependent mechanism regulating flagellar motility. Molecular Microbiology **76:**1295-1305.
79. **Farris, C., S. Sanowar, M. W. Bader, R. Pfuetzner, and S. I. Miller.** 2010. Antimicrobial peptides activate the Rcs regulon through the outer membrane lipoprotein RcsF. Journal of Bacteriology **192:**4894-4903.
80. **Federle, M. J., and B. L. Bassler.** 2003. Interspecies communication in bacteria. The Journal of Clinical Investigation **112:**1291-1299.
81. **Felisberto-Rodrigues, C., E. Durand, M. S. Aschtgen, S. Blangy, M. Ortiz-Lombardia, B. Douzi, C. Cambillau, and E. Cascales.** 2011. Towards a structural comprehension of bacterial type VI secretion systems: characterization of the TssJ-TssM complex of an *Escherichia coli* pathovar. PLoS Pathogens **7:**e1002386.
82. **Feng, J., M. R. Atkinson, W. McCleary, J. B. Stock, B. L. Wanner, and A. J. Ninfa.** 1992. Role of phosphorylated metabolic intermediates in the regulation of glutamine synthetase synthesis in *Escherichia coli*. Journal of Bacteriology **174:**6061-6070.
83. **Filippova, E. V., M. Chruszcz, T. Skarina, O. Kagan, M. Cymborowski, A. Savchenko, A. M. Edwards, A. Joachimiak, W. Minor.** 2007. Crystal structure of PA0076 from *Pseudomonas aeruginosa* PAO1 at 2.05 A resolution. Midwest Center for Structural Genomics.
84. **Filloux, A., A. Hachani, and S. Bleves.** 2008. The bacterial type VI secretion machine: yet another player for protein transport across membranes. Microbiology **154:**1570-1583.
85. **Finlay, B. B., and S. Falkow.** 1997. Common themes in microbial pathogenicity revisited. Microbiology and Molecular Biology Reviews **61:**136-169.
86. **Francis, M. S., H. Wolf-Watz, and A. Forsberg.** 2002. Regulation of type III secretion systems. Current Opinion in Microbiology **5:**166-172.
87. **Frank, J., M. Radermacher, P. Penczek, J. Zhu, Y. Li, M. Ladjadj, and A. Leith.** 1996. SPIDER and WEB: processing and visualization of images in 3D electron microscopy and related fields. J Struct Biol **116:**190-199.
88. **French, C. T., I. J. Toesca, T. H. Wu, T. Teslaa, S. M. Beaty, W. Wong, M. Liu, I. Schroder, P. Y. Chiou, M. A. Teitell, and J. F. Miller.** 2011. Dissection of the *Burkholderia* intracellular life cycle using a photothermal nanoblade. Proceedings of the National Academy of Sciences **108:**12095-12100.
89. **Fronzes, R., P. J. Christie, and G. Waksman.** 2009. The structural biology of type IV secretion systems. Nature Reviews Microbiology **7:**703-714.
90. **Fuqua, C., M. R. Parsek, and E. P. Greenberg.** 2001. Regulation of gene expression by cell-to-cell communication: acyl-homoserine lactone quorum sensing. Annual Review of Genetics **35:**439-468.
91. **Galan, J. E.** 2009. Common themes in the design and function of bacterial effectors. Cell Host & Microbe **5:**571-579.

92. **Galan, J. E., and H. Wolf-Watz.** 2006. Protein delivery into eukaryotic cells by type III secretion machines. Nature **444:**567-573.
93. **Gerlach, R. G., D. Jackel, B. Stecher, C. Wagner, A. Lupas, W. D. Hardt, and M. Hensel.** 2007. Salmonella Pathogenicity Island 4 encodes a giant non-fimbrial adhesin and the cognate type 1 secretion system. Cellular Microbiology **9:**1834-1850.
94. **Gode-Potratz, C. J., and L. L. McCarter.** 2011. Quorum sensing and silencing in *Vibrio parahaemolyticus*. Journal of Bacteriology **193:**4224-4237.
95. **Gooderham, W. J., and R. E. Hancock.** 2009. Regulation of virulence and antibiotic resistance by two-component regulatory systems in *Pseudomonas aeruginosa*. FEMS Microbiology Reviews **33:**279-294.
96. **Goodman, A. L., B. Kulasekara, A. Rietsch, D. Boyd, R. S. Smith, and S. Lory.** 2004. A signaling network reciprocally regulates genes associated with acute infection and chronic persistence in *Pseudomonas aeruginosa*. Developmental Cell **7:**745-754.
97. **Gueguen, E., and E. Cascales.** 2013. Promoter swapping unveils the role of the *Citrobacter rodentium* CTS1 type VI secretion system in interbacterial competition. Applied and Environmental Microbiology **79:**32-38.
98. **Guindon, S., J. F. Dufayard, V. Lefort, M. Anisimova, W. Hordijk, and O. Gascuel.** 2010. New algorithms and methods to estimate maximum-likelihood phylogenies: assessing the performance of PhyML 3.0. Systematic Biology **59:**307-321.
99. **Hachani, A., N. S. Lossi, A. Hamilton, C. Jones, S. Bleves, D. Albesa-Jove, and A. Filloux.** 2011. Type VI secretion system in Pseudomonas aeruginosa: secretion and multimerization of VgrG proteins. Journal of Biological Chemistry **286:**12317-12327.
100. **Hall, H. K., and J. W. Foster.** 1996. The role of fur in the acid tolerance response of *Salmonella* typhimurium is physiologically and genetically separable from its role in iron acquisition. Journal of Bacteriology **178:**5683-5691.
101. **Harrington, S. M., E. G. Dudley, and J. P. Nataro.** 2006. Pathogenesis of enteroaggregative *Escherichia coli* infection. FEMS Microbiology Letters **254:**12-18.
102. **Hassan, K. A., A. Johnson, B. T. Shaffer, Q. Ren, T. A. Kidarsa, L. D. Elbourne, S. Hartney, R. Duboy, N. C. Goebel, T. M. Zabriskie, I. T. Paulsen, and J. E. Loper.** 2010. Inactivation of the GacA response regulator in *Pseudomonas fluorescens* Pf-5 has far-reaching transcriptomic consequences. Environmental Microbiology **12:**899-915.
103. **Hassett, D. J., P. A. Sokol, M. L. Howell, J. F. Ma, H. T. Schweizer, U. Ochsner, and M. L. Vasil.** 1996. Ferric uptake regulator (Fur) mutants of *Pseudomonas aeruginosa* demonstrate defective siderophore-mediated iron uptake, altered aerobic growth, and decreased superoxide dismutase and catalase activities. Journal of Bacteriology **178:**3996-4003.
104. **Hayes, C. S., S. K. Aoki, and D. A. Low.** 2010. Bacterial contact-dependent delivery systems. Annual Review of Genetics **44:**71-90.
105. **Henderson, I. R., F. Navarro-Garcia, M. Desvaux, R. C. Fernandez, and D. Ala'Aldeen.** 2004. Type V protein secretion pathway: the autotransporter story. Microbiology and Molecular Biology Reviews **68:**692-744.
106. **Hengge, R.** 2009. Principles of c-di-GMP signalling in bacteria. Nature Review Microbiology **7:**263-273.
107. **Hense, B. A., C. Kuttler, J. Muller, M. Rothballer, A. Hartmann, and J. U. Kreft.** 2007. Does efficiency sensing unify diffusion and quorum sensing? Nature Review Microbiology **5:**230-239.

108. **Hickman, J. W., and C. S. Harwood.** 2008. Identification of FleQ from *Pseudomonas aeruginosa* as a c-di-GMP-responsive transcription factor. Molecular Microbiology **69:**376-389.
109. **Hiron, A., M. Falord, J. Valle, M. Debarbouille, and T. Msadek.** 2011. Bacitracin and nisin resistance in *Staphylococcus aureus*: a novel pathway involving the BraS/BraR two-component system (SA2417/SA2418) and both the BraD/BraE and VraD/VraE ABC transporters. Molecular Microbiology **81:**602-622.
110. **Hoang, T. T., A. J. Kutchma, A. Becher, and H. P. Schweizer.** 2000. Integration-proficient plasmids for *Pseudomonas aeruginosa*: site-specific integration and use for engineering of reporter and expression strains. Plasmid **43:**59-72.
111. **Holland, I. B., L. Schmitt, and J. Young.** 2005. Type 1 protein secretion in bacteria, the ABC-transporter dependent pathway (review). Molecular Membrane Biology **22:**29-39.
112. **Holm, L., and P. Rosenstrom.** 2010. Dali server: conservation mapping in 3D. Nucleic Acids Research **38:**W545-549.
113. **Hood, R. D., P. Singh, F. Hsu, T. Guvener, M. A. Carl, R. R. Trinidad, J. M. Silverman, B. B. Ohlson, K. G. Hicks, R. L. Plemel, M. Li, S. Schwarz, W. Y. Wang, A. J. Merz, D. R. Goodlett, and J. D. Mougous.** 2010. A type VI secretion system of *Pseudomonas aeruginosa* targets a toxin to bacteria. Cell Host & Microbe **7:**25-37.
114. **Hooper, L. V., and J. I. Gordon.** 2001. Commensal host-bacterial relationships in the gut. Science **292:**1115-1118.
115. **Hsu, F., S. Schwarz, and J. D. Mougous.** 2009. TagR promotes PpkA-catalysed type VI secretion activation in *Pseudomonas aeruginosa*. Molecular Microbiology **72:**1111-1125.
116. **Ikeda, J. S., A. Janakiraman, D. G. Kehres, M. E. Maguire, and J. M. Slauch.** 2005. Transcriptional regulation of sitABCD of *Salmonella enterica* serovar Typhimurium by MntR and Fur. Journal of Bacteriology **187:**912-922.
117. **Imperi, F., F. Ciccosanti, A. B. Perdomo, F. Tiburzi, C. Mancone, T. Alonzi, P. Ascenzi, M. Piacentini, P. Visca, and G. M. Fimia.** 2009. Analysis of the periplasmic proteome of *Pseudomonas aeruginosa*, a metabolically versatile opportunistic pathogen. Proteomics **9:**1901-1915.
118. **Ishikawa, T., P. K. Rompikuntal, B. Lindmark, D. L. Milton, and S. N. Wai.** 2009. Quorum sensing regulation of the two hcp alleles in *Vibrio cholerae* O1 strains. PLoS One **4:**e6734.
119. **Ishikawa, T., D. Sabharwal, J. Broms, D. L. Milton, A. Sjostedt, B. E. Uhlin, and S. N. Wai.** 2012. Pathoadaptive conditional regulation of the type VI secretion system in *Vibrio cholerae* O1 strains. Infection and Immunity **80:**575-584.
120. **Izore, T., V. Job, and A. Dessen.** 2011. Biogenesis, regulation, and targeting of the type III secretion system. Structure **19:**603-612.
121. **Jacobs, M. A., A. Alwood, I. Thaipisuttikul, D. Spencer, E. Haugen, S. Ernst, O. Will, R. Kaul, C. Raymond, R. Levy, L. Chun-Rong, D. Guenthner, D. Bovee, M. V. Olson, and C. Manoil.** 2003. Comprehensive transposon mutant library of *Pseudomonas aeruginosa*. Proceedings of the National Academy of Sciences **100:**14339-14344.
122. **Janakiraman, A., and J. M. Slauch.** 2000. The putative iron transport system SitABCD encoded on SPI1 is required for full virulence of *Salmonella* typhimurium. Molecular Microbiology **35:**1146-1155.
123. **Jani, A. J., and P. A. Cotter.** 2010. Type VI secretion: not just for pathogenesis anymore. Cell Host & Microbe **8:**2-6.

124. **Jobichen, C., S. Chakraborty, M. Li, J. Zheng, L. Joseph, Y. K. Mok, K. Y. Leung, and J. Sivaraman.** 2010. Structural basis for the secretion of EvpC: a key type VI secretion system protein from *Edwardsiella tarda*. PLoS One **5:**e12910.
125. **Kanamaru, S.** 2009. Structural similarity of tailed phages and pathogenic bacterial secretion systems. Proceedings of the National Academy of Sciences **106:**4067-4068.
126. **Kanamaru, S., P. G. Leiman, V. A. Kostyuchenko, P. R. Chipman, V. V. Mesyanzhinov, F. Arisaka, and M. G. Rossmann.** 2002. Structure of the cell-puncturing device of bacteriophage T4. Nature **415:**553-557.
127. **Kapitein, N., G. Bonemann, A. Pietrosiuk, F. Seyffer, I. Hausser, J. K. Locker, and A. Mogk.** 2013. ClpV recycles VipA/VipB tubules and prevents non-productive tubule formation to ensure efficient type VI protein secretion. Molecular Microbiology **87:**1013-1028.
128. **Khajanchi, B. K., J. Sha, E. V. Kozlova, T. E. Erova, G. Suarez, J. C. Sierra, V. L. Popov, A. J. Horneman, and A. K. Chopra.** 2009. N-acylhomoserine lactones involved in quorum sensing control the type VI secretion system, biofilm formation, protease production, and in vivo virulence in a clinical isolate of *Aeromonas hydrophila*. Microbiology **155:**3518-3531.
129. **Kitaoka, M., S. T. Miyata, T. M. Brooks, D. Unterweger, and S. Pukatzki.** 2011. VasH is a transcriptional regulator of the type VI secretion system functional in endemic and pandemic *Vibrio cholerae*. Journal of Bacteriology **193:**6471-6482.
130. **Korgaonkar, A. K., and M. Whiteley.** 2011. *Pseudomonas aeruginosa* enhances production of an antimicrobial in response to N-acetylglucosamine and peptidoglycan. Journal of Bacteriology **193:**909-917.
131. **Korotkov, K. V., M. Sandkvist, and W. G. Hol.** 2012. The type II secretion system: biogenesis, molecular architecture and mechanism. Nature Reviews Microbiology **10:**336-351.
132. **Koskiniemi, S., J. G. Lamoureux, K. C. Nikolakakis, C. t'Kint de Roodenbeke, M. D. Kaplan, D. A. Low, and C. S. Hayes.** 2013. Rhs proteins from diverse bacteria mediate intercellular competition. Proceedings of the National Academy of Sciences **110:**7032-7037.
133. **Krishnan, K., and P. D. Moens.** 2009. Structure and functions of profilins. Biophysical Reviews **1:**71-81.
134. **Kulasekara, H. D., and S. I. Miller.** 2007. Threonine phosphorylation times bacterial secretion. Nature Cell Biology **9:**734-736.
135. **Kunkel, T. A., J. D. Roberts, and R. A. Zakour.** 1987. Rapid and efficient site-specific mutagenesis without phenotypic selection. Methods in Enzymology **154:**367-382.
136. **Lambertsen, L., C. Sternberg, and S. Molin.** 2004. Mini-Tn7 transposons for site-specific tagging of bacteria with fluorescent proteins. Environmental Microbiology **6:**726-732.
137. **Lapouge, K., M. Schubert, F. H. Allain, and D. Haas.** 2008. Gac/Rsm signal transduction pathway of gamma-proteobacteria: from RNA recognition to regulation of social behaviour. Molecular Microbiology **67:**241-253.
138. **Latasa, C., A. Roux, A. Toledo-Arana, J. M. Ghigo, C. Gamazo, J. R. Penades, and I. Lasa.** 2005. BapA, a large secreted protein required for biofilm formation and host colonization of *Salmonella enterica* serovar Enteritidis. Molecular Microbiology **58:**1322-1339.

139. **Lee, S. H., and J. E. Galan.** 2004. *Salmonella* type III secretion-associated chaperones confer secretion-pathway specificity. Molecular Microbiology **51:**483-495.
140. **Lee, V. T., J. M. Matewish, J. L. Kessler, M. Hyodo, Y. Hayakawa, and S. Lory.** 2007. A cyclic-di-GMP receptor required for bacterial exopolysaccharide production. Molecular Microbiology **65:**1474-1484.
141. **Leiman, P. G., F. Arisaka, M. J. van Raaij, V. A. Kostyuchenko, A. A. Aksyuk, S. Kanamaru, and M. G. Rossmann.** 2010. Morphogenesis of the T4 tail and tail fibers. Virology Journal **7:**355.
142. **Leiman, P. G., M. Basler, U. A. Ramagopal, J. B. Bonanno, J. M. Sauder, S. Pukatzki, S. K. Burley, S. C. Almo, and J. J. Mekalanos.** 2009. Type VI secretion apparatus and phage tail-associated protein complexes share a common evolutionary origin. Proceedings of the National Academy of Sciences **106:**4154-4159.
143. **Leiman, P. G., P. R. Chipman, V. A. Kostyuchenko, V. V. Mesyanzhinov, and M. G. Rossmann.** 2004. Three-dimensional rearrangement of proteins in the tail of bacteriophage T4 on infection of its host. Cell **118:**419-429.
144. **LeRoux, M., J. A. De Leon, N. J. Kuwada, A. B. Russell, D. Pinto-Santini, R. D. Hood, D. M. Agnello, S. M. Robertson, P. A. Wiggins, and J. D. Mougous.** 2012. Quantitative single-cell characterization of bacterial interactions reveals type VI secretion is a double-edged sword. Proceedings of the National Academy of Sciences **109:**19804-19809.
145. **Lesic, B., M. Starkey, J. He, R. Hazan, and L. G. Rahme.** 2009. Quorum sensing differentially regulates *Pseudomonas aeruginosa* type VI secretion locus I and homologous loci II and III, which are required for pathogenesis. Microbiology **155:**2845-2855.
146. **Leung, K. Y., B. A. Siame, H. Snowball, and Y. K. Mok.** 2011. Type VI secretion regulation: crosstalk and intracellular communication. Current Opinion in Microbiology **14:**9-15.
147. **Leverrier, P., J. P. Declercq, K. Denoncin, D. Vertommen, A. Hiniker, S. H. Cho, and J. F. Collet.** 2011. Crystal structure of the outer membrane protein RcsF, a new substrate for the periplasmic protein-disulfide isomerase DsbC. The Journal of Biological Chemistry **286:**16734-16742.
148. **Lewenza, S., M. M. Mhlanga, and A. P. Pugsley.** 2008. Novel inner membrane retention signals in *Pseudomonas aeruginosa* lipoproteins. Journal of Bacteriology **190:**6119-6125.
149. **Li, M., I. Le Trong, M. A. Carl, E. T. Larson, S. Chou, J. A. De Leon, S. L. Dove, R. E. Stenkamp, and J. D. Mougous.** 2012. Structural basis for type VI secretion effector recognition by a cognate immunity protein. PLoS Pathogens **8:**e1002613.
150. **Liu, H., S. J. Coulthurst, L. Pritchard, P. E. Hedley, M. Ravensdale, S. Humphris, T. Burr, G. Takle, M. B. Brurberg, P. R. Birch, G. P. Salmond, and I. K. Toth.** 2008. Quorum sensing coordinates brute force and stealth modes of infection in the plant pathogen *Pectobacterium atrosepticum*. PLoS Pathogens **4:**e1000093.
151. **Lossi, N. S., E. Manoli, A. Forster, R. Dajani, T. Pape, P. Freemont, and A. Filloux.** 2013. The HsiB1C1 (TssB-TssC) complex of the *Pseudomonas aeruginosa* type VI secretion system forms a bacteriophage tail sheathlike structure. The Journal of Biological Chemistry **288:**7536-7548.

152. **Lu, H. M., S. Mizushima, and S. Lory.** 1993. A periplasmic intermediate in the extracellular secretion pathway of *Pseudomonas aeruginosa* exotoxin A. Journal of Bacteriology **175:**7463-7467.
153. **Ludtke, S. J., P. R. Baldwin, and W. Chiu.** 1999. EMAN: semiautomated software for high-resolution single-particle reconstructions. Journal of Structural Biology **128:**82-97.
154. **Ma, A. T., S. McAuley, S. Pukatzki, and J. J. Mekalanos.** 2009. Translocation of a *Vibrio cholerae* type VI secretion effector requires bacterial endocytosis by host cells. Cell Host & Microbe **5:**234-243.
155. **Ma, A. T., and J. J. Mekalanos.** 2010. In vivo actin cross-linking induced by *Vibrio cholerae* type VI secretion system is associated with intestinal inflammation. Proceedings of the National Academy of Sciences **107:**4365-4370.
156. **Ma, L. S., F. Narberhaus, and E. M. Lai.** 2012. IcmF Family Protein TssM Exhibits ATPase Activity and Energizes Type VI Secretion. The Journal of Biological Chemistry **287:**15610-15621.
157. **MacIntyre, D. L., S. T. Miyata, M. Kitaoka, and S. Pukatzki.** 2010. The *Vibrio cholerae* type VI secretion system displays antimicrobial properties. Proceedings of the National Academy of Sciences **107:**19520-19524.
158. **Makino, K., H. Shinagawa, M. Amemura, T. Kawamoto, M. Yamada, and A. Nakata.** 1989. Signal transduction in the phosphate regulon of *Escherichia coli* involves phosphotransfer between PhoR and PhoB proteins. Journal of Molecular Biology **210:**551-559.
159. **Marchler-Bauer, A., J. B. Anderson, F. Chitsaz, M. K. Derbyshire, C. DeWeese-Scott, J. H. Fong, L. Y. Geer, R. C. Geer, N. R. Gonzales, M. Gwadz, S. He, D. I. Hurwitz, J. D. Jackson, Z. Ke, C. J. Lanczycki, C. A. Liebert, C. Liu, F. Lu, S. Lu, G. H. Marchler, M. Mullokandov, J. S. Song, A. Tasneem, N. Thanki, R. A. Yamashita, D. Zhang, N. Zhang, and S. H. Bryant.** 2009. CDD: specific functional annotation with the Conserved Domain Database. Nucleic Acids Research **37:**D205-210.
160. **Mattei, P. J., E. Faudry, V. Job, T. Izore, I. Attree, and A. Dessen.** 2011. Membrane targeting and pore formation by the type III secretion system translocon. FEBS Journal **278:**414-426.
161. **McCleary, W. R., J. B. Stock, and A. J. Ninfa.** 1993. Is acetyl phosphate a global signal in *Escherichia coli*? Journal of Bacteriology **175:**2793-2798.
162. **McGinness, K. E., T. A. Baker, and R. T. Sauer.** 2006. Engineering controllable protein degradation. Molecular Cell **22:**701-707.
163. **Michel, G., S. Bleves, G. Ball, A. Lazdunski, and A. Filloux.** 1998. Mutual stabilization of the XcpZ and XcpY components of the secretory apparatus in *Pseudomonas aeruginosa*. Microbiology **144 ( Pt 12):**3379-3386.
164. **Moore, M. M., D. L. Fernandez, and R. L. Thune.** 2002. Cloning and characterization of *Edwardsiella ictaluri* proteins expressed and recognized by the channel catfish Ictalurus punctatus immune response during infection. Diseases of Aquatic Organisms **52:**93-107.
165. **Moscoso, J. A., H. Mikkelsen, S. Heeb, P. Williams, and A. Filloux.** 2011. The *Pseudomonas aeruginosa* sensor RetS switches Type III and Type VI secretion via c-di-GMP signalling. Environmental Microbiology **13:**3128-3138.
166. **Mougous, J. D., M. E. Cuff, S. Raunser, A. Shen, M. Zhou, C. A. Gifford, A. L. Goodman, G. Joachimiak, C. L. Ordonez, S. Lory, T. Walz, A. Joachimiak, and J. J.**

**Mekalanos.** 2006. A virulence locus of *Pseudomonas aeruginosa* encodes a protein secretion apparatus. Science **312:**1526-1530.
167. **Mougous, J. D., C. A. Gifford, T. L. Ramsdell, and J. J. Mekalanos.** 2007. Threonine phosphorylation post-translationally regulates protein secretion in *Pseudomonas aeruginosa*. Nature Cell Biology **9:**797-803.
168. **Mougous, J. D., R. H. Senaratne, C. J. Petzold, M. Jain, D. H. Lee, M. W. Schelle, M. D. Leavell, J. S. Cox, J. A. Leary, L. W. Riley, and C. R. Bertozzi.** 2006. A sulfated metabolite produced by stf3 negatively regulates the virulence of *Mycobacterium tuberculosis*. Proceedings of the National Academy of Sciences **103:**4258-4263.
169. **Mulks, M. H., and A. G. Plaut.** 1978. IgA protease production as a characteristic distinguishing pathogenic from harmless neisseriaceae. The New England Journal of Medicine **299:**973-976.
170. **Murdoch, S. L., K. Trunk, G. English, M. J. Fritsch, E. Pourkarimi, and S. J. Coulthurst.** 2011. The opportunistic pathogen *Serratia marcescens* utilises Type VI Secretion to target bacterial competitors. Journal of Bacteriology **193:**6057-6069.
171. **Murray, T. S., M. Egan, and B. I. Kazmierczak.** 2007. *Pseudomonas aeruginosa* chronic colonization in cystic fibrosis patients. Current Opinion in Pediatrics **19:**83-88.
172. **Nagai, H., E. D. Cambronne, J. C. Kagan, J. C. Amor, R. A. Kahn, and C. R. Roy.** 2005. A C-terminal translocation signal required for Dot/Icm-dependent delivery of the *Legionella* RalF protein to host cells. Proceedings of the National Academy of Sciences **102:**826-831.
173. **Narita, S., and H. Tokuda.** 2006. An ABC transporter mediating the membrane detachment of bacterial lipoproteins depending on their sorting signals. FEBS Letters **580:**1164-1170.
174. **Nataro, J. P., and J. B. Kaper.** 1998. Diarrheagenic *Escherichia coli*. Clinical Microbiology Reviews **11:**142-201.
175. **Newman, J. R., and C. Fuqua.** 1999. Broad-host-range expression vectors that carry the L-arabinose-inducible *Escherichia coli* araBAD promoter and the araC regulator. Gene **227:**197-203.
176. **Ng, W. L., and B. L. Bassler.** 2009. Bacterial quorum-sensing network architectures. Annual Review of Genetics **43:**197-222.
177. **Oberhardt, M. A., J. Puchalka, K. E. Fryer, V. A. Martins dos Santos, and J. A. Papin.** 2008. Genome-scale metabolic network analysis of the opportunistic pathogen *Pseudomonas aeruginosa* PAO1. Journal of Bacteriology **190:**2790-2803.
178. **Ohi, M., Y. Li, Y. Cheng, and T. Walz.** 2004. Negative Staining and Image Classification - Powerful Tools in Modern Electron Microscopy. Biological Procedures Online **6:**23-34.
179. **Osipiuk, J., X. Xu, H. Cui, A. Savchenko, A. Edwards, and A. Joachimiak.** 2011. Crystal structure of secretory protein Hcp3 from *Pseudomonas aeruginosa*. Journal of Structural and Functional Genomics **12:**21-26.
180. **Parret, A. H., and R. De Mot.** 2002. *Escherichia coli's* uropathogenic-specific protein: a bacteriocin promoting infectivity? Microbiology **148:**1604-1606.
181. **Parsek, M. R., and E. P. Greenberg.** 2005. Sociomicrobiology: the connections between quorum sensing and biofilms. Trends in Microbiology **13:**27-33.

182. **Paul, K., V. Nieto, W. C. Carlquist, D. F. Blair, and R. M. Harshey.** 2010. The c-di-GMP binding protein YcgR controls flagellar motor direction and speed to affect chemotaxis by a "backstop brake" mechanism. Molecular Cell **38:**128-139.
183. **Paulsen, I. T., C. M. Press, J. Ravel, D. Y. Kobayashi, G. S. Myers, D. V. Mavrodi, R. T. DeBoy, R. Seshadri, Q. Ren, R. Madupu, R. J. Dodson, A. S. Durkin, L. M. Brinkac, S. C. Daugherty, S. A. Sullivan, M. J. Rosovitz, M. L. Gwinn, L. Zhou, D. J. Schneider, S. W. Cartinhour, W. C. Nelson, J. Weidman, K. Watkins, K. Tran, H. Khouri, E. A. Pierson, L. S. Pierson, 3rd, L. S. Thomashow, and J. E. Loper.** 2005. Complete genome sequence of the plant commensal Pseudomonas fluorescens Pf-5. Nature Biotechnology **23:**873-878.
184. **Pell, L. G., V. Kanelis, L. W. Donaldson, P. L. Howell, and A. R. Davidson.** 2009. The phage lambda major tail protein structure reveals a common evolution for long-tailed phages and the type VI bacterial secretion system. Proceedings of the National Academy of Sciences **106:**4160-4165.
185. **Pennetier, C., L. Dominguez-Ramirez, and J. Plumbridge.** 2008. Different regions of Mlc and NagC, homologous transcriptional repressors controlling expression of the glucose and N-acetylglucosamine phosphotransferase systems in *Escherichia coli*, are required for inducer signal recognition. Molecular Microbiology **67:**364-377.
186. **Pettersson, J., R. Nordfelth, E. Dubinina, T. Bergman, M. Gustafsson, K. E. Magnusson, and H. Wolf-Watz.** 1996. Modulation of virulence factor expression by pathogen target cell contact. Science **273:**1231-1233.
187. **Pezza, R. J., M. A. Villarreal, G. G. Montich, and C. E. Argarana.** 2002. Vanadate inhibits the ATPase activity and DNA binding capability of bacterial MutS. A structural model for the vanadate-MutS interaction at the Walker A motif. Nucleic Acids Research **30:**4700-4708.
188. **Phan, J., J. E. Tropea, and D. S. Waugh.** 2004. Structure of the *Yersinia pestis* type III secretion chaperone SycH in complex with a stable fragment of YscM2. Acta Crystallographica Section D: Biological Crystallography **60:**1591-1599.
189. **Pieper, R., S. T. Huang, J. M. Robinson, D. J. Clark, H. Alami, P. P. Parmar, R. D. Perry, R. D. Fleischmann, and S. N. Peterson.** 2009. Temperature and growth phase influence the outer-membrane proteome and the expression of a type VI secretion system in *Yersinia pestis*. Microbiology **155:**498-512.
190. **Potvin, E., D. E. Lehoux, I. Kukavica-Ibrulj, K. L. Richard, F. Sanschagrin, G. W. Lau, and R. C. Levesque.** 2003. In vivo functional genomics of *Pseudomonas aeruginosa* for high-throughput screening of new virulence factors and antibacterial targets. Environmental Microbiology **5:**1294-1308.
191. **Pugsley, A. P.** 1993. The complete general secretory pathway in Gram-negative bacteria. Microbiology and Molecular Biology Reviews **57:**50-108.
192. **Pukatzki, S., A. T. Ma, A. T. Revel, D. Sturtevant, and J. J. Mekalanos.** 2007. Type VI secretion system translocates a phage tail spike-like protein into target cells where it cross-links actin. Proceedings of the National Academy of Sciences **104:**15508-15513.
193. **Pukatzki, S., A. T. Ma, D. Sturtevant, B. Krastins, D. Sarracino, W. C. Nelson, J. F. Heidelberg, and J. J. Mekalanos.** 2006. Identification of a conserved bacterial protein secretion system in *Vibrio cholerae* using the *Dictyostelium* host model system. Proceedings of the National Academy of Sciences **103:**1528-1533.

194. **Pukatzki, S., S. B. McAuley, and S. T. Miyata.** 2009. The type VI secretion system: translocation of effectors and effector-domains. Current Opinion in Microbiology **12:**11-17.
195. **Rao, P. S., Y. Yamada, Y. P. Tan, and K. Y. Leung.** 2004. Use of proteomics to identify novel virulence determinants that are required for *Edwardsiella tarda* pathogenesis. Molecular Microbiology **53:**573-586.
196. **Rappas, M., D. Bose, and X. Zhang.** 2007. Bacterial enhancer-binding proteins: unlocking sigma54-dependent gene transcription. Current Opinion in Structural Biology **17:**110-116.
197. **Rashid, R. A., P. I. Tarr, and S. L. Moseley.** 2006. Expression of the *Escherichia coli* IrgA homolog adhesin is regulated by the ferric uptake regulation protein. Microbial Pathogenesis **41:**207-217.
198. **Ravaud, S., M. A. Do Cao, M. Jidenko, C. Ebel, M. Le Maire, J. M. Jault, A. Di Pietro, R. Haser, and N. Aghajari.** 2006. The ABC transporter BmrA from *Bacillus subtilis* is a functional dimer when in a detergent-solubilized state. Biochemical Journal **395:**345-353.
199. **Records, A. R., and D. C. Gross.** 2010. Sensor kinases RetS and LadS regulate *Pseudomonas syringae* type VI secretion and virulence factors. Journal of Bacteriology **192:**3584-3596.
200. **Rietsch, A., I. Vallet-Gely, S. L. Dove, and J. J. Mekalanos.** 2005. ExsE, a secreted regulator of type III secretion genes in *Pseudomonas aeruginosa*. Proceedings of the National Academy of Sciences **102:**8006-8011.
201. **Rietsch, A., M. C. Wolfgang, and J. J. Mekalanos.** 2004. Effect of metabolic imbalance on expression of type III secretion genes in *Pseudomonas aeruginosa*. Infection and Immunity **72:**1383-1390.
202. **Rogge, M. L., and R. L. Thune.** 2011. Regulation of the *Edwardsiella ictaluri* type III secretion system by pH and phosphate concentration through EsrA, EsrB, and EsrC. Applied and Environmental Microbiology **77:**4293-4302.
203. **Rossi, V., D. K. Banfield, M. Vacca, L. E. Dietrich, C. Ungermann, M. D'Esposito, T. Galli, and F. Filippini.** 2004. Longins and their longin domains: regulated SNAREs and multifunctional SNARE regulators. Trends in Biochemical Sciences **29:**682-688.
204. **Russell, A. B., R. D. Hood, N. K. Bui, M. LeRoux, W. Vollmer, and J. D. Mougous.** 2011. Type VI secretion delivers bacteriolytic effectors to target cells. Nature **475:**343-347.
205. **Russell, A. B., M. LeRoux, K. Hathazi, D. M. Agnello, T. Ishikawa, P. A. Wiggins, S. N. Wai, and J. D. Mougous.** 2013. Diverse type VI secretion phospholipases are functionally plastic antibacterial effectors. Nature **496:**508-512.
206. **Russell, A. B., P. Singh, M. Brittnacher, N. K. Bui, R. D. Hood, M. A. Carl, D. M. Agnello, S. Schwarz, D. R. Goodlett, W. Vollmer, and J. D. Mougous.** 2012. A widespread bacterial type VI secretion effector superfamily identified using a heuristic approach. Cell Host & Microbe **11:**538-549.
207. **Ryder, C., M. Byrd, and D. J. Wozniak.** 2007. Role of polysaccharides in *Pseudomonas aeruginosa* biofilm development. Current Opinion in Microbiology **10:**644-648.
208. **Sandkvist, M., L. O. Michel, L. P. Hough, V. M. Morales, M. Bagdasarian, M. Koomey, V. J. DiRita, and M. Bagdasarian.** 1997. General secretion pathway (eps)

genes required for toxin secretion and outer membrane biogenesis in *Vibrio cholerae*. Journal of Bacteriology **179:**6994-7003.
209. **Sauer, K., A. K. Camper, G. D. Ehrlich, J. W. Costerton, and D. G. Davies.** 2002. *Pseudomonas aeruginosa* displays multiple phenotypes during development as a biofilm. Journal of Bacteriology **184:**1140-1154.
210. **Schlenker, C., and C. M. Surawicz.** 2009. Emerging infections of the gastrointestinal tract. Best Practice & Research Clinical Gastroenterology **23:**89-99.
211. **Schrodinger, LLC.** 2010. The PyMOL Molecular Graphics System, Version 1.3r1.
212. **Schuck, P.** 2000. Size-distribution analysis of macromolecules by sedimentation velocity ultracentrifugation and lamm equation modeling. Biophysics Journal **78:**1606-1619.
213. **Schulein, R., P. Guye, T. A. Rhomberg, M. C. Schmid, G. Schroder, A. C. Vergunst, I. Carena, and C. Dehio.** 2005. A bipartite signal mediates the transfer of type IV secretion substrates of *Bartonella henselae* into human cells. Proceedings of the National Academy of Sciences **102:**856-861.
214. **Schumacher, J., N. Joly, M. Rappas, X. Zhang, and M. Buck.** 2006. Structures and organisation of AAA+ enhancer binding proteins in transcriptional activation. Journal of Structural Biology **156:**190-199.
215. **Schwarz, S., R. D. Hood, and J. D. Mougous.** 2010. What is type VI secretion doing in all those bugs? Trends in Microbiology **18:**531-537.
216. **Schwarz, S., T. E. West, F. Boyer, W. C. Chiang, M. A. Carl, R. D. Hood, L. Rohmer, T. Tolker-Nielsen, S. J. Skerrett, and J. D. Mougous.** 2010. *Burkholderia* type VI secretion systems have distinct roles in eukaryotic and bacterial cell interactions. PLoS Pathogens **6:**e1001068.
217. **Sexton, J. A., J. L. Miller, A. Yoneda, T. E. Kehl-Fie, and J. P. Vogel.** 2004. *Legionella pneumophila* DotU and IcmF are required for stability of the Dot/Icm complex. Infection and Immunity **72:**5983-5992.
218. **Shalom, G., J. G. Shaw, and M. S. Thomas.** 2007. In vivo expression technology identifies a type VI secretion system locus in *Burkholderia pseudomallei* that is induced upon invasion of macrophages. Microbiology **153:**2689-2699.
219. **Sheng, L., Y. Lv, Q. Liu, Q. Wang, and Y. Zhang.** 2013. Connecting type VI secretion, quorum sensing, and c-di-GMP production in fish pathogen *Vibrio alginolyticus* through phosphatase PppA. Veterinary Microbiology **162:**652-662.
220. **Shi, L., S. Deng, M. J. Marshall, Z. Wang, D. W. Kennedy, A. C. Dohnalkova, H. M. Mottaz, E. A. Hill, Y. A. Gorby, A. S. Beliaev, D. J. Richardson, J. M. Zachara, and J. K. Fredrickson.** 2008. Direct involvement of type II secretion system in extracellular translocation of *Shewanella oneidensis* outer membrane cytochromes MtrC and OmcA. Journal of Bacteriology **190:**5512-5516.
221. **Shingler, V.** 1996. Signal sensing by sigma 54-dependent regulators: derepression as a control mechanism. Molecular Microbiology **19:**409-416.
222. **Silverman, J. M., L. S. Austin, F. Hsu, K. G. Hicks, R. D. Hood, and J. D. Mougous.** 2011. Separate inputs modulate phosphorylation-dependent and -independent type VI secretion activation. Molecular Microbiology **82:**1277-1290.
223. **Silverman, J. M., Y. R. Brunet, E. Cascales, and J. D. Mougous.** 2012. Structure and regulation of the type VI secretion system. Annual Review of Microbiology **66:**453-472.
224. **Skrabanek, L., H. K. Saini, G. D. Bader, and A. J. Enright.** 2008. Computational prediction of protein-protein interactions. Molecular Biotechnology **38:**1-17.

225. **Smith, E. E., D. G. Buckley, Z. Wu, C. Saenphimmachak, L. R. Hoffman, D. A. D'Argenio, S. I. Miller, B. W. Ramsey, D. P. Speert, S. M. Moskowitz, J. L. Burns, R. Kaul, and M. V. Olson.** 2006. Genetic adaptation by *Pseudomonas aeruginosa* to the airways of cystic fibrosis patients. Proceedings of the National Academy of Sciences **103:**8487-8492.
226. **Sory, M. P., A. Boland, I. Lambermont, and G. R. Cornelis.** 1995. Identification of the YopE and YopH domains required for secretion and internalization into the cytosol of macrophages, using the cyaA gene fusion approach. Proceedings of the National Academy of Sciences **92:**11998-12002.
227. **Stebbins, C. E., and J. E. Galan.** 2001. Maintenance of an unfolded polypeptide by a cognate chaperone in bacterial type III secretion. Nature **414:**77-81.
228. **Stebbins, C. E., and J. E. Galan.** 2003. Priming virulence factors for delivery into the host. Nature Reviews of Molecular Cell Biology **4:**738-743.
229. **Stover, C. K., X. Q. Pham, A. L. Erwin, S. D. Mizoguchi, P. Warrener, M. J. Hickey, F. S. Brinkman, W. O. Hufnagle, D. J. Kowalik, M. Lagrou, R. L. Garber, L. Goltry, E. Tolentino, S. Westbrock-Wadman, Y. Yuan, L. L. Brody, S. N. Coulter, K. R. Folger, A. Kas, K. Larbig, R. Lim, K. Smith, D. Spencer, G. K. Wong, Z. Wu, I. T. Paulsen, J. Reizer, M. H. Saier, R. E. Hancock, S. Lory, and M. V. Olson.** 2000. Complete genome sequence of *Pseudomonas aeruginosa* PA01, an opportunistic pathogen. Nature **406:**959-964.
230. **Suarez, G., J. C. Sierra, T. E. Erova, J. Sha, A. J. Horneman, and A. K. Chopra.** 2010. A type VI secretion system effector protein, VgrG1, from *Aeromonas hydrophila* that induces host cell toxicity by ADP ribosylation of actin. Journal of Bacteriology **192:**155-168.
231. **Suhr, M., I. Benz, and M. A. Schmidt.** 1996. Processing of the AIDA-I precursor: removal of AIDAc and evidence for the outer membrane anchoring as a beta-barrel structure. Molecular Microbiology **22:**31-42.
232. **Sutherland, M. C., T. L. Nguyen, V. Tseng, and J. P. Vogel.** 2012. The Legionella IcmSW complex directly interacts with DotL to mediate translocation of adaptor-dependent substrates. PLoS Pathogens **8:**e1002910.
233. **Tanaka, S. Y., S. Narita, and H. Tokuda.** 2007. Characterization of the *Pseudomonas aeruginosa* Lol system as a lipoprotein sorting mechanism. The Journal of Biological Chemistry **282:**13379-13384.
234. **Taylor, D. N., A. L. Bourgeois, C. D. Ericsson, R. Steffen, Z. D. Jiang, J. Halpern, R. Haake, and H. L. Dupont.** 2006. A randomized, double-blind, multicenter study of rifaximin compared with placebo and with ciprofloxacin in the treatment of travelers' diarrhea. The American Journal of Tropical Medicine and Hygiene **74:**1060-1066.
235. **Tetsch, L., and K. Jung.** 2009. The regulatory interplay between membrane-integrated sensors and transport proteins in bacteria. Molecular Microbiology **73:**982-991.
236. **Tetsch, L., C. Koller, I. Haneburger, and K. Jung.** 2008. The membrane-integrated transcriptional activator CadC of *Escherichia coli* senses lysine indirectly via the interaction with the lysine permease LysP. Molecular Microbiology **67:**570-583.
237. **Thanabalu, T., E. Koronakis, C. Hughes, and V. Koronakis.** 1998. Substrate-induced assembly of a contiguous channel for protein export from *E.coli*: reversible bridging of an inner-membrane translocase to an outer membrane exit pore. The EMBO Journal **17:**6487-6496.

238. **Thibault, J., E. Faudry, C. Ebel, I. Attree, and S. Elsen.** 2009. Anti-activator ExsD forms a 1:1 complex with ExsA to inhibit transcription of type III secretion operons. The Journal of Biological Chemistry **284:**15762-15770.
239. **Torres, C., C. Galian, C. Freiberg, J. R. Fantino, and J. M. Jault.** 2009. The YheI/YheH heterodimer from *Bacillus subtilis* is a multidrug ABC transporter. Biochimica et Biophysica Acta: Molecular and Cell Biology of Lipids **1788:**615-622.
240. **Van Veldhoven, P. P., and G. P. Mannaerts.** 1987. Inorganic and organic phosphate measurements in the nanomolar range. Analytical Biochemistry **161:**45-48.
241. **VanRheenen, S. M., G. Dumenil, and R. R. Isberg.** 2004. IcmF and DotU are required for optimal effector translocation and trafficking of the *Legionella pneumophila* vacuole. Infection and Immunity **72:**5972-5982.
242. **Ventre, I., A. L. Goodman, I. Vallet-Gely, P. Vasseur, C. Soscia, S. Molin, S. Bleves, A. Lazdunski, S. Lory, and A. Filloux.** 2006. Multiple sensors control reciprocal expression of *Pseudomonas aeruginosa* regulatory RNA and virulence genes. Proceedings of the National Academy of Sciences **103:**171-176.
243. **Vergunst, A. C., M. C. van Lier, A. den Dulk-Ras, T. A. Stuve, A. Ouwehand, and P. J. Hooykaas.** 2005. Positive charge is an important feature of the C-terminal transport signal of the VirB/D4-translocated proteins of *Agrobacterium*. Proceedings of the National Academy of Sciences **102:**832-837.
244. **Wagner, C., M. Polke, R. G. Gerlach, D. Linke, Y. D. Stierhof, H. Schwarz, and M. Hensel.** 2011. Functional dissection of SiiE, a giant non-fimbrial adhesin of Salmonella enterica. Cellular Microbiology **13:**1286-1301.
245. **Waksman, G., and R. Fronzes.** 2010. Molecular architecture of bacterial type IV secretion systems. Trends in Biochemical Sciences **35:**691-698.
246. **Wang, Q., J. G. Frye, M. McClelland, and R. M. Harshey.** 2004. Gene expression patterns during swarming in *Salmonella* typhimurium: genes specific to surface growth and putative new motility and pathogenicity genes. Molecular Microbiology **52:**169-187.
247. **Ward, A., C. L. Reyes, J. Yu, C. B. Roth, and G. Chang.** 2007. Flexibility in the ABC transporter MsbA: Alternating access with a twist. Proceedings of the National Academy of Sciences **104:**19005-19010.
248. **Weber, B., M. Hasic, C. Chen, S. N. Wai, and D. L. Milton.** 2009. Type VI secretion modulates quorum sensing and stress response in *Vibrio anguillarum*. Environmental Microbiology **11:**3018-3028.
249. **Weiss, V., and B. Magasanik.** 1988. Phosphorylation of nitrogen regulator I (NRI) of *Escherichia coli*. Proceedings of the National Academy of Sciences **85:**8919-8923.
250. **Winsor, G. L., D. K. Lam, L. Fleming, R. Lo, M. D. Whiteside, N. Y. Yu, R. E. Hancock, and F. S. Brinkman.** 2011. *Pseudomonas* Genome Database: improved comparative analysis and population genomics capability for *Pseudomonas* genomes. Nucleic Acids Research **39:**D596-600.
251. **Wolff, N., J. M. Ghigo, P. Delepelaire, C. Wandersman, and M. Delepierre.** 1994. C-terminal secretion signal of an *Erwinia chrysanthemi* protease secreted by a signal peptide-independent pathway: proton NMR and CD conformational studies in membrane-mimetic environments. Biochemistry **33:**6792-6801.
252. **Worrall, L. J., E. Lameignere, and N. C. Strynadka.** 2011. Structural overview of the bacterial injectisome. Current Opinion Microbiology **14:**3-8.

253. **Wu, H. Y., P. C. Chung, H. W. Shih, S. R. Wen, and E. M. Lai.** 2008. Secretome analysis uncovers an Hcp-family protein secreted via a type VI secretion system in *Agrobacterium tumefaciens*. Journal of Bacteriology **190:**2841-2850.
254. **Xu, H., and T. R. Hoover.** 2001. Transcriptional regulation at a distance in bacteria. Current Opinion in Microbiology **4:**138-144.
255. **Yahr, T. L., and E. P. Greenberg.** 2004. The genetic basis for the commitment to chronic versus acute infection in *Pseudomonas aeruginosa*. Molecular Cell **16:**497-498.
256. **Zhang, L., A. J. Hinz, J. P. Nadeau, and T. F. Mah.** 2011. *Pseudomonas aeruginosa tssC1* Links Type VI Secretion and Biofilm-Specific Antibiotic Resistance. Journal of Bacteriology **193:**5510-5513.
257. **Zhang, W., S. Xu, J. Li, X. Shen, Y. Wang, and Z. Yuan.** 2011. Modulation of a thermoregulated type VI secretion system by AHL-dependent quorum sensing in *Yersinia pseudotuberculosis*. Archives of Microbiology **193:**351-363.
258. **Zheng, J., and K. Y. Leung.** 2007. Dissection of a type VI secretion system in *Edwardsiella tarda*. Molecular Microbiology **66:**1192-1206.
259. **Zheng, J., O. S. Shin, D. E. Cameron, and J. J. Mekalanos.** 2010. Quorum sensing and a global regulator TsrA control expression of type VI secretion and virulence in *Vibrio cholerae*. Proceedings of the National Academy of Sciences **107:**21128-21133.
260. **Zou, T., X. Yao, B. Qin, M. Zhang, L. Cai, W. Shang, D. I. Svergun, M. Wang, S. Cui, and Q. Jin.** 2012. Crystal structure of Pseudomonas aeruginosa Tsi2 reveals a stably folded superhelical antitoxin. Journal of Molecular Biology **417:**351-361.

# VITA

Julie Michelle Silverman was born in Albany, NY on March 22, 1985. She graduated from Bethlehem Central High School in 2003. Prior to starting graduate school, Dr. Silverman attended Binghamton University from 2003 to 2007 where she graduated with a Bachelor of Science in Biochemsitry. At Binghamton University, she worked as an undergraduate research in the laboratory of Dr. David G. Davies, where she studied *P. aeruginosa* biofilm dispersion. In 2013, Dr. Silverman received a Doctor of Philosophy degree from the University of Washignton Department of Microbiology. For her graduate work, she studied the type VI secretion system in the laboratory of Dr. Joseph D. Mougous.